Office de la Propriété Intellectuelle du Canada
Un organisme d'Industrie Canada

Canadian Intellectual Property Office
An agency of Industry Canada

CA 2820184 A1 2010/02/18

(21) 2 820 184

(12) DEMANDE DE BREVET CANADIEN
CANADIAN PATENT APPLICATION

(13) A1

(22) Date de dépôt/Filing Date: 2009/08/12

(41) Mise à la disp. pub./Open to Public Insp.: 2010/02/18

(62) Demande originale/Original Application: 2 733 976

(30) Priorités/Priorities: 2008/08/14 (US61/088,936); 2008/08/14 (US61/088,921); 2008/08/15 (US61/089,389); 2008/08/28 (US61/092,531); 2009/08/05 (US12/535,952); 2009/08/06 (US12/536,987); 2009/08/06 (US12/536,982); 2009/08/06 (US12/536,992)

(51) Cl.Int./Int.Cl. *C25B 9/18* (2006.01), *C25B 1/04* (2006.01), *H01L 31/0236* (2006.01), *H01L 31/042* (2006.01), *H01L 31/18* (2006.01), *H01L 31/052* (2006.01)

(71) Demandeur/Applicant:
MH SOLAR CO., LTD., TW

(72) Inventeur/Inventor:
SATER, BERNARD L., US

(74) Agent: SMART & BIGGAR

(54) Titre : CELLULES PHOTOVOLTAIQUES AVEC SURFACES TRAITEES ET APPLICATIONS APPARENTEES US2009053576

(54) Title: PHOTOVOLTAIC CELLS WITH PROCESSED SURFACES AND RELATED APPLICATIONS

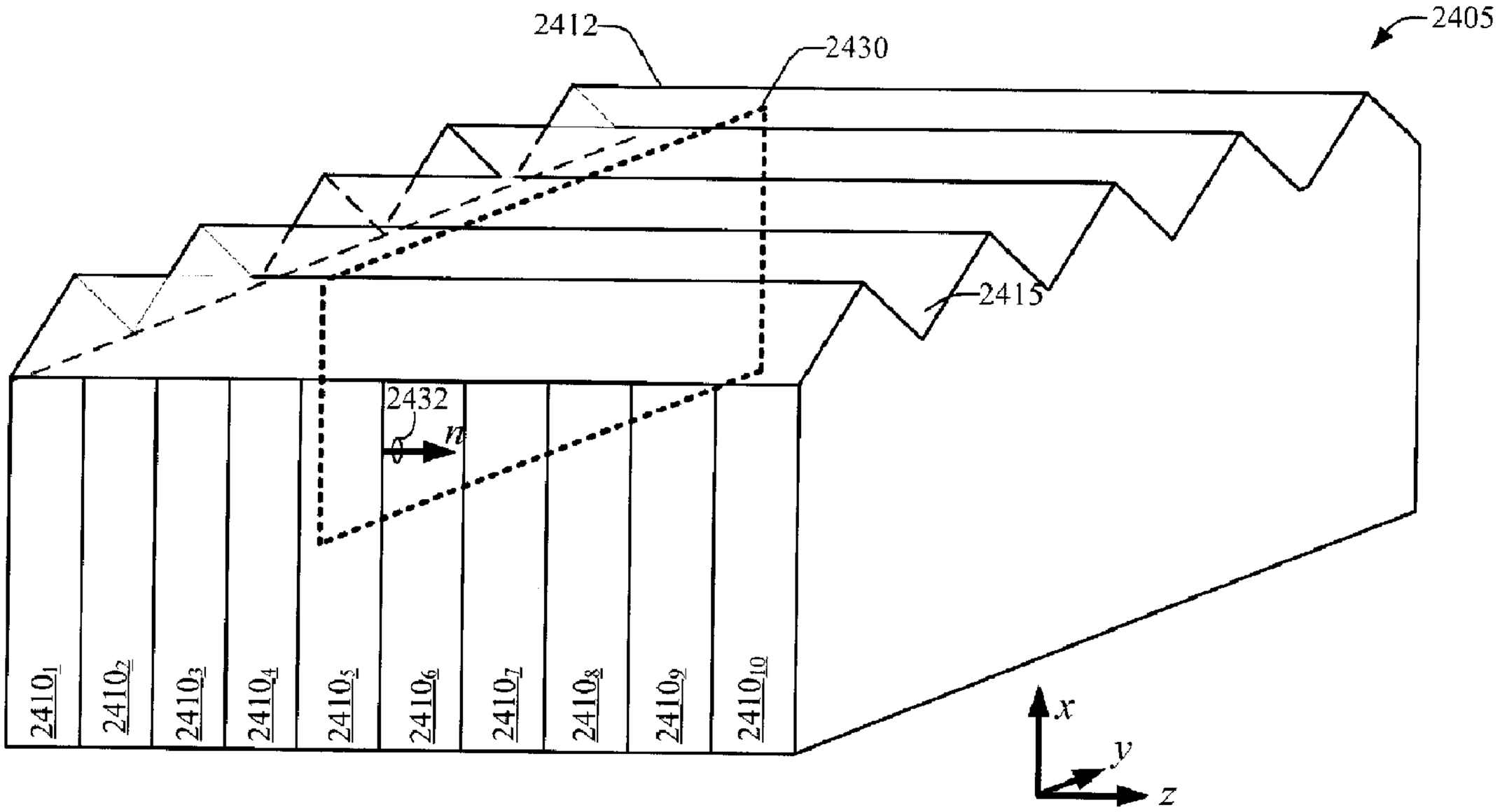

(57) Abrégé/Abstract:
Photovoltaic cells and processes that mitigate recombination losses of photogenerated carriers are provided. To reduce recombination losses, diffuse doping layers in active photovoltaic (PV) elements are coated with patterns of dielectric material(s) that reduce contact between metal contacts and the active PV element. Various patterns can be utilized, and one or more surfaces of the PV element can be coated with one or more dielectrics. Vertical Multi-Junction photovoltaic cells can be produced with

CA 2820184 A1 2010/02/18

(21) 2 820 184

(13) A1

(57) Abrégé(suite)/Abstract(continued):
patterned PV elements, or unit cells. While patterned PV elements can increase series resistance of VMJ photovoltaic cells, and patterning one or more surfaces in the PV element can add complexity to a process utilized to produce VMJ photovoltaic cells, reduction of carrier losses at diffuse doping layers in a PV element increases efficiency of photovoltaic cells, and thus provide with PV operational advantages that outweigh increased manufacturing complexity. System to fabricate the photovoltaic cells is provided.

50669-106D1

Abstract

Photovoltaic cells and processes that mitigate recombination losses of photogenerated carriers are provided. To reduce recombination losses, diffuse doping layers in active photovoltaic (PV) elements are coated with patterns of dielectric material(s) that reduce contact between metal contacts and the active PV element. Various patterns can be utilized, and one or more surfaces of the PV element can be coated with one or more dielectrics. Vertical Multi-Junction photovoltaic cells can be produced with patterned PV elements, or unit cells. While patterned PV elements can increase series resistance of VMJ photovoltaic cells, and patterning one or more surfaces in the PV element can add complexity to a process utilized to produce VMJ photovoltaic cells, reduction of carrier losses at diffuse doping layers in a PV element increases efficiency of photovoltaic cells, and thus provide with PV operational advantages that outweigh increased manufacturing complexity. System to fabricate the photovoltaic cells is provided.

50669-106D1

PHOTOVOLTAIC CELLS WITH PROCESSED SURFACES AND RELATED APPLICATIONS

[0001] This application is a divisional of Canadian National Phase Patent Application No. 2,733,976 filed August 12, 2009.

BACKGROUND

[0002] Limited supply and increasing demand of fossil energy resources and associated global environmental damage have driven global efforts to diversify utilization energy resources and related technologies. One such resource is solar energy, which employs photovoltaic (PV) technology for conversion of light into electricity. In addition, solar energy can be exploited for heat generation (e.g., in solar furnaces, steam generators, and the like). Solar technology is typically implemented in a series of PV cells, or solar cells, or panels thereof that receive sunlight and convert the sunlight into electricity, which can be subsequently delivered into a power grid. Significant progress has been achieved in design and production of solar panels, which has effectively increased efficiency while reducing manufacturing

cost thereof. As more highly efficient solar cells are developed, size of the cell is decreasing leading to an increase in the practicality of employing solar panels to provide a competitive renewable energy substitute to dwindling and highly demanded non-renewable sources. To this end, solar energy collection systems like solar concentrators can be deployed to convert solar energy into electricity which can be delivered to power grids, and to harvest heat as well. In addition to development of solar concentrator technology, development on solar cells directed to utilization is solar concentrators has been pursued.

[0003] High Intensity Solar Cell technology, referred to as a vertical multi-junction (VMJ) solar cell, is an integrally bonded series-connected array of miniature vertical junction unit cells that are edge illuminated with electrical contacts on the ends. The unique VMJ cell design can inherently provides high-voltage low-series resistance output characteristics, making it ideally suited for efficient performance in high intensity photovoltaic concentrators. Another key feature of the VMJ Cell is its design simplicity that leads to low manufacturing cost.

[0004] The efficacy of VMJ can be evidenced on performance data taken on an experimental VMJ cell with 40 series-connected junctions over the range of 100 to 2500 suns intensities where the output power density exceeded 400,000 watts/m^2 at 25 volts with near 20% efficiency. It should be appreciated that the foregoing performance in VMJ solar cells is accomplished with low manufacturing cost(s) and low manufacturing complexity. Such aspects are believe to be the needed drivers for feasible technical performance and economic efficiencies needed to enable photovoltaic concentrator systems to be significantly more cost effective and viable in solving global energy problems. Furthermore any increase in cell efficiency (e.g., more watts in output) should directly decrease concentrator system size (e.g., less cost associated with bill of materials) resulting in lower $/watt photovoltaic power cost.

[0005] It is to be noted that lower $/watt cost is substantially relevant to solar cell technology adoption and market penetration since global energy demand is steadily increasing, not only in emerging but in developed countries as well, while traditional fossil fuel costs are escalating. Also there are widespread increasing concerns for all associated problems; such as environmental pollution, global warming, and national security and economic perils linked with dependency on foreign fuel supplies. These environment, economic and security factors coupled with growing public awareness are driving intense interest in finding more cost-effective

and environmentally friendly renewable energy solutions. Of all available renewable energy resources, solar has the substantially greatest potential for satisfying demand in an efficient and sustainable manner. In fact, the earth receives more energy in the form of sunlight every periods of few minutes than mankind can consume from substantially all other resources over an entire year.

[0006] Even though photovoltaic power is widely recognized as an ideal renewable energy technology, its associated cost(s) can be a major impediment to adoption and market penetration. Before gaining market share and adoption, photovoltaic-based power needs to become cost-competitive with traditional power sources, including coal-fired power which is well developed, adopted among consumers and substantially cost effective. Moreover access to low cost electrical power is considered essential in all global economies; so terawatts (e.g., thousands of Giga Watts) of photovoltaic power systems can be needed. Market studies show installed photovoltaic power systems must drop to a benchmark cost of $3/watt, or less, before being cost-competitive without subsidies in large utility scale applications. Since installed photovoltaic system costs currently exceed $6/watt, substantial cost improvements are still required.

[0007] Attempting to achieve lower $/watt performance has been the principal goal of most research and development in photovoltaic technologies during the past several decades. Despite the industry spending billions of dollars pursuing a variety of technologies with the objective of rendering photovoltaic energy more cost-effective, existing photovoltaic industry still requires substantial subsidies to support sales, which can be an indicator of detrimental conditions for market development and industry development.

[0008] Currently silicon solar cells, which remain substantially the same as at the time of initial discovery and development in 1960s, dominate ~ 93% of photovoltaic markets. Existing photovoltaic industry in an endeavor to lower costs has relied heavily on the availability of low cost scrap-grade semiconductor silicon to manufacture conventional solar cells. It should be noted that such scrap-grade silicon, often referred to as solar-grade silicon, is primarily the heads and tails of ingots left over from wafer production and off-spec material rejected by semiconductor device manufacturers requiring higher quality prime-grade silicon wafers. Although photovoltaic sales have increased rapidly, growing ~ 40% annually over the past decade with production volume estimated at 3.8 Gigawatts (GW) in 2007, sales are

now hampered by shortages and higher prices in solar-grade silicon. Although prime-grade silicon is available, it is not considered an option since it would further increase manufacturing costs several fold.

[0009] For typical conventional solar cells over half the manufacturing cost is raw semiconductor poly-silicon used to produce the wafers for solar cells. As a result, a typical 14% efficiency solar cell is rated at 0.014 W/cm^2 and has more than $3/watt (or $0.042/cm^2) in silicon wafer cost before any additional manufacturing. Consequently, the existing photovoltaic industry has to address and resolve the fact that starting silicon material cost(s) alone exceeds the benchmark price utilities need for large scale applications. As a contrasting aspect, semiconductor manufacturers producing microprocessor chips that sell at over $100/cm^2 on an area basis can afford cost(s) associated with utilization of prime-grade silicon wafers.

[0010] The shortages in solar-grade silicon and the photovoltaic industry's inability to achieve important benchmark cost, along with the advent of new more efficient triple-junction solar cells developed for space applications, have recently generated considerable renewed interest photovoltaic concentrators. The obvious advantage of photovoltaic concentrators is the potential cost benefit resulting from using large areas of inexpensive materials (glass mirror reflectors or plastic lenses) to concentrate sunlight onto much smaller areas of expensive solar cells, hence using cheap materials to replace expensive materials. Designing photovoltaic concentrators for 1000 suns intensity would significantly reduce expensive semiconductor silicon requirements by ~ 99.9%, which means 1000 MW of VMJ cells are possible using same amount of expensive semiconductor silicon currently required for 1 MW of conventional solar cells. Pragmatically, this is considered a practical approach to alleviate any silicon shortage concern.

[0011] Substantial work on solar concentrators has mostly focused on developing silicon concentrator solar cell designs for high intensities; much of work considerable developed during the era of the 1970s energy crisis, which at the time demonstrated moderate to unsatisfactory results cost benefits. Research and development initially targeting silicon cells for concentrator systems for operation at 500 suns intensity was conducted; however that target was lowered to 250 suns when unresolved development difficulties were encountered in attempting to overcome series-resistance problems in the solar cell designs being investigated. For example, high series-resistance losses in concentrator solar cells were well recognized as being

a major problem, which conventional VMJ solar cell technology has addressed and resolved. It is to be noted that a substantial portion of solar cells developed for concentrator technology are quite complex and expensive to manufacture, with 6 or 7 high-temperature steps (>1000°C) and 6 or 7 photolithography masking steps. This complexity was attributed to design attempts to minimize series-resistance losses that basically limited maximum intensity operation in the best of these designs to no more than 250 suns. Such complexity and associated costs hindered substantial development of concentrator technologies and associated solar cell technologies, and promoted development of alternative technologies like thin-film solar cell technologies.

[0012] Vertical Multi-Junction (VMJ) solar cell technology is substantially different from conventional concentrator solar cells. The VMJ solar cell technology provides at least two advantages with respect to other technologies: (1) it does not require photolithography, and (2) a single high-temperature diffusion step, at temperatures greater than 1000°C, can be employed to form both junctions. Consequently, lower manufacturing cost is a given. In addition, VMJ solar cells can be operated at high intensities; e.g., operation at 2500 suns. It is readily apparent from such operation that series-resistance is not a problem in VMJ cell design; even at intensities an order of magnitude higher conventional wisdom suggested it was not economically viable. Also the current density in VMJ unit cells at 2500 suns is typically near 70 A/cm^2, a radiation level that can be substantially detrimental to most solar cells based on other technologies.

[0013] As stated above, the renewed interest in photovoltaic concentrators is largely due to the development Triple-Junction Solar Cells made with III-V materials containing gallium (Ga), phosphorus (P), arsenide (As), indium (In) and germanium (Ge). Triple-junction cell may use 20 to 30 different semiconductors layered in series upon germanium wafers: doped layers of $GaInP_2$ and GaAs grown in a metal-organic chemical vapor deposition (MOCVD) reactor where each type of semiconductor will have a characteristic band gap energy that causes it to absorb sunlight most efficiently at a certain color. The semiconductors layers are carefully chosen to absorb nearly the entire solar spectrum, thus generating electricity from as much of the sunlight as possible. These multi-junction devices are the most efficient solar cells to date, reaching a record high of 40.7% efficiency under modest solar concentration and

laboratory conditions. But since they are expensive to manufacture, they require application in photovoltaic concentrators.

[0014] However the demand and cost of III-V solar cell materials are rapidly increasing. As an example, in 12 months (12/2006-12/2007) the cost of pure gallium increased from about $350 per Kg to $680 per kg and germanium prices increased substantially to $1000-$1200 per Kg. The price of indium which was $94 per Kg in 2002 increased to nearly $1000 per Kg in 2007. In addition the demand for indium is projected to continue to increase with large-scale manufacturing of thin-film CIGS (CuInGaSe) solar cells started by several new companies in 2007. Moreover, indium is a rare element that is widely used to form transparent electrical coatings in the form of indium-tin oxide for liquids crystal displays and large flat-panel monitors. Realistically, these materials appear not viable long term photovoltaic (PV) solutions needed to provide terawatts of low cost power in solving major global energy problems.

[0015] While III-V semiconductor solar cell of area 0.26685 cm^2 may generate a power of 2.6 watts, or about 10 W/cm^2, and it has been estimated that such technology may eventually produce electricity at 8-10 cents/kWh, substantially similar to the price of electricity from conventional sources, further analysis may be needed to support such estimate. However, VMJ solar cells showed output power exceeding 40 W/cm^2 at 2500 suns intensity using the least costly semiconductor material with low cost manufacturing. (This output power is over 400,000 W/m^2.) In addition to complex PV technologies based on advanced materials, Si-based solar cell technology remains substantially dominant in photovoltaic elements and applications. Moreover, should a global need occur, silicon is the only semiconductor material with an existing industrial base that would be capable of supplying terawatts of photovoltaic power within the foreseeable future for widespread global application.

SUMMARY

[0016] The following presents a simplified summary in order to provide a basic understanding of some aspects described herein. This summary is not an extensive overview nor is intended to identify key/critical elements or to delineate the scope of the various aspects described herein. Its sole purpose is to present some concepts in a simplified form as a prelude to the more detailed description that is presented later.

[0017] The subject innovation provides semiconductor-based photovoltaic cells and processes that mitigate recombination losses of photogenerated carriers. In an aspect, to reduce recombination losses, diffuse doping layers in active photovoltaic elements are coated with patterns of dielectric material(s) that reduce contact between metal contacts and the active PV element. Various patterns can be utilized, and one or more surfaces of the PV element can be coated with one or more dielectrics. Vertical Multi-Junction (VMJ) solar cells can be produced with patterned PV elements, or unit cells. Patterned PV elements can increase series resistance of VMJ solar cells, and patterning one or more surfaces in the PV element can add complexity to a process utilized to produce VMJ solar cells; yet, reduction of carrier losses at diffuse doping layers can increase efficiency of solar cells and thus provide with PV operational advantages that outweigh increased manufacturing complexity. A system that enables fabrication of the semiconductor-based PV cells is also provided.

[0018] Aspects or features described herein, and associated advantages, such as reduction of recombination losses of photogenerated carriers, can be exploited in any class of photovoltaic cells such as solar cells, thermophotovoltaic cells, or cells excited with laser sources of photons. Additionally, aspects of the subject innovation also can be implemented in other class(es) of energy-conversion cells such as betavoltaic cells.

[0019] The subject innovation mitigates bulk recombination losses in a vertical multi junction (VMJ) cell *via* a texturing on its light receiving surface. The textures can be in form of cavity shaped grooves - as "V" shaped cross section configurations, "U" shaped cross configurations, and the like - wherein a plane that includes such cross section configuration is substantially perpendicular to the direction of stacking the unit cells that form the VMJ. In one aspect, a plane that includes substantially repetitive cross sections (*e.g.* cross-sectioning a direction that grooves are extended thereon) is substantially perpendicular to the direction of

stacking the unit cells. Such an arrangement facilitates directing the refracted light away from the p+ and n+ diffused doped regions of the VMJ– while at the same time creating desired carriers in a decreasing volume. Accordingly, incident light can be refracted in the plane that includes the cross section configuration, and which is substantially perpendicular to the direction of stacking the unit cells.

[0020] It is to be appreciated that the texturing for the VMJ of the subject innovation is different from prior art for conventional silicon photovoltaic cell textures – both in terms of orientation of PN junctions; and/or interaction with incident light. For example, conventional silicon photovoltaic cells are typically textured to incline the penetration of the light, so that more of the longer wavelengths are absorbed closer to PN junctions (positioned horizontally) for better current collection of carriers – and hence mitigate poor spectral response to longer wavelengths in the solar spectrum. In contrast, such is not required in the VMJ of the subject innovation that includes vertical junctions, and hence already provides for an enhanced spectral response to the longer wavelengths in the solar spectrum.

[0021] In a particular aspect, an outcome for implementing grooves of the subject innovation (*e.g.*, V grooves) is to mitigate bulk recombination losses by reducing the bulk volume - (as opposed to conventional solar surfaces with texturing, which reduce reflection, or cause reflected or refracted light to become closer to the junctions). In particular, the VMJ cell has demonstrated better carrier current collection for both the short wavelengths and the long wavelengths, wherein the short wavelength response is due to eliminating a highly doped horizontal junction at the top surface, and the long wavelength respond is due to the enhanced collection efficiency of vertical junctions.) As another example, if instead of the cavity shaped grooved texture of the subject innovation, other textures (*e.g.*, random, pyramids, domes, and similar raised configurations) were implemented as part of the VMJ, incident light becomes refracted in all directions, resulting in light absorption in the p+ and n+ diffused regions and hence reduced efficiency.

[0022] According to a related methodology, initially a VMJ can be formed by stacking multiple cell units, wherein each cell itself can include a plurality of parallel semiconductor substrates or layers that are stacked together. Each layer can consist of impurity doped semiconductor material that form a PN junction, and further include a "built –in" electrostatic drift field that enhance minority carrier movement toward such PN junction. Subsequently a plurality of such cell units are integrated to shape a

VMJ. Next, on a surface of the VMJ cell that receives light, cavity shaped grooves can be formed (*e.g.*, *via* a dicing saw) - wherein the plane that includes the cross section configuration is substantially perpendicular to the direction of stacking the unit cells, which form the VMJ. Accordingly, incident light can be refracted in the plane that includes the repetitive cross section configurations, and which is substantially perpendicular to the direction of stacking the unit cells (*e.g.*, hence supply a higher absorption for a given depth.) Moreover, various back surface(s) and side surface(s) with reflection coatings can be implemented in conjunction with various aspects of the subject innovation.

[0023] In a related aspect, a grooved surface of the subject innovation further improves carrier collection, while reducing bulk recombination losses. For example, the V-grooves can be positioned perpendicular to the p+nn+ (or n+pp+) unit cells, to increase optical absorption paths of the longer wavelengths in the solar spectrum and enable light absorption being substantially confined within the n-type bulk region of p+nn+ unit cells. Moreover, such V-grooves can have an anti-reflection coating applied to improved incident light absorption in the cell.

[0024] In a related aspect, the subject innovation mitigates bulk recombination losses in a vertical multi junction (VMJ) cell *via* a texturing on its light receiving surface. The textures can be in form of cavity shaped grooves - as "V" shaped cross section configurations, "U" shaped cross configurations, and the like - wherein a plane that includes such cross section configuration is substantially perpendicular to the direction of stacking the unit cells that form the VMJ. In one aspect, a plane that includes substantially repetitive cross sections (*e.g.* cross-sectioning a direction that grooves are extended thereon) is substantially perpendicular to the direction of stacking the unit cells. Such an arrangement facilitates directing the refracted light away from the p+ and n+ diffused doped regions of the VMJ– while at the same time creating desired carriers in a decreasing volume. Accordingly, incident light can be refracted in the plane that includes the cross section configuration, and which is substantially perpendicular to the direction of stacking the unit cells.

[0025] It is to be appreciated that the texturing for the VMJ of the subject innovation is different from prior art for conventional silicon photovoltaic cell textures – both in terms of orientation of PN junctions; and/or interaction with incident light. For example, conventional silicon photovoltaic cells are typically textured to incline the penetration of the light, so that more of the longer wavelengths

are absorbed closer to PN junctions (positioned horizontally) for better current collection of carriers – and hence mitigate poor spectral response to longer wavelengths in the solar spectrum. In contrast, such is not required in the VMJ of the subject innovation that includes vertical junctions, and hence already provides for an enhanced spectral response to the longer wavelengths in the solar spectrum.

[0026] In a particular aspect, an outcome for implementing grooves of the subject innovation (*e.g.*, V grooves) is to mitigate bulk recombination losses by reducing the bulk volume - (as opposed to conventional solar surfaces with texturing, which reduce reflection, or cause reflected or refracted light to become closer to the junctions). In particular, the VMJ cell has demonstrated better carrier current collection for both the short wavelengths and the long wavelengths, wherein the short wavelength response is due to eliminating a highly doped horizontal junction at the top surface, and the long wavelength respond is due to the enhanced collection efficiency of vertical junctions.) As another example, if instead of the cavity shaped grooved texture of the subject innovation, other textures (*e.g.*, random, pyramids, domes, and similar raised configurations) were implemented as part of the VMJ, incident light becomes refracted in all directions, resulting in light absorption in the p+ and n+ diffused regions and hence reduced efficiency.

[0027] According to a related methodology, initially a VMJ can be formed by stacking multiple cell units, wherein each cell itself can include a plurality of parallel semiconductor substrates or layers that are stacked together. Each layer can consist of impurity doped semiconductor material that form a PN junction, and further include a "built –in" electrostatic drift field that enhance minority carrier movement toward such PN junction. Subsequently a plurality of such cell units are integrated to shape a VMJ. Next, on a surface of the VMJ cell that receives light, cavity shaped grooves can be formed (*e.g.*, *via* a dicing saw) - wherein the plane that includes the cross section configuration is substantially perpendicular to the direction of stacking the unit cells, which form the VMJ. Accordingly, incident light can be refracted in the plane that includes the repetitive cross section configurations, and which is substantially perpendicular to the direction of stacking the unit cells (*e.g.*, hence supply a higher absorption for a given depth.) Moreover, various back surface(s) and side surface(s) with reflection coatings can be implemented in conjunction with various aspects of the subject innovation.

[0028] In a related aspect, a grooved surface of the subject innovation further improves carrier collection, while reducing bulk recombination losses. For example, the V-grooves can be positioned perpendicular to the p+nn+ (or n+pp+) unit cells, to increase optical absorption paths of the longer wavelengths in the solar spectrum and enable light absorption being substantially confined within the n-type bulk region of p+nn+ unit cells. Moreover, such V-grooves can have an anti-reflection coating applied to improved incident light absorption in the cell.

[0029] In another aspect, the subject innovation supplies a buffer zone(s) at end layers of a high voltage silicon vertical multi junction (VMJ) photovoltaic cell, to provide a barrier that protects the active layers while providing an ohmic contact. Such buffer zone(s) can be in form of an inactive layer(s) arrangement that is additionally stacked upon and/or below end layers of the VMJ cell. The VMJ cell itself can include a plurality of cell units, wherein each cell unit employs several active layers (e.g., three) to form a PN junction and a "built –in" electrostatic drift field (which enhances minority carrier movement toward the PN junction.)

[0030] As such, various active layers such as nn+ and/or p+n junctions located at either ends of a VMJ cell (and as part of cell units thereof) can be safeguarded against adverse forms of stress and/or strain (e.g., thermal/mechanical compression, torsion, moment, shear and the like - which can be induced in the VMJ during fabrication and/or operation thereof.) Moreover, the buffer zone can be formed *via* materials that have substantially low resistivity ohmic contact, either metals or semiconductors, such that it will not contribute any substantial series resistance loss in the photovoltaic cell at operating conditions. For example, the buffer zone can be formed by employing low resistivity silicon wafers that are p-type doped, so that when using other p-type dopants such as aluminum alloys in manufacturing the VMJ photovoltaic cell, it will mitigate a risk of auto-doping (in contrast to employing n-type wafers that can create unwanted pn junctions – when an object is to create a substantially low resistivity ohmic contact. It is to be appreciated that the subject innovation can be implemented as part of any class of photovoltaic cells such as solar cells or thermophotovoltaic cells. Additionally, aspects of the subject innovation also can be implemented in other class(es) of energy-conversion cells such as betavoltaic cells.

[0031] In related aspects, the buffer zone can be in form of a rim on a surface of an end layer of a cell unit, which acts as a protective boundary for such active layer

and further frames the VMJ cell for ease of handling and transportation. Likewise, by enabling a secure grip to the VMJ cell, such rim formation also eases operation related to the anti reflective coating (e.g., coating can be applied uniformly when the cell is securely maintained during operation, such as by mechanically clamping thereon.) Moreover, the buffer zones (e.g., the inactive layers positioned at ends of the VMJ) can be physically positioned adjacent to other buffer zones during the deposition – and hence any unwanted dielectric coating material that inadvertently penetrates down onto the contact surfaces can be readily removed without damaging active unit cells. The buffer zone can be formed from substantially low resistivity and highly doped silicon (e.g., a thickness of approximately 0.008") Such buffer zone can subsequently contact conductive leads that partition or separate a VMJ cell from another VMJ cell in a photovoltaic cell array.

[0032] According to a further aspect, the buffer zone can be sandwiched between an electrical contact, and the active layers of the VMJ cells. Moreover, such buffer zones can have thermal expansion characteristics that substantially match those of the active layers, hence mitigating performance degradation (e.g., mitigation of stress/strain caused when leads are welded or soldered in manufacturing.) For example, highly doped low resistivity silicon layers can be employed, which match the thermal expansion coefficient (3×10^{-6}/°C) of all active unit cells. Accordingly, substantially strong ohmic contacts can be provided to the active unit cells, which additionally mitigate stress problems caused by welding/ soldering and/or from mismatched thermal expansion coefficients in contact materials. Other examples include introducing metallic layers, such as tungsten (4.5×10^{-6}/°C), or molybdenum (5.3×10^{-6}/°C), which are chosen for thermal expansion coefficients substantially similar to the active silicon (3×10^{-6}/°C) p+nn+ unit cells. The metallization applied to the outer layers of the low resistivity silicon layers of the buffer zone, or to the metallic layers of electrodes that are alloyed to the active unit cells, can be welded or soldered without introducing deleterious stress to the high intensity solar cell or photovoltaic cell– wherein such outer layers serve as ohmic contacts; rather than segments of unit cells in series with the other unit cells.

[0033] Various aspect of the subject innovation can be implemented as part of wafers having miller indices (111) for orientation of associated crystal planes of the buffer zones, which are considered mechanically stronger and slower etching than (100) crystal orientation silicon typically used in making active VMJ unit cells.

Accordingly, low resistivity silicon layers can have a different crystal orientation than that of the active unit cells, wherein by employing such alternative orientation, a device with improved mechanical strength/end contacts is provided. Put differently, edges of (100) orientated unit cells typically etch faster and essentially round off corners of the active unit cells with such crystal orientation – as compared to the inactive (111) orientated end layers - hence resulting in a more stable device structure with higher mechanical strength for welding or otherwise connecting end contacts.

[0034] In a related aspect, the subject innovation employs a vertical multi junction (VMJ) photovoltaic cell, to provide electrolysis for compounds (*e.g.*, water), *via* incident lights and current generation for an electrolysis thereof (*e.g.*, generation of hydrogen and oxygen). Such VMJ includes a plurality of cell units in contact with the electrolyte, wherein each cell unit employs several active layers (*e.g.*, three) to form a PN junction and a "built –in" electrostatic drift field (which enhances minority carrier movement toward the PN junction.) The VMJ can be partially or totally submerged within water/electrolytes, as part of a transparent housing such as glass or plastic, wherein as light encounters such VMJ a plurality of electrolysis electrodes (anodes/cathodes) can be formed through out the VMJ. Current flowing among such electrolysis electrodes flows through the water and decompose the water to hydrogen and oxygen, whenever threshold voltage of electrolysis is reached. Typically, such decomposition threshold voltage lies within a range of 1.18 volts to 1.6 volt to split the water and create hydrogen and oxygen. It is to be appreciated that higher voltages can be reached through the stacked plurality of cell units (*e.g.*, a plurality of cells connected in series). In addition, catalyst additives can further be employed to increase hydrogen and oxygen evolution efficiency, and reduce semiconductor corrosion caused by high electrode potential and the electrolyte solutions. Moreover, the electrolyte can be formed of any solution that does not adversely affect stacked layers that form the VMJ cell (*e.g.*, iridium-based material made of iridium, a binary alloy thereof, or an oxide thereof.)

[0035] In a related aspect, the VMJ is partially or totally submerged in the water/electrolyte, and can include raised metal areas (*e.g.*, VMJ electrodes) that protrude above the silicon of the VMJ cell to increase contact area with the water and electrolyte, and enhance hydrogen production. Such protrusions can be of several millimeters, for example. According to a further aspect, substantially thin layers of electro-catalyst materials, such as platinum, RuO_2, or titanium, can be incorporated in

to the metallization during VMJ cell fabrication to enhance the formation of hydrogen. Moreover, considerable flexibility exists in choosing electro-catalyst material since the n+ negative (-) side of the metallization can be different from that for the p+ positive (+) side. It is to be appreciated that one skilled in the art can readily select catalyst materials that will enhance hydrogen production and are stable and compatible with VMJ cell fabrication. Moreover, ultrasonic units can be employed to free the generated oxygen or hydrogen bubbles that remain attached to electrolysis electrodes. It is to be appreciated the flow of the electrolyte can also remove such formed bubbles.

[0036] According to a related methodology, the electrolyte solution is introduced into a container that contains the VMJ, wherein it is fully or substantially immersed. Such system is then subjected to incident light and a current flow generated from the VMJ. The incident light on the VMJ can generate electric current throughout the electrolyte solution, and any location wherein a threshold for decomposing water is reached or passes (*e.g.*, around 1.6 volts) electrolysis of water occurs. For example, across each unit cell a voltage of 0.6 volts can be generated (*e.g.*, for a 1000 suns) and between regions of a first unit cell and a third unit cell electrolysis can occur. Accordingly, various collection mechanisms (*e.g.*, membranes, sieved plates, and the like) to collect the generated oxygen and hydrogen gas, can be positioned between regions that voltage exceed the threshold for water electrolysis (*e.g.*, around 1.6 volts) and decomposition of water is expected. It is to be appreciated that such collection mechanisms can also be positioned in the downstream flow of the electrolyte to collect generated oxygen and hydrogen gases.

[0036a] According to a further aspect of the present invention, there is provided an electrolysis system comprising: a vertical multi junction (VMJ) photovoltaic cell that includes a plurality of integrally bonded cell units, each cell unit with a plurality of layers that form a PN junction(s); a textured surface of the VMJ photovoltaic cell for receipt of incident light, the textured surface for mitigation of bulk recombination losses for the VMJ photovoltaic cell, the textured surface facilitates confining light refraction of an incident light in a plane that cross sections the textured surface, the plane includes substantially repetitive cross sectional patterns, wherein light absorption is mitigated in p+ and n+ diffused doped regions of the VMJ: an electrolyte that receives a current generated by the VMJ photovoltaic cell, a plurality of anodes and a plurality of cathodes formable by the integrally bonded cell units on a surface of the VMJ, to create the current that decomposes the electrolyte, and a plurality of metal layer protrusions, each protrusion bonded to one of the plurality of anodes and to one of the plurality of cathodes.

[0036b] According to another aspect of the present invention, there is provided a method of electrolyzing an electrolyte comprising: integrally bonding a plurality of active layers to form a VMJ photovoltaic cell; generating a current from the VMJ cell for electrolysis of an electrolyte; forming a plurality of anodes and cathodes that protrude from a surface of the VMJ cell, and forming a plurality of metal layer protrusions, each protrusion bonded to one of the plurality of anodes and to one of the plurality of cathodes.

[0036c] According to still another aspect of the present invention, there is provided an electrolysis system comprising: decomposing means for decomposing an electrolyte *via* incident light comprising a plurality of anodes and cathodes on a surface of the decomposing means and comprising a plurality of metal layer protrusions, each protrusion bonded to one of the plurality of anodes and to one of the plurality of cathodes; and means for mitigating bulk combination losses for the decomposing means, wherein refracted light is substantially confined in a plane that cross sections the means for mitigating bulk combination losses, the plane includes substantially repetitive cross sectional patterns; wherein light absorption is mitigated in p+ and n+ diffused doped regions of the decomposing means.

[0037] To the accomplishment of the foregoing and related ends, certain illustrative aspects are described herein in connection with the following description and the annexed drawings. These aspects are indicative of various ways which can be practiced, all of which are intended to be covered herein. Other advantages and novel features may become apparent from the following detailed description when considered in conjunction with the drawings.

BRIEF DESCRIPTION OF THE DRAWINGS

[0038] Fig. 1 illustrates a schematic perspective of a textured or grooved surface as part of vertical multi junction (VMJ) cell in accordance with an aspect of the subject innovation.

[0039] Fig. 2 illustrates exemplary cross sections for implementing grooves of the subject innovation.

[0040] Fig. 3 illustrates an exemplary stacking of cell units to form a VMJ with a grooved surface according to an aspect of the subject innovation.

[0041] Fig. 4 illustrates a particular unit cell that in part forms a VMJ according to an aspect of the subject innovation.

[0042] Fig. 5 illustrates a related methodology of creating a VMJ with grooved surfaces to mitigate bulk recombination losses according to an aspect of the subject innovation.

[0043] Fig. 6 illustrates a schematic block diagram of an arrangement for buffer zones as part of a vertical multi junction (VMJ) cell in accordance with an aspect of the subject innovation.

[0044] Fig. 7 illustrates a particular aspect of a unit cell, an array of which can from a VMJ cell in accordance with a particular aspect of the subject innovation.

[0045] Fig. 8 illustrates an exemplary cross section for a buffer zone in form of a rim formation on surfaces of unit cells located at either end of a VMJ.

[0046] Fig. 9 illustrates a related methodology of employing buffer zones at end layers of a high voltage silicon vertical multi junction (VMJ) photovoltaic cell, to provide a barrier that protects the active layers thereof.

[0047] Fig. 10 illustrates a schematic cross sectional view for a solar assembly that includes a modular arrangement of photovoltaic (PV) cells, which can implement VMJs with buffer zones.

[0048] Fig. 11 illustrates a schematic block diagram of an electrolysis system that employs a vertical multi junction (VMJ) cell for water electrolysis in accordance with an aspect of the subject innovation.

[0049] Fig. 12 illustrates protrusions of metal layers from a surface of the VMJ that can facilitate the electrolysis process.

[0050] Fig. 13 illustrates a voltage gradient across the VMJ and throughout the stacked cells as part thereof.

[0051] Fig. 14 illustrates a methodology of water electrolysis *via* a VMJ according to an aspect of the subject innovation.

[0052] Fig. 15 illustrates a VMJ cell that can be employed for electrolysis of the subject innovation.

[0053] Fig. 16 illustrates a single cell unit, a plurality of which form the VMJ for electrolysis of the subject innovation.

[0054] Fig. 17 illustrates a VMJ cell with a grooved surface to improve efficiency of the electrolysis process.

[0055] Fig. 18 illustrates exemplary grooving for a surface of a VMJ employed for electrolysis according to an aspect of the subject innovation.

[0056] FIGs. 19A and 19B are diagrams of example configuration of patterned surfaces of PV elements in accordance with aspects disclosed in the subject application. FIG. 19C displays a diagram of example set of precursors and derived PV elements that can be produced through doping in accordance with aspects described herein.

[0057] FIGs. 20A-20C illustrate diagrams of example configurations of patterned dielectric coating of PV elements and an illustrative VMJ stack in accordance with aspects described herein. FIG. 20D illustrates a VMJ PV cell processed to expose a specific crystalline surface.

[0058] FIGs. 21A-21C illustrate diagrams of example configurations of patterned dielectric coating of PV elements and an illustrative VMJ stack in accordance with aspects described herein.

[0059] FIG. 22 illustrates a cross-section diagram of an example configuration of patterned dielectric coating of an active PV element with a reduced diffuse doping layer in accordance with aspects described herein.

[0060] FIGs. 23A and 23B illustrate diagrams of example configurations of patterned dielectric coatings of a PV element in accordance with aspects described herein.

[0061] FIG. 24 presents a perspective illustration of an embodiment of a photovoltaic cell with textured surface in accordance with aspects described herein.

[0062] FIG. 25 is a flowchart of an example method for producing a photovoltaic cell with reduced carrier recombination losses according to aspects disclosed herein.

[0063] FIG. 26 displays a flowchart of an example method for producing VMJ solar cells with reduced carrier recombination losses according to aspects described herein.

[0064] FIG. 27 is a block diagram of an example system that enables fabrication of solar cells in accordance with aspects described herein.

DETAILED DESCRIPTION

[0065] The subject innovation is now described with reference to the drawings, wherein like reference numerals are used to refer to like elements throughout. In the following description, for purposes of explanation, numerous specific details are set forth in order to provide a thorough understanding of the present invention. It may be evident, however, that the present invention may be practiced without these specific details. In other instances, well-known structures and devices are shown in block diagram form in order to facilitate describing the present invention.

[0066] In the subject description, appended claims, or drawings, the term "or" is intended to mean an inclusive "or" rather than an exclusive "or." That is, unless specified otherwise, or clear from context, "X employs A or B" is intended to mean any of the natural inclusive permutations. That is, if X employs A; X employs B; or X employs both A and B, then "X employs A or B" is satisfied under any of the foregoing instances. Moreover, articles "a" and "an" as used in the subject specification and annexed drawings should generally be construed to mean "one or more" unless specified otherwise or clear from context to be directed to a singular form.

[0067] Moreover, with respect to nomenclature of impurity doped materials that are part of the photovoltaic cells described herein, for doping with donor impurities, the terms "n-type" and "N-type" are employed interchangeably, so are the terms "n+-type" and "N+-type." For doping with acceptor impurities, the terms "p-type" and "P-type" are also utilized interchangeably, and so are the terms "p+-type" and "P+-type." For clarity, doping type also appears abbreviated, e.g., n-type is labeled as N, p+-type is indicated as P+, etc. Multi-layer photovoltaic elements or unit cells are labeled as a set of letters, each of which indicates doping type of the layer; for instance, a p-type/n-type junction is labeled PN, whereas a p+-type/n-type/n+-type

junctions is indicated with P+NN+; labeling of other junction combinations also adhere to this notation.

[0068] **Fig. 1** illustrates a schematic perspective of a grooved surface 100 as part of a vertical multi junction (VMJ) cell 120 in accordance with an aspect of the subject innovation. Such an arrangement for texturing 100 enables the refracted light to be directed away from the p+ and n+ diffused doped regions – while at the same time creating desired carriers. Accordingly, incident light can be refracted in the plane 110 having a normal vector *n*. Such plane 110 is parallel to the PN junction planes of the VMJ 120, and can include the cross section configuration of the grooves 100. Moreover, an anti-reflection coating can be applied to the textured 100 surface to increase incident light absorption in the cell. Put differently, the orientation of the plane 110 is substantially perpendicular to the direction of stacking the unit cells 111, 113, 115. It is to be appreciated that other non-perpendicular orientations can also be contemplated (e.g., crystalline planes being exposed at various angles) and all such aspects are to be considered within the realm of the subject innovation.

[0069] **Fig. 2** illustrates exemplary textures for grooving a surface of the VMJ, which receives light thereon. Such grooving can be in form of cavity shaped grooves – for example, as "V" shaped cross section configurations having a variety of angles , (*e.g.*, $0^{o} <$ $< 180^{o}$)"U" shaped cross configurations, and the like - wherein the plane that includes the cross section configuration is substantially perpendicular to the direction of stacking the unit cells that form the VMJ, and/or substantially parallel to the PN junctions of the VMJ. It is to be appreciated that the texturing 210, 220, 230 for the VMJ of the subject innovation is different from prior art for conventional silicon photovoltaic cell textures, in orientation of PN junctions and/or interaction with incident light. For example, conventional silicon photovoltaic cells are typically textured to incline the penetration of the light, so that more of the longer wavelengths are absorbed closer to PN junctions (positioned horizontally) for better current collection of carriers – and hence mitigate poor spectral response to longer wavelengths in the solar spectrum. In contrast, such is not required in the VMJ of the subject innovation that includes vertical junctions, and which already provides an enhanced spectral response to the longer wavelengths in the solar spectrum.

[0070] Rather, one aspect for implementing grooves of the subject innovation (*e.g.*, V grooves) is to mitigate bulk recombination losses by reducing the bulk volume - (as opposed to conventional solar surfaces with texturing, which reduce

reflection, or cause reflected or refracted light to become closer to the junctions). In particular, VMJ cell has demonstrated better carrier current collection for both the short wavelengths and the long wavelengths, wherein the short wavelength response is due to eliminating a highly doped horizontal junction at the top surface and the long wavelength respond is due to the enhanced collection efficiency of vertical junctions.) As another example, if instead of the cavity shaped grooved texture of the subject innovation, other textures (*e.g.*, random, pyramids, domes, and similar raised configurations) were implemented as part of the VMJ, incident light becomes refracted in all directions, resulting in light absorption in the p+ and n+ diffused regions and hence reduced efficiency. It is to be appreciated that such "U" and "V" shaped grooves are exemplary in nature and other configurations are well within the realm of the subject innovation.

[0071] **Fig. 3** illustrates an arrangement of unit cells 311, 313, 317 that can implement grooved texture on a side 345 in accordance with an aspect of the subject innovation. As explained earlier, The VMJ 315 itself is formed from a plurality integrally bonded cell units 311, 313, 317 (1 to k, k being an integer), wherein each cell unit itself is formed from stacked substrates or layers (not shown). For example, each cell unit 311 can include a plurality of parallel semiconductor substrates stacked together, and consisting of impurity doped semiconductor material, which form a PN junction and a "built –in" electrostatic drift field that enhance minority carrier movement toward such PN junction. It is to be appreciated that various N+-type and P-type doping layer formation can be implemented as part of the cell units and such arrangements are well within the realm of the subject innovation.

[0072] Accordingly, the textures on a light receiving surface 345 facilitate refracted light to be directed away from the p+ and n+ diffused doped regions – while at the same time creating desired carriers are created. Hence, incident light can be refracted in the plane that includes the cross section configuration, and which is substantially perpendicular to the direction of stacking the unit cells (*e.g.*, perpendicular to vector *n*.)

[0073] **Fig. 4** illustrates a particular aspect of a unit cell, an array of which can form a VMJ cell having a textured grooving of the subject innovation. The unit cell 400 includes layers 411, 413, 415 stacked together in a substantially parallel arrangement. Such layers 411, 413, 415 can further include impurity doped semiconductor material, wherein layer 413 is of one conductivity type and layer 411

is of an opposing conductivity type - to define a PN junction at intersection 412. Likewise, layer 415 can be of the same conductivity type as layer 413-yet with substantially higher impurity concentration, hence generating a built-in electrostatic drift field that enhances minority carrier movements toward the PN junction 412. Such unit cells can be integrally bonded together to form a VMJ, and surface grooved according to various aspects of the subject innovation.

[0074] According to a further aspect, to fabricate the VMJ from a plurality of cells 400, initially identical PNN+ (or NPP+) junctions can be formed to a depth of approximately 3 to10 μm into flat wafers of high resistivity (*e.g.*, more than 100 ohm-cm) of N type (or P type) silicon -having a thickness of approximately 0.008 inch. Subsequently, such PNN+ wafers are stacked together with a thin layer of aluminum interposed therebetween, wherein each wafer's PNN+ junction and crystal orientation can be oriented in the same direction. Moreover, aluminum-silicon eutectic alloys can be employed, or metals such as molybdenum, or tungsten, which have thermal coefficient(s) that substantially matches the thermal coefficient of silicon. Next, the silicon wafers and aluminum interfaces can be alloyed together, such that the stacked assembly can be bonded together. Buffer zones with substantially low resistivity can also be supplied in form of an inactive layer(s) arrangement that is additionally stacked upon and/or below end layers of the VMJ cell – hence implementing a barrier that protects the active layers against adverse forms of stress and/or strain (*e.g.*, thermal/mechanical compression, torsion, moment, shear and the like - which can be induced in the VMJ during fabrication and/or operation thereof.) The surface of such cell can then be grooved to mitigate bulk recombination losses, as described in detail *supra*. It is to be appreciated that other material, such as germanium and titanium can also be employed. Likewise, aluminum-silicon eutectic alloys can also be employed.

[0075] **Fig. 5** illustrates a related methodology 500 of grooving a surface of a VMJ that receives light. While the exemplary method is illustrated and described herein as a series of blocks representative of various events and/or acts, the subject innovation is not limited by the illustrated ordering of such blocks. For instance, some acts or events may occur in different orders and/or concurrently with other acts or events, apart from the ordering illustrated herein, in accordance with the innovation. In addition, not all illustrated blocks, events or acts, may be required to implement a methodology in accordance with the subject innovation. Moreover, it

will be appreciated that the exemplary method and other methods according to the innovation may be implemented in association with the method illustrated and described herein, as well as in association with other systems and apparatus not illustrated or described.

[0076] Initially, and at 510 multiple cell units with PN junctions are formed as described in detail *supra*. As explained earlier each cell unit itself can include a plurality of parallel semiconductor substrates that are stacked together. Each layer can consist of impurity doped semiconductor material that form a PN junction, and further include a "built –in" electrostatic drift field that enhance minority carrier movement toward such PN junction. Subsequently, and at 520 of plurality of such cell units are integrated to shape a VMJ, wherein buffer zones can also be implemented as a protection for such cells (*e.g.*, stress/strain induced thereon during fabrication.) Next and at 530, on a surface of the VMJ cell that receives light cavity shaped grooves can be formed (*e.g.*, *via* a dicing saw) - wherein the plane that includes the cross section configuration is substantially perpendicular to the direction of stacking the unit cells that form the VMJ. Subsequently, and at 540 incident light can be refracted in the plane that includes the cross section configuration (and/or parallel to the PN junctions), and which is substantially perpendicular to the direction of stacking the unit cells

[0077] **Fig. 6** illustrates a schematic block diagram of an arrangement for buffer zones as part of vertical multi junction (VMJ) cell in accordance with an aspect of the subject innovation. The VMJ 615 itself is formed from a plurality of integrally bonded cell units 611, 617 (1 to n, n being an integer), wherein each cell unit itself is formed from stacked substrates or layers (not shown). For example, each cell unit 611, 617 can include a plurality of parallel semiconductor substrates stacked together, and consisting of impurity doped semiconductor material, which form a PN junction and a "built –in" electrostatic drift field that enhance minority carrier movement toward such PN junction. Accordingly, various active layers such as nn+ and/or p+n junctions, or pp+ and/or pn+ junctions, located at either ends of a VMJ cell 615 (and as part of cell units thereof) can be safeguarded against adverse forms of stress and/or strain (e.g., thermal/mechanical compression, torsion, moment, shear and the like - which can be induced in the VMJ during fabrication and/or operation thereof.)

[0078] Moreover, each of the buffer zones 610 612 can be formed *via* material that have substantially low resistivity ohmic contact (e.g., any range with upper limit

less than approximately 0.5 ohm-cm), while mitigating and/or eliminating unwanted auto doping. For example, the buffer zones 610, 612 can be formed by employing low resistivity wafers that are p-type doped, with other p-type dopants such as aluminum alloys, to mitigate a risk of auto-doping (in contrast to employing n-type wafers that can create unwanted pn junctions – when it is desired to create a substantially low resistivity ohmic contact.)

[0079] **Fig. 7** illustrates a particular aspect of a unit cell, an array of which can form a VMJ cell. The unit cell 700 includes layers 711, 713, 715 stacked together in a substantially parallel arrangement. Such layers 711, 713, 715 can further include impurity doped semiconductor material, wherein layer 713 is of one conductivity type and layer 711 is of an opposing conductivity type - to define a PN junction at intersection 712. Likewise, layer 715 can be of the same conductivity type as layer 713-yet with substantially higher impurity concentration, hence generating a built-in electrostatic drift field that enhances minority carrier movements toward the PN junction 712. Such unit cells can be integrally bonded together to form a VMJ, wherein a buffer zone of the subject innovation can be positioned to safe guard the VMJ and associated unit cells and/or layers that form them.

[0080] According to a further aspect, to fabricate the VMJ from a plurality of cells 700, initially identical PNN+ (or NPP+) junctions can be formed to a depth of approximately 3 to10 μm into flat wafers of high resistivity (e.g., more than 100 ohm-cm) of N type (or P type) silicon - having a thickness of approximately 0.008 inch. Subsequently, such PNN+ wafers are stacked together with a thin layer of aluminum interposed between each wafer, wherein each wafer's PNN+ junction and crystal orientation can be oriented in the same direction. Moreover, aluminum-silicon eutectic alloys can be employed, or metals such as molybdenum or tungsten with thermal coefficient(s) that substantially matches the thermal coefficient of silicon. Next, the silicon wafers and aluminum interfaces can be alloyed together, such that the stacked assembly can be bonded together. Moreover, aluminum-silicon eutectic alloys can also be employed. It is to be appreciated that various N+-type and P-type doping layers can be implemented as part of the cell units and such arrangements are well within the realm of the subject innovation.

[0081] Buffer zones with substantially low resistivity can also be supplied in form of an inactive layer(s) arrangement that is additionally stacked upon and/or

below end layers of the VMJ cell – hence implementing a barrier that protects the active layers against adverse forms of stress and/or strain (e.g., thermal/mechanical compression, torsion, moment, shear and the like - which can be induced in the VMJ during fabrication and/or operation thereof.)

[0082] **Fig. 8** illustrates an exemplary cross section for a buffer zone in form of a rim formation 810 (812) on surfaces of an end layer 831 (841) of unit cells 830 (840), which in part forms the VMJ cell 800. Such rim formations 810, 812 act as a protective boundary for active layers of the cell units, and further partially frame the VMJ cell 800 for ease of handling and transportation (e.g., a low resistivity buffer zone and edge or end contact of the VMJ cell.) Likewise, by enabling a secure grip to the VMJ cell 800, the rim formation also eases operation related to the anti reflective coating (e.g., coating can be applied uniformly when the cell is securely maintained during operation, such as by mechanically clamping thereon.) Moreover, such rim formations can physically be positioned adjacent to other rim formations during the deposition process, wherein any unwanted dielectric coating material that inadvertently penetrates down onto the contact surfaces can be readily removed without damaging the unit cells 830, 840. The rim formation 810 (812) representing the buffer zone can be formed from substantially low resistivity and highly doped silicon (e.g., a thickness of approximately 0.008"), wherein the rim formation can subsequently contact conductive leads that partition a VMJ cell from another VMJ cell in a photovoltaic cell array. Moreover, because of the substantially low resistivity of the buffer zone, the conductive leads are not required to have full electrical contact to the buffer zone. As such, they can be partial contacts, such as a point contact, or a series of point contacts, while nevertheless providing good electrical contact. It is to be appreciated that Fig. 8 is exemplary in nature, and other variations - such as the buffer zone 810 formed in manufacturing reaching the surfaces of 800 with 810 bonding to active layers 841 – are well within the realm of the subject innovation. For example, the shape of 810 can represent a partial lead contact to the metalized layer on the buffer zone as discussed earlier.

[0083] The conductive leads can be in form of electrode layers, which are formed by depositing a first conductive material on a substrate – and can comprise; tungsten, silver, copper, titanium, chromium, cobalt, tantalum, germanium, gold, aluminum, magnesium, manganese, indium, iron, nickel, palladium, platinum, zinc, alloys thereof, indium-tin oxide, other conductive and semiconducting metal oxides,

nitrides and silicides, polysilicon, doped amorphous silicon, and various metal composition alloys. In addition, other doped or undoped conducting or semi-conducting polymers, oligomers or monomers, such as PEDOT/PSS, polyaniline, polythiothene, polypyrrole, their derivatives, and the like can be employed for electrodes. Furthermore, since some metals can have a layer of oxide formed thereupon that can adversely affect the performance of the VMJ cell, non-metal material such as amorphous carbon can also be employed for electrode formation. It is to be appreciated that the rim formation of Fig. 8 is exemplary in nature and other configurations for the buffer zone such as, rectangular, circular, cross sections having a range of surface contact with the active layers are well within the realm of the subject innovation.

[0084] Moreover, various aspect of the subject innovation can be implemented as part of wafers having miller indices (111) for orientation of associated crystal planes of the buffer zones, which are considered mechanically stronger and slower etching than (100) crystal orientation silicon typically used in fabricating active VMJ unit cells. Accordingly, low resistivity silicon layers can have a different crystal orientation than that of the active unit cells, wherein by employing such alternative orientation, a device with improved mechanical strength/end contacts is provided. Put differently, edges of (100) orientated unit cells typically etch faster to essentially round off corners of the active unit cells with such crystal orientation – as compared to the inactive (111) orientated end layers, hence resulting in a more stable device structure with higher mechanical strength for welding or otherwise connecting end contacts.

[0085] **Fig. 9** illustrates a related methodology 900 of employing buffer zones at end layers of a high voltage silicon vertical multi junction (VMJ) photovoltaic cell, to provide a barrier that protects the active layers thereof. While the exemplary method is illustrated and described herein as a series of blocks representative of various events and/or acts, the subject innovation is not limited by the illustrated ordering of such blocks. For instance, some acts or events may occur in different orders and/or concurrently with other acts or events, apart from the ordering illustrated herein, in accordance with the innovation. In addition, not all illustrated blocks, events or acts, may be required to implement a methodology in accordance with the subject innovation. Moreover, it will be appreciated that the exemplary method and other methods according to the innovation may be implemented in

association with the method illustrated and described herein, as well as in association with other systems and apparatus not illustrated or described. Initially, and at 910 multiple cell units with PN junctions are formed as described in detail *supra*. As explained earlier each cell unit itself can include a plurality of parallel semiconductor substrates that are stacked together. Each layer can consist of impurity doped semiconductor material that form a PN junction, and further include a "built –in" electrostatic drift field that enhance minority carrier movement toward such PN junction. Subsequently and at 920, a plurality of such cell units are integrated to shape a VMJ. Next and at 930 a buffer zone can be implemented that contacts end layers of the VMJ, to provide a barrier that protects the active layers thereof. Such buffer zone(s) can be in form of an inactive layer(s) arrangement that is additionally stacked upon and/or below end layers of the VMJ cell. The VMJ can then be implemented as part of a photovoltaic cell at 940.

[0086] **Fig. 10** illustrates a schematic cross sectional view 1000 for a solar assembly that includes a modular arrangement 1020 of photovoltaic (PV) cells 1023, 1025, 1027 (1 through k, where k is an integer). Each PV cell can employ a plurality of VMJs with buffer zones according to an aspect of the subject innovation. Typically, each of the PV cells (also referred to as photovoltaic cells) 1023, 1025, 1027 can convert light (*e.g.*, sunlight) into electrical energy. The modular arrangement 1020 of the PV cells can include standardized units or segment that facilitate construction and provide for a flexible arrangement.

[0087] In one exemplary aspect, each of the photovoltaic cells 1023, 1025, 1027 can be a dye-sensitized solar cell (DSC) that includes a plurality of glass substrates (not shown), wherein deposited thereon are transparent conducting coating, such as a layer of fluorine-doped tin oxide, for example. Such DSC can further include a semiconductor layer such as TiO_2 particles, a sensitizing dye layer, an electrolyte and a catalyst layer such as Pt- (not shown)- which can be sandwiched between the glass substrates. A semiconductor layer can further be deposited on the coating of the glass substrate, and the dye layer can be sorbed on the semiconductor layer as a monolayer, for example. Hence, an electrode and a counter electrode can be formed with a redox mediator to control of electron flows therebetween.

[0088] Accordingly, the cells 1023, 1025, 1027 experience cycles of excitation, oxidation, and reduction, which produce a flow of electrons, *e.g.*, electrical energy. For example, incident light 1005 excites dye molecules in the dye layer,

wherein the photo excited dye molecules subsequently inject electrons into the conduction band of the semiconductor layer. Such can cause oxidation of the dye molecules, wherein the injected electrons can flow through the semiconductor layer to form an electrical current. Thereafter, the electrons reduce electrolyte at catalyst layer, and reverse the oxidized dye molecules to a neutral state. Such cycle of excitation, oxidation, and reduction can be continuously repeated to provide electrical energy.

[0089] **Fig. 11** illustrates a schematic block diagram of an electrolysis system that employs a vertical multi junction (VMJ) cell 1110 for electrolysis in accordance with an aspect of the subject innovation. The VMJ 1110 can be partially or totally submerged within water/electrolytes, as part of a transparent housing such as quartz, glass or plastic 1130. As incident light 1135 encounters a surface 1137 of such VMJ 1110 a plurality of electrolysis electrodes in form of anodes and/or cathodes can be formed throughout the VMJ, and/or on a surface 1137 thereon. Current flowing among such electrolysis electrodes that are formed on the surface 1137, then flows through the water and decompose the water to hydrogen and oxygen - whenever threshold voltage of electrolysis is reached. The VMJ 1110 includes a plurality of integrally bonded cell units 1111, 1117 (1 to n, where n is an integer), wherein each cell unit itself is formed from stacked substrates or layers (not shown). For example, each cell unit 1111, 1117 can include a plurality of parallel semiconductor substrates stacked together, and consisting of impurity doped semiconductor material, which form a PN junction and a "built –in" electrostatic drift field that enhance minority carrier movement toward such PN junction. When incident light 1135 is directed to the surface 1137, in various regions of the VMJ 1110, then a plurality of cathodes and anodes can be formed that subsequently function as electrodes for the electrolysis operation.

[0090] Current flowing among such electrolysis electrodes flows through the electrolyte and decompose the water to hydrogen and oxygen, whenever threshold voltage of electrolysis is reached. Typically, such decomposition threshold voltage lies within a range of 1.18 volts to 1.6 volt to split the water and create hydrogen and oxygen. It is to be appreciated that higher voltages can be reached through the stacked plurality of cell units (*e.g.*, a plurality of cells connected in series). In addition, catalyst material can further be employed to increase hydrogen and oxygen evolution efficiency and reducing semiconductor corrosion caused by high electrode

potential and electrolyte solutions. Moreover, the electrolyte can be formed of any solution that does not adversely affect stacked layers that form the VMJ cell (*e.g.*, iridium-based catalyst made of iridium, a binary alloy thereof, or an oxide thereof.) In related aspects, ultrasonic transducers can operatively interact with the electrolysis system to free oxygen or hydrogen bubbles, which remain attached to the electrolysis electrodes.

[0091] The VMJ 1110 can further be positioned on a heat regulating assembly 1119, which removes generated heat from hot spot areas to maintain temperature gradient for the VMJ cell within predetermined levels. Such heat regulating assembly 1119 can be in form of a heat sink arrangement, which includes a plurality of heat sinks to be surface mounted to a back side of the VMJ, wherein each heat sink can further include a plurality of fins (not shown) extending substantially perpendicular the back side. The fins can expand a surface area of the heat sink to increase contact with cooling medium (*e.g.*, electrolyte, cooling fluid such as water), which can be further employed to dissipate heat from the fins and/or photovoltaic cells. As such, heat from the VMJ can be conducted through the heat sink and into surrounding electrolyte, and/or substance that does not affect electrolysis operation. Moreover, heat from the VMJ cell can be conducted through thermal conducting paths (*e.g.*, metal layers), to the heat sinks to mitigate direct physical or thermal conduct of the heat sinks to the VMJ cells, and provide a scalable solution for proper operation of the electrolysis.

[0092] In a related aspect, the heat sinks can be positioned in a variety of planar or three dimensional arrangements as to monitor, regulate and over all manage heat flow away from the VMJ cell. Moreover, each heat sink can further employ thermo/electrical structures (not shown) that can have a shape of a spiral, twister, corkscrew, maze, or other structural shapes with a denser pattern distribution of lines in one portion and a relatively less dense pattern distribution of lines in other portions. For example, one portion of such structures can be formed of a material that provides relatively high isotropic conductivity and another portion can be formed of a material that provides high thermal conductivity in another direction. Accordingly, each thermo/electrical structure of the heat regulating assembly provides for a heat conducting path that can dissipate heat from the hot spots and into the various heat conducting layers, or associated heat sinks, of the heat regulating device, and hence facilitate the electrolysis operation. It is to be appreciated that the heat sinks can be

cooled *via* an independent cooling medium that is separate from the electrolyte medium.

[0093] **Fig. 12** illustrates a further aspect of the subject innovation that includes protrusions 1211, 1215 of metal layers that are associated with electrodes of a single unit cell 1201. Such protrusions 1211, 1215 protrude (*e.g.*, several millimeters) from a surface 1241 of the VMJ 1200 to facilitate the electrolysis process, *via* increasing a contact surface area. In addition, substantially thin layers of electro-catalyst materials, such as platinum, RuO_2, or titanium, can be incorporated in to the metallization during VMJ cell fabrication to enhance hydrogen production. Moreover, considerable flexibility exists in choosing electro-catalyst material since the n negative (-) side 1211 of the metallization can be different from that for the p+ positive (+) side 1215. It is to be appreciated that one skilled in the art can readily select catalyst materials that will enhance hydrogen production and are stable and compatible with VMJ cell fabrication. As incident light 1235 reaches the surface 1241 of the VMJ, a plurality of cathodes/anodes can be formed thereon. For example, in regions on the VMJ at the negatively charged cathode, a **reduction** reaction takes place, with electrons (e^-) from the cathode being given to hydrogen captions to form hydrogen gas (the half reaction balanced with acid):

Cathode (reduction): $2\mathbf{H}^+(aq) + 2e^- \rightarrow \mathbf{H}_2(g)$
electrons (e^-) from the cathode being given to hydrogen captions to form hydrogen gas (the half reaction balanced with acid).

[0094] At the positively charged anode, an **oxidation** reaction occurs, generating oxygen gas and giving electrons to the cathode to complete the circuit:

Anode (oxidation): $2\mathbf{H_2O}(l) \rightarrow \mathbf{O}_2(g) + 4\mathbf{H}^+(aq) + 4e^-$

[0095] The same half reactions can also be balanced with base as listed below. In general, not all half reactions should be balanced with acid or base. In general, to add half reactions they typically should both be balanced with either acid or base.

Cathode (reduction): $2\mathbf{H_2O}(l) + 2e^- \rightarrow \mathbf{H}_2(g) + 2\mathbf{OH}^-(aq)$
Anode (oxidation): $4\mathbf{OH}^-(aq) \rightarrow \mathbf{O}_2(g) + 2\mathbf{H_2O}(l) + 4e^-$

Combining either half reaction pair yields the same overall decomposition of water into oxygen and hydrogen:

Overall reaction: $2\mathbf{H_2O}(l) \rightarrow 2\mathbf{H}_2(g) + \mathbf{O}_2(g)$

[0096] As indicated above, the number of hydrogen molecules produced is thus twice the number of oxygen molecules. Assuming equal temperature and pressure for both gases, the produced hydrogen gas has therefore twice the volume of the produced oxygen gas. The number of electrons pushed through the water is twice the number of generated hydrogen molecules and four times the number of generated oxygen molecules. As explained earlier, if a water-soluble **electrolyte** is added, the conductivity of the water rises considerably. Accordingly, the electrolyte disassociates into captions and anions; wherein the anions rush towards the anode and neutralize the buildup of positively charged H^+ therein; similarly, the captions rush towards the cathode and neutralize the buildup of negatively charged OH therein. Such allows the continued flow of electricity. It is to be appreciated that the choice of electrolyte should be considered in conjunction with the material employed for the VMJ cell, as not to adversely affect its material and operation. Additional factors in choosing an electrolyte pertain to the fact that an anion from the electrolyte is in competition with the hydroxide ions to give up an electron. An electrolyte anion with less standard electrode potential than hydroxide will likely be oxidized instead of the hydroxide, and hence no oxygen gas will be produced. Likewise, a cation with a greater standard electrode potential than a hydrogen ion will be reduced, and no hydrogen gas will be produced. To mitigate such circumstances, the following captions have lower electrode potential than H^+ and are therefore suitable for use as electrolyte captions: Li^+, Rb^+, K^+, Cs^+, Ba^{2+}, Sr^{2+}, Ca^{2+}, Na^+, and Mg^{2+}. Sodium and lithium can also be used, if so does not adversely affect the VMJ cell - as they form inexpensive, soluble salts.

[0097] **Fig. 13** illustrates a voltage-distance graph for various points on the VMJ 1310, wherein the unit cells 1311, 1317 intersect or share a common boundary. As illustrated, the VMJ 1310 includes a plurality of unit cells 1311, 1317 that are serially connected, wherein the voltage can increase as a linear function of number of cells that are stacked together (*e.g.*, from left to right on the horizontal axis). As illustrated in Fig. 13, voltage difference between both ends of $cell_1$ is 0.6 volts, and by stacking $cell_2$ thereon, such voltage difference in the combined cells is increased to 1.2 volts. Likewise, by stacking $cell_3$ thereon, the voltage difference can be increased to 1.8 volts. As such, electrolysis can occur between any two points on a surface of the VMJ that exceeds the threshold value for decomposing the water. For example, for an open circuit voltage of a 40 junction VMJ cell at 1000 suns 32 volts can be

generated (*e.g.*, 0.8 volts per unit cell.) Assuming electrolysis in initiated at 1.6 volts only two unit cells are sufficient to provide the voltage. In another aspect, as the current loading increases, the voltage determined by the VMJ cell IV characteristics at maximum power at 1000 suns drops to 24 volts, or 0.6 volts per unit cell. As such, three unit cells can be required, which contribute to 1.8 volts for powering the electrolysis reaction. (Typically an over voltage may also be required for electrolysis at higher current densities.)

[0098] It is further to be appreciated that although the electrolysis is described in context of a single VMJ, the subject innovation is not so limited and can be implemented as part of a plurality of VMJ cells (*e.g.*, in parallel and/or series, or operatively separate from each other). By determining current relationships formed among various regions of the VMJ that demonstrate different voltages, one can tailor a VMJ cell design to provide additional contacting area for handling higher currents where needed. For example, the contacting current densities can be reduced by increasing metallization thickness at various points, if so is required. Moreover, various forms of pressurization can be employed to improve electrolysis efficiency and/or collection (*e.g.*, sieving mechanisms, filtering mechanisms, and the like) for products of decompositions (*e.g.*, hydrogen, oxygen). It is to be appreciated that the subject innovation is not limited to electrolysis of water and electrolysis of other compounds that can suitably interact with the VMJ are well within the realm of the subject innovation.

[0099] **Fig. 14** illustrates a related methodology 1400 of water electrolysis *via* a VMJ according to an aspect of the subject innovation. While the exemplary method is illustrated and described herein as a series of blocks representative of various events and/or acts, the subject innovation is not limited by the illustrated ordering of such blocks. For instance, some acts or events may occur in different orders and/or concurrently with other acts or events, apart from the ordering illustrated herein, in accordance with the innovation. In addition, not all illustrated blocks, events or acts, may be required to implement a methodology in accordance with the subject innovation. Moreover, it will be appreciated that the exemplary method and other methods according to the innovation may be implemented in association with the method illustrated and described herein, as well as in association with other systems and apparatus not illustrated or described. Initially and at 1410, the electrolyte solution is introduced into a container that contains the VMJ, wherein it is fully or

substantially immersed. Such system is then subjected to incident light at 1420, and a current flow generated from the VMJ. The incident light can generate water electrolysis throughout the electrolyte solution at 1430, and any location wherein a threshold for decomposing water is reached or passes (*e.g.*, around 1.2 volts) electrolysis occurs. For example, across each unit cell a voltage of 0.6 volts can be generated (*e.g.*, for a 1000 suns) and between regions of a first unit cell and a third unit cell electrolysis can occur. Accordingly, various collection mechanisms (*e.g.*, membranes, sieved plates, and the like) can be positioned between regions that voltage exceed the threshold for electrolysis (*e.g.*, around 1.6), and hence collect the generated hydrogen gas at 1440. It is to be appreciated that other collections mechanisms such as collection down stream can also be employed.

[00100] **Fig. 15** illustrates a VMJ cell that can be employed for electrolysis in accordance with an aspect of the subject innovation. The VMJ 1515 itself is formed from a plurality of integrally bonded cell units 1511, 1517 (1 to n, n being an integer), wherein each cell unit itself is formed from stacked substrates or layers (not shown). For example, each cell unit 1511, 1517 can include a plurality of parallel semiconductor substrates stacked together, and consisting of impurity doped semiconductor material, which form a PN junction and a "built –in" electrostatic drift field that enhance minority carrier movement toward such PN junction. Moreover, by implementing a buffer zone(s) 1510, 1512 various active layers such as nn+ and/or p+n junctions located at either ends of a VMJ cell 1515 (and as part of cell units thereof) can be safeguarded against adverse forms of stress and/or strain (*e.g.*, thermal/mechanical compression, torsion, moment, shear and the like - which can be induced in the VMJ during fabrication and/or operation thereof.) Each of such buffer zones 1510 1512 can be formed *via* material that have substantially low resistivity ohmic contact (*e.g.*, any range with upper limit less than approximately 0.5 ohm-cm), while mitigating and/or eliminating unwanted auto doping. For example, the buffer zones 1510, 1512 can be formed by employing low resistivity wafers that are p-type doped, with other p-type dopants such as aluminum alloys, to mitigate a risk of auto-doping (in contrast to employing n-type wafers that can create unwanted pn junctions – when it is desired to create a substantially low resistivity ohmic contact.) Catalytic materials (*e.g.*, platinum, titanium, and the like) can also be employed at end contacts of the VMJ, to facilitate the electrolysis operation, for example.)

[00101] **Fig. 16** illustrates a particular aspect of a unit cell 1600, an array of which can form a VMJ cell for the electrolysis of the subject innovation. The unit cell 1600 includes layers 1611, 1613, 1615 stacked together in a substantially parallel arrangement. Such layers 1611, 1613, 1615 can further include impurity doped semiconductor material, wherein layer 1613 is of one conductivity type and layer 1611 is of an opposing conductivity type - to define a PN junction at intersection 1612. Likewise, layer 1615 can be of the same conductivity type as layer 1613-yet with substantially higher impurity concentration, hence generating a built-in electrostatic drift field that enhances minority carrier movements toward the PN junction 1612. Such unit cells can be integrally bonded together to form a VMJ (*e.g.*, using catalytic material for such bondage to enhance electrolysis), which performs electrolysis as described in detail *supra*.

[00102] According to a further aspect, to fabricate the VMJ from a plurality of cells 1600, initially identical PNN+ (or NPP+) junctions can be formed to a depth of approximately 3 to10 *μm* inch into flat wafers of high resistivity (*e.g.*, more than 100 ohm-cm) of N type (or P type) silicon -having a thickness of approximately 0.008 inch. Subsequently, such PNN+ wafers are stacked together with a thin layer of aluminum interposed between each wafer, wherein each wafer's PNN+ junction and crystal orientation can be oriented in the same direction. Moreover, aluminum-silicon eutectic alloys can be employed, or metals such as germanium and titanium, or metals such as molybdenum or tungsten that have thermal coefficient(s) that substantially matches the thermal coefficient of silicon can also be employed. Next, the silicon wafers and aluminum alloy interfaces can be alloyed together, such that the stacked assembly can be bonded together (*e.g.*, further including catalytic material.) It is to be appreciated that other material, such as germanium and titanium can also be employed. Likewise, aluminum-silicon eutectic alloys can also be employed. It is further to be appreciated that the electrolyte should be chosen such that it does not adversely affect the operation of the VMJ, and/or result in chemical reactions harmful to the VMJ. It is to be appreciated that various N+-type and P-type doping layer formation can be implemented as part of the cell units and such arrangements are well within the realm of the subject innovation.

[00103] **Fig. 17** illustrates a further aspect of the subject innovation that includes a VMJ employed for electrolysis with a textured surface. A schematic

perspective of a grooved surface 1700 is depicted as part of a vertical multi junction (VMJ) cell 1720 in accordance with an aspect of the subject innovation. Such an arrangement for texturing 1700 enables the refracted light to be directed away from the p+ and n+ diffused doped regions – while at the same time creating desired carriers. Accordingly, incident light can be refracted in the plane 1710 having a normal vector *n*. Such plane 1710 is parallel to the PN junction planes of the VMJ 1720, and can include the cross section configuration of the grooves 1700. Put differently, the orientation of the plane 1710 is substantially perpendicular to the direction of stacking the unit cells 1711, 1713, 1715. Such grooved surface can increase efficiency of the electrolysis process.

[00104] **Fig. 18** illustrates exemplary textures for grooving a surface of the VMJ, which receives light thereon for electrolysis of an electrolyte. Such grooving can be in form of cavity shaped grooves – for example, as "V" shaped cross section configurations having a variety of angles θ, (*e.g.*, $0^\circ < \theta < 180^\circ$)"U" shaped cross configurations, and the like - wherein the plane that includes the cross section configuration is substantially perpendicular to the direction of stacking the unit cells that form the VMJ, and/or substantially parallel to the PN junctions of the VMJ. It is to be appreciated that the texturing 1810, 1820, 1830 for the VMJ of the subject innovation is different from prior art for conventional silicon photovoltaic cell textures, in orientation of PN junctions and/or interaction with incident light. For example, conventional silicon photovoltaic cells are typically textured to incline the penetration of the light, so that more of the longer wavelengths are absorbed closer to PN junctions (positioned horizontally) for better current collection of carriers – and hence mitigate poor spectral response to longer wavelengths in the solar spectrum. In contrast, such is not required in the VMJ of the subject innovation that includes vertical junctions, and which already provides an enhanced spectral response to the longer wavelengths in the solar spectrum.

[00105] Rather, one aspect for implementing grooves of Fig. 7(*e.g.*, V grooves) is to mitigate bulk recombination losses by reducing the bulk volume - (as opposed to conventional solar surfaces with texturing, which reduce reflection, or cause reflected or refracted light to become closer to the junctions). In particular, VMJ cell has demonstrated better carrier current collection for both the short wavelengths and the long wavelengths, wherein the short wavelength response is due to eliminating a highly doped horizontal junction at the top surface and the long wavelength respond is

due to the enhanced collection efficiency of vertical junctions.) As another example, if instead of the cavity shaped grooved texture of the subject innovation, other textures (*e.g.*, random, pyramids, domes, and similar raised configurations) were implemented as part of the VMJ, incident light becomes refracted in all directions, resulting in light absorption in the p+ and n+ diffused regions and hence reduced efficiency. Moreover, reflection coatings can be applied to the back side of the VMJ cell to further enhance light absorption.

[00106] In another aspect, the subject innovation relates to improving performance of photovoltaic cells, e.g., solar cells, particularly high-intensity solar cells such as edge-illuminated or vertical junction structures that can produce a substantially high power output under high intensity radiation levels. Various designs of PV elements that form unit cells employed to fabricate VMJ photovoltaic cells are set forth herein unit to reduce recombination losses of photogenerated carriers via patterned contacts.

[00107] The VMJ cell has an inherent theoretical limit efficiency exceeding 30% at 1000 suns intensity so further performance improvements are possible using experimental understanding and insight from computer simulations and modeling analysis. Although conventional one-sun solar cells are easily modeled with good results using analytical equations, such is not the case for edge-illuminated VMJ cells at operating at high intensities, because at high intensities, even second order effects can have substantial effect(s) on the cell operating efficiency. While aspects or features of the subject innovation are illustrated with solar cells, such aspects or features and associated advantages, such as reduction of recombination losses of photogenerated carriers, can be exploited in other photovoltaic cells, e.g., thermophotovoltaic cells, or cells excited with laser source(s) of photons. Moreover, aspects of the subject innovation also can be implemented in other classes of energy-conversion cells such as betavoltaic cells.

[00108] The physics of electron-hole carrier pairs produced in solar cells at high intensities is rather complex as many physical parameters come into play, including, but not limited to: surface recombination velocities, carriers mobility and concentrations, emitters (e.g., diffusions) reverse saturation currents, minority carrier lifetimes, band gap narrowing, built-in electrostatic fields, and various recombination mechanisms. Mobility decreases rapidly with increasing carrier density and Auger recombination increases rapidly with intensity as the cube of the carrier density. To

incorporate such aspects into modeling of VMJ solar cell performance, computer simulations (e.g., two-dimensional numerical computational analysis of photogenerated carrier transport in a semiconductor) can provide insight into physical parameters in vertical junction unit cells, or PV elements, operating or for operation at high intensities. Such simulations provide an analysis and design instrument to understand possible sources of performance efficiencies and to increase performance of VMJ cells at high intensities. It should be appreciated that while even though conventional one-sun solar cells are easily modeled with good results using simple analytical equations, such is not the case for edge-illuminated VMJ photovoltaic cells operating at high illumination intensities, because at high intensities, even second order effects can have a dramatic effect of the cell operating efficiency

[00109] Computational simulations based upon models of contact-to-contact VMJ unit cells that incorporate an array of semiconductor physics reveal specific regions in VMJ unit cells where recombination losses of photogenerated carriers occur at high intensities. At least some of such regions present complex loss mechanisms that are intensity dependent. Computer simulation(s) reveal regions in PV elements, or VMJ unit cells, that can be improved upon in order to reduce recombination losses and improve performance of VMJ cells. Aspects of the subject innovation provide such improvements.

[00110] Series resistance has been considered a significant source of design issues for conventional concentrator solar cells. The VMJ photovoltaic cell design proved more than adequate in this regard, showing series resistance is not a problem even at 2500 suns intensity. However, in some situations, it can be advantageous to tradeoff an increase in series resistance for less design simplicity, in order to improve efficiency of VMJ photovoltaic cells for photovoltaic concentrators operating near 1000 suns.

[00111] It should be appreciated that design for operation at substantially higher intensities, such as 2500 suns where VMJ cells are still capable of operating efficiently, can require substantially more demanding and expensive concentrator system engineering in optics, structures, sun tracking, and thermal control, while not likely contributing any better overall performance or economic benefits. Therefore, aspects or features of solar cells, and associated process(es) for production thereof, set forth in the subject innovation can increase efficiency performance of high-intensity VMJ cells operating in the range of 1000 suns or higher. Efficiency increase can

make VMJ solar cells or other solar cells that exploit aspects of the subject innovation more cost effective and viable, even though it can involve additional manufacturing and a potential increase in series resistance for intensities greater than 1000 suns. Aspects or features described herein can provide adequate engineering tradeoffs to make photovoltaic concentrator systems using solar cells, VMJ cells or otherwise, that exploit aspects of the subject innovation more viable and cost effective in providing lower $/watt performance.

[00112] Computer modeling analysis of conventional VMJ unit cell design, e.g., P+NN+ slab with deep junctions, using realistic parameters for good silicon processing (minority-carrier lifetimes, surface recombination velocity, etc.) at intensities greater than 500 suns, showed the following percentage recombination losses for some specific regions:

- P+ diffusion 22.7 %
- P+ contact 5.3 %
- N+ diffusion 32.8 %
- N+ contact 11.4 %

Therefore, this analysis suggests the heavily doped P+ and N+ diffused emitter regions with their metal contacts account for over half of all recombination losses in unit cells that form the VMJ solar cell, and that an optimized diffused N+ emitter may be different in design from an optimum diffused P+ emitter, due in part to differences in mobility. Relative magnitude of recombination losses originated in N+ and P+ regions can be switched for N+PP+ unit cell(s), or P+NN+ unit cell(s) with shallow P+N junction(s). In an aspect, the subject innovation is directed to reducing recombination losses in the foregoing diffusion regions in order to improve the performance of VMJ cells.

[00113] High minority-carrier lifetimes and low surface recombination velocities were successfully achieved in conventional VMJ cell development with open-circuit voltage $V_{oc} = 0.8$ volts per unit cell junction at high intensities. V_{oc} is determined by sunlight-generated currents and diffused emitter reverse saturation currents (J_o), with both the P+N and NN+ junctions present in the unit cell(s) of a VMJ solar cell contributing to the open-circuit voltage. The optimum junctions from an electrical point of view are the lowest J_o; using $J_o = 1x10^{-13}$ Acm^{-2}, which is representative of high-quality low reverse saturation currents in diffused junctions, the

analysis showed diffusion depths of approximately 3 to10 μm are sufficient depths for both the P+ and N+ diffusions, even when considering infinite recombination velocities at the ohmic metal contacts.

[00114] It is to be noted that even though deep and gradual NN+ diffusion profiles will provide a built-in electrostatic drift field that will enhance the minority carrier movement towards the junction barrier for ultimate collection and reduce recombination in this region, computer simulations reveal NN+ junction enhancement becomes less effective at high intensities, which can result in higher recombination in N+ region as shown above.

[00115] Experiments and computational modeling and simulation have identified that prime areas for improving performance are in reducing recombination losses in the heavily doped P+ and N+ diffused and metal contacts regions for VMJ unit cells operating at high intensities. Since a high-quality oxide passivated surface can have a recombination velocity as low as a few cm/second, which is significantly less than that at the metal contacts, and considering that the drift fields created by diffusion profiles become less effective at high intensities, aspects of the subject innovation provide reduced metal contact area and diffusion area via patterned dielectric coating of PV elements, or VMJ unit cells, to improve performance of VMJ solar cells.

[00116] With respect to the drawings, **FIG. 19A** illustrates a diagram 1900 of a photovoltaic element 1910 with a patterned dielectric coating 1920 between one of the surfaces of the PV element and a metal contact 1925. Note that surfaces of PV element 1910, dielectric coating 1920, and metal contact 1925 are illustrated as not in contact for clarity. However, in solar cell(s) discussed herein, such surfaces are in contact. Pattern dielectric coating 1920 is illustrated as disconnected elliptical regions assembled in a periodic array or lattice. The PV element 1910 is typically a slab of N-type semiconductor material, wherein the semiconductor material is one of Si; Ge; GaAs, InAs, or other III-V semiconducting compounds; II-VI semiconducting compounds; CuGaSe; CuInSe; CuInGaSe. The slab can include a doped P+ diffuse region 1916 (labeled as P+) on a first surface of the slab and a doped N+ diffuse region 1914 (labeled as N+) on a second surface substantially parallel to the first surface. Thickness of the active PV element 1910 affords an N-type (N) layer 1912 among the diffused doped layers 1914 and 1916. Thickness of diffusion layers 1914

and 1916 can range from 3-10 μm, and are determined by doping process employed to introduce carriers into a slab of N-type material (e.g., slab 1912). Inclusion of diffuse doped layers can be accomplished with substantially any doping means, e.g., techniques and dopant materials, typically employed in semiconductor processing. Dopant materials can include phosphorous and boron, for N+ and P+ doping, respectively. For purposes of explanation, interfaces between diffuse layers N+ 1914 and P+ 1916 and N-type (N) layer 1912 are idealized as sharp abrupt boundaries; however, such interfaces can be irregular, with areas of intermixing between neutral and doped materials. The degree of intermixing dictated, at least in part, by the mechanisms or means employed to generate the doped diffuse regions.

[00117] While aspects or features of the subject innovation are illustrated for an initially N-type slab of semiconductor material as precursor of PV element 1910, such aspects or features can also be implemented or accomplished in an initially intrinsic, e.g., nominally undoped, precursor of PV element 1910. Moreover, in alternative or additional scenarios, P-type precursor(s) can be employed: PV element 1910 can be a slab of P-type doped semiconductor material that can include P+ diffuse layer 1916 on a first surface, and its vicinity, of the slab and N+-doping diffuse layer 1914 a second surface, and its vicinity, substantially parallel to the first surface, as described supra.

[00118] In an aspect of the subject innovation, patterned dielectric coating 1920 reduces formation of metal-diffuse doping layer interface (e.g., metal and N+ layer 1914 interface) upon metallization of active PV element 1910—openings in a patterned dielectric coating are the regions where the metal and diffuse doping layer form an interface. Since such interfaces have high recombination losses, the reduction of the metal-diffuse doping layer contact thus mitigates nonradiative losses of photogenerated carriers (e.g., electrons and holes), with ensuing increase in photovoltaic efficiency of PV element 1910. In addition, coating a PV element, e.g., 1910, with dielectric material produces passivation of surface states and thus reduces surface recombination losses. Patterning of dielectric coating can be accomplished through photolithographic techniques, or substantially any other technique that allows controlled patterning of a dielectric surface; for instance, wet etching. Such photolithographic techniques generally afford pattern formation through multiple processing steps of masking and removal of the dielectric material in the dielectric

coating. Alternatively or additionally, patterning of dielectric coating can be accomplished through deposition techniques, e.g., vapor coating like chemical vapor deposition (CVD) and its variations, plasma etched CVD (PECVD); molecular beam epitaxy (MBE), etc., in the presence of a mask that shadows deposited material in order to dictate a specific pattern.

[00119] It should be appreciated that dielectric coating layer 1920 can adopt various planar geometries and configurations that provide electrical contact among N+-doping diffuse layer 1914 and metal contact 1925. As indicated supra, in example diagram 1920, dielectric coating 1920 adopts a square-lattice arrangement of elliptical disconnected areas. Other lattices of dielectric regions also can be formed. Such lattices can include triangular lattice, monoclinic lattice, face-centered square lattice, or the like. Alternative or additional arrangements of portion(s) of dielectric material within a patterned dielectric coating can include disconnected or connected stripes of dielectric material. It is to be noted that a patterned dielectric coating, such as coating 1920, can be placed among metal contact 1935 and P+ diffuse doping layer 1916 (see, e.g., **FIG. 19B**). Location of patterned dielectric coating 1920 is dictated by the neutral-doped junction that has dominant losses at operating radiation intensity in a solar concentrator or other solar-electric energy conversion apparatus or device. For example, in PV element 1910 (e.g., a P+NN+ unit cell), N+ diffused region, or layer, and its contact to metal 1925 can have substantially larger losses at high electromagnetic radiation intensities, thus patterned dielectric coating 1920 in the configuration displayed in diagram 1900 can be the substantially least expensive configuration to reduce recombination (e.g., radiative and nonradiative) losses and improve performance of the PV element 1910, particularly at high intensities.

[00120] It should be appreciated that substantially any pattern of dielectric material (e.g., a disconnected array of openings, such as the space between dielectric elliptic areas in dielectric coating 1920) can reduce recombination losses at a single diffuse layer (e.g., N+ layer 1914) because metallization applied in a later step can assure all or substantially all open, contact areas are mutually connected when fully bonded to the next planar unit cell within the VMJ cell structure. Unit cell(s) employed to produce a VMJ photovoltaic cell as described herein consist of PV element 1910 coated with a dielectric pattern and metalized as described supra. Thus, such unit cell(s) are different from conventional unit cell(s) employed for fabrication of conventional VMJ solar cells. It is noted that smaller contact area(s) amongst

metal and doped layer may contribute to an increase in series resistance in a stack of PV elements such as 1910 that form a solar cell; thus, an advantageous pattern for reducing the contact area ratio is a high density of closely spaced smaller openings for optimizing performance for a given intensity. Recombination losses can include radiative or nonradiative recombination of photogenerated carriers, wherein nonradiative recombination can comprise Auger scattering, carrier-phonon relaxation, or the like. Auger recombination rate increases as the cube of carrier density, e.g., density of photogenerated carriers; doubling the volume of a photovoltaic device can lead to a sixteen-fold increase in recombination losses when Auger bulk scattering in accounted for. Thus, thinner slabs 1910 or substantially any design modification that renders PV element 1910 thinner, such as the use of light trapping with textured surfaces, such as V-grooved surfaces, U-grooved surfaces ..., or back side reflectors, can be utilized to mitigate bulk Auger recombination at high intensities through reduction of the thickness of unit cells that form a VMJ photovoltaic cell. Collection efficiency in PV cells can increase significantly when VMJ unit cells as designed in accordance with aspects described herein afford a 50% reduction in recombination losses.

[00121] It should be appreciated that substantially any dielectric material can be employed for dielectric coating 1920. In an aspect, dielectric coating can be a thermal oxide layer, which has a low surface recombination velocity. It should further be appreciated that making electrical contacts to end of unit cells, or PV elements, of semiconductor-based (e.g., Si-based) VMJ photovoltaic cells with patterned openings in the dielectric can require a full electrical contact that can be provided by low resistivity silicon that thermally matches or substantially matches the thermal expansion coefficient of the unit cells, or a metal such as molybdenum or tungsten which have thermal coefficient(s) that nearly matches the thermal coefficient(s) of silicon. Likewise, for a VMJ solar cell based on a semiconductor material or compound other than silicon, metallization of patterned dielectric coating, e.g., 1920 or 1960, can be effected with conductive material(s), e.g., metals or low-resistivity doped semiconductors, that have thermal coefficient(s) that nearly matches thermal coefficient(s) of semiconductor material of the unit cells that form the VMJ solar cells.

[00122] With respect to metal layers, metal contact layer 1925 and metal contact layer 1935 can be disparate. For example, a first metal contact layer (e.g.,

layer 1925) can include dopants, and a second contact layer (e.g., layer 1935) can incorporate a diffusion barrier in order to mitigates autodoping.

[00123] **FIG. 19B** is a diagram 1950 of a photovoltaic element 1910 with patterned dielectric coatings in both diffusion doping regions. In diagram 1950, a first patterned dielectric coating 1920 between a N+ diffuse doping layer 1914 and a first metal contact 1925, and a second patterned dielectric coating 1960 between a P+ diffuse doping layer 1916 and a second metal contact 1935. Aspects of dielectric coating 1960 are substantially the same as those of dielectric coating 1920. As mentioned above, metal contact layer 1925 and 1935 can be disparate.

[00124] It is to be noted that mitigation of recombination losses of photogenerated carriers and ensuing increased PV element performance provided by the introduction of the second patterned dielectric coating outweighs the added complexity and possible extra expense(s) of additional processing act(s) associated with preparation of a second patterned dielectric coating.

[00125] To ensure efficient operation of PV element 1910 in a photovoltaic device, the first pattern in dielectric coating 1920 is to be correlated with the second pattern in coating 1960 so as to have a set of one or more opening(s), and section(s) of metal layers 1925, in opposition. When patterned dielectric coating 1920 is "out-of-phase" with respect to patterned dielectric coating 1960, and the dielectric coatings mutually occlude section(s) of respective metal layers 1925, resistance among unit cells in a stack of PV elements 1910 increases and efficiency of a VMJ solar cell decreases.

[00126] Additionally or alternatively, openings formed through pattern dielectric coating 1920 can be different in size, e.g., different area, that openings generated via dielectric coating 1960. For instance, it can be more desirable to have the openings area for the N+ contacts wider than those for the P+ contacts in PV element 1910, or P+NN+ unit cells, to more effectively reduce overall losses, particularly if there are higher losses at the N+ diffused region and metal contacts. As described above, such disparate among opening sizes can be implemented or exploited irrespective of the particular pattern of the dielectric coating.

[00127] **FIG. 19C** displays a diagram of example set of precursors and derived PV element(s) that can be produced through doping in accordance with aspects described herein. As indicated supra, three precursor types can be employed to produce PV elements that are processed to introduce patterned dielectric coating(s)

and metal contact(s) as described herein: (i) N-type doped precursor 1980, (ii) P-type doped precursor 1985, and (iii) intrinsic precursor 1990. Precursors are semiconducting materials such as Si; Ge; GaAs, InAs, or other III-V semiconducting compounds; II-VI semiconducting compounds; CuGaSe; CuInSe; CuInGaSe. Upon doping, N-type precursor 1980 can lead to PV element 1982, which includes an N+-type diffuse doping region and a P+-type doping region, such PV element is PV element 1910. In addition, doping of precursor 1980 can lead to PV element 1984, with layers, or regions, of N-type and P-type diffuse doping. Precursor 1985 enable formation of PV elements 1986 and 1988, with N+ and P+ diffuse doping layers in PV element 1986, and N+ diffuse doping and P-type doping in element 1988. Various doping of intrinsic precursor 1990 result in PV elements 1992-1998. In PV element 1992, P-type and N-type regions of doping are included; PV element 1994 includes N+-type and P-type doping layers; PV element 1996 includes N-type and P+-type doping layers; and N+-type and P+-type layer are included in PV element 1998. While the different regions of doping introduced in the precursor materials 1980, 1985, and 1990 are illustrated as extended regions, such regions can be spatially confined or nearly-confined, as described herein. The various PV elements illustrated herein can be coated with a patterned dielectric material and metalized as described herein in order to form unit cell(s) that can stacked to produce a monolithic photovoltaic cells in accordance with aspects of the subject innovation. In an aspect, patterned contacts formed through coating with patterned dielectric material in P+NN+ PV elements, or unit cells, can be employed for terrestrial PV concentrators, whereas P+PN+ PV elements, or unit cells, can be more radiation hardened and thus exploited for space applications.

[00128] **FIG. 20A** is a diagram 2000 of a cross section of a PV element with a single surface patterned with a dielectric coating. The pattern of dielectric material results in sections 2005 of dielectric deposited atop an N+ diffuse doping layer 2014. It is to be noted that an additional, or alternative, configuration of a PV element with a patterned dielectric coating on P+ diffuse doping layer 2016 is possible. In PV element illustrated in diagram 2000, an N-type region 2012 separates diffuse doping regions 2014 and 2016. As discussed above, such configuration can be effective at mitigation of recombination losses associated with operation of the PV element at high intensity.

[00129] **FIG. 20B** illustrates PV elements of diagram 2030 upon metallization with metal contacts 2025 and 2035. The presence of the patterned dielectric coating regions 2005 on N+ diffusion layer 2014 reduce the electric coupling among electric contacts 2025 and 2035. As discussed above, metal contact layers can be disparate.

[00130] **FIG. 20C** illustrates an example embodiment of a VMJ photovoltaic cell 2060 in which constituent unit cells 2070_1-2070_M (M is a positive integer) stacked along direction 2080 exploit a one-side, asymmetric patterned dielectric coating (e.g., coating with dielectric regions 2005) on N+ diffuse doping layer. The VMJ solar cell that results from the stack of unit cells 2070_λ ($\lambda = 1, 2 \ldots M$), which are PV elements, is a monolithic (e.g., integrally bonded), axially oriented structure. In an aspect, based on semiconducting material of unit cell(s), two classes of VMJ photovoltaic cells can be formed: (a) homogeneouse and (b) heterogeneous. In (a), units cell(s) 2070_1-2070_M are based on the same or substantially the same precursor, whereas in (b) the unit cell(s) are based on disparate precursors. Disparate precursors can be based on the same semiconducting compounds, e.g., Si; Ge; GaAs, InAs, or other III-V semiconducting compounds; II-VI semiconducting compounds; CuGaSe; CuInSe; CuInGaSe, but differ in doping type or, for alloyed compounds, in alloying concentrations. Heterogeneous VMJ photovoltaic cells can exploit various portions of the emission spectrum of a source of electromagnetic radiation, e.g., solar light spectrum. A VMJ solar cell can produce a serial voltage $\Delta V \cong M \cdot \Delta V_C$ along direction 2080, wherein ΔV_C is a voltage in a constituent PV element 2070_λ. In an aspect, M ~ 40 is typically utilized to form a VMJ solar cell. A 1 cm^2 VMJ with M ~ 40 can output nearly 25 volts under typical operation conditions, such as incident photon flux, radiation wavelength, temperature, or the like. It should be appreciated that performance of a stack of PV elements is limited by the PV element with lowest performance because such element is a current output bottleneck in the series connection; namely, the current output is reduced to the current output of the lowest performing unit cell. Therefore, to optimize performance, stacks of active PV elements, or unit cells, that form the VMJ photovoltaic cell can be current-matched or nearly current-matched based on a performance characterization conducted in a test-bed under conditions (e.g., radiation wavelength(s), concentration intensity) substantially similar to those expected under normal operating conditions of a solar

collector system in the field. The current that is matched is current produced by a PV element, or unit cell, upon solar-electric energy conversion.

[00131] In addition, the monolithic stack of PV elements 2070_1-2070_M that produces the VMJ solar cell can be processed, e.g., sawn, cut, etched, peeled, or the like, in order to expose or nearly expose a specific crystalline plane (*qrs*), with *q*, *r*, *s* Miller indices, which are integer numbers, to sunlight when the VMJ solar cell is part of a PV module or device. In an aspect, to achieve substantive passivation of surface states, specific crystalline plane(s) can (100) planes. **FIG. 20D** illustrates a VMJ PV cell 2090 produced through a stack of PV elements, or unit cells, 2092 with patterned contacts in the fashion presented in FIG. 20C, the VMJ PV cell processed to expose a specific crystalline surface *(qrs)*, indicated with a normal vector 2094 oriented in direction ⟨*qrs*⟩. It is noted that any PV elements with patterned contacts described herein can be utilized to form a VMJ PV cell that exposes crystalline plane *(qrs)*. In addition, as part of the processing, and based on direction ⟨*qrs*⟩, a portion 2096 of the VMJ PV cell can be removed to generate a flat surface to facilitate or enable utilization of the VMJ PV cell in a PV device or module.

[00132] **FIG. 21A** is a diagram that illustrates example dielectric coating pattern(s) to a PV element. Patterns 2130 and 2140 correspond to patterns for a first and second surface in a PV element. Openings in the dielectric coating are lines, or stripes, with a defined width *w* 2135 and pitch separation w_P 2145 from each other. In an aspect, such structure of openings in pattern dielectric coating provide a reduction in contact area of $(1 + w/w_P)^{-1}$; for instance, when $w = w_P$ the reduction there is a 50% reduction in contact area. However, because smaller contact area may contribute to an increase in series resistance, the preferred pattern of lines, or stripes, for reducing the contacts area ratios are high density of closely spaced smaller lines, or stripes, openings. The density can be varied to optimize performance for a given radiation intensity at which the PV element is expected to operate as part of a solar cell, or PV cell, in a PV module. Additional or alternative patterns on opposite surfaces of a PV element 1910, or a wafer, also are possible as well as advantageous. As illustrated, lines, or stripes, openings can be made on opposite sides of each PV element 1910, or a wafer, and misoriented 90 degrees from one side to the other; namely, stripes in patterned dielectric coating 2130 are oriented at an angle of 1935 degrees with respect to the ⟨100⟩ direction, whereas stripes in patterned dielectric coating 2140 are aligned

at an angle of 45 degrees with respect to ⟨100⟩. It is noted that other relative misorientations are also possible and advantageous. Moreover, as indicated above, openings formed through patterned dielectric coating 2130 can be different in size, e.g., span a different area, that openings generated via dielectric coating 2140. For instance, it can be generally more desirable to have openings area for the N+ contacts wider than those for the P+ contacts in a PV element with P+NN+ unit cell(s), to more effectively reduce overall losses, particularly when there are higher losses at the N+ diffused region and metal contacts. In the alternative, it can be desirable to implement openings area for the P+ contacts wider than those for the N+ contacts to mitigate recombination losses in N+PP+ unit cell(s) (e.g., PV element 1986).

[00133] At fabrication of vertical multi-junction solar cell(s), which includes stacking and alloying surface-patterned PV elements described herein, the differently oriented, dielectric areas when bonded together with metallization can form low-resistance contact points in a defined pattern. In an aspect, the contact points, facilitated through the openings in dielectric coatings 2130 and 2140, are directly aligned and mutually adjacent in a controlled pattern, with P+ contacts of one wafer interfacing at points to N+ contacts of the next wafer in order to keep series resistance low in finished VMJ cells. As described supra, in an aspect, fabricated VMJ cells can be sawn to have a preferred ⟨100⟩ crystal orientation at the illuminated surface in order to establish the lowest surface states for passivation. Thus, as illustrated in the FIG. 21A, relative orientation of the lines, or stripes, on a first surface of a patterned PV element can be relatively misoriented at an angle γ such as 90 degrees from the lines or stripes in a second surface, wherein the first and second surfaces include the ⟨100⟩ crystal direction, e.g., are normal to the (100) crystalline plane. Other orientations of lines or stripes are also possible and advantageous. Likewise, relative misorientation γ of lines or stripes at different surfaces can be implemented. In an aspect, misorientation γ is a finite real number; e.g., dielectric coating patterns are not mutually aligned at disparate surfaces. Additionally, since VMJ photovoltaic cells described herein can be processed to expose or substantially expose any crystalline plane (*qrs*), stripes in a dielectric coating can be oriented at an angle a with respect to crystalline directions ⟨*qrs*⟩, with *q*, *r*, and *s* Miller indices. In particular, stripes in a patterned dielectric coating on a first surface can include stripes oriented at a first angle α with respect to ⟨*qrs*⟩, whereas stripes in a patterned dielectric coating in a

second surface can be oriented at a second angle β (α≠β) with respect to ⟨*qrs*⟩; thus, providing a misorientation γ=α−β.

[00134] **FIG. 21B** illustrates a cross-section diagram of a PV element 2150 with dielectric coating patterns deposited on both a P+ diffuse doping layer 2176 and an N+ diffuse doping layer 2174. In PV element 2150, N-type region 2172 separates diffuse doping regions 2014 and 2016. The illustrated cross section is a cut that illustrates alignment of dielectric regions on a first surface, e.g., dielectric regions 2155, with those dielectric regions on a second surface, e.g., dielectric regions 2165. It should be appreciated that other cross-section cuts can display misaligned regions of dielectric material the first surface and second surface. As discussed above, such alignment facilitates to retain series resistance among PV elements 2150 when stacked to form a VMJ solar cell, since metal contact in P+ diffuse doping layer can match a metal contact in a subsequently stacked N+ diffuse doping layer, as illustrated in **FIG. 21C**. It should be appreciated that, as indicated above, spacing amongst dielectric regions 2155 can be different from spacing amongst dielectric regions 2165.

[00135] **FIG. 22** illustrates a cross-section diagram of an example PV element 2200 with dielectric coating regions 2205, originated through deposition of patterned dielectric coating 2202, that facilitate or enable to reduce at least one of a metal contact area in a surface of the PV element upon metallization thereof. In PV element 2200, N+ diffusion region(s) 2214 is structured to reduce doping layer volume and thus mitigate recombination losses of photogenerated carriers. Regions of N+ doping can be determined by the openings structure in the patterned dielectric coating; e.g., N+ diffuse region(s) 2214 can be stripes oriented along pitch spacing(s) in a striped pattern of dielectric coating 2202. Such regions are formed through utilization of dielectric coating regions 2205 as a mask to control or manipulate N+ doping. Based at least in part on the patterned dielectric coating 2202, and topology of deposited regions 2205, N+ diffuse doping area(s) or volume(s) 2214 can be fully confined or quasi-confined, e.g., confined in two or less directions and extended in a third direction. In a feature of PV element 2200, regions of N-type material 2212 are interspersed with N+ diffuse doping regions 2214. In addition, P+ diffuse doping region 2216 is not coated with a patterned dielectric material.

[00136] Upon metallization, e.g., surface of P+ diffuse layer 2216 and patterned surface of confined, disconnected N+ diffuse doping region (e.g., set of

regions 2214) are coated with a metal contact, a set of metalized PV elements can be stacked, and processed, e.g., soldered or alloyed through a high temperature manufacture step, to form a VMJ photovoltaic cell with reduced recombination losses in accordance with aspects described herein.

[00137] **FIG. 23A** illustrates a cross-section diagram of a PV element 2300 with dielectric coating patterns deposited on opposed diffuse doping regions. In an aspect, a first dielectric coating pattern (e.g., a striped pattern 2330 oriented along a direction 135 degrees rotated with respect to the ⟨100⟩ crystalline direction) is utilized to reduce metal contact surface at a first diffuse doping region, while a second dielectric coating pattern (e.g., a striped pattern 2340 oriented 45 degrees with respect to the ⟨100⟩ crystalline direction). Both N+ and P+ diffuse doping regions can include, respectively, doping regions 2314 and 2316 confined in two or more directions. Openings in the dielectric coating patterns can serve as masks to generate reduced-volume doping diffuse layers; the openings formed between regions 2305 and 2325 of coated dielectric. Reduction of metal contact surface and volume of doping regions at both diffuse doping layers can provide enhanced mitigation of carrier recombination losses with respect to dielectric coating and doping volume reduction in a single doping region. As discussed above, benefit of improved PV performance of a VMJ produced with patterned PV elements, or unit cells, surpass additional processing complexity and costs associated with surface patterning. Moreover, openings formed through pattern dielectric coating 2330 can be different in size, e.g., span a different area, than openings generated via dielectric coating 2340, in order to further control recombination losses originated from diffuse doping areas. For instance, it can be more desirable to have openings that produce larger N+ doping regions than those that produce P+ doping regions, to more effectively reduce overall losses, particularly when there are higher losses at the N+ diffused region and metal contacts.

[00138] **FIG. 23B** illustrates a cross-section of patterned PV element 2350 with metal contact layers 2365 and 2375, which can be mutually different as discussed above. The illustrated cross-section cut displays metal regions 2365 (e.g., among spaces of dielectric material) on the surface of N+ diffuse doping layer aligned with metal regions 2375 (e.g., region among spaces of dielectric material) on the surface of P+ diffuse doping layer. In PV element 2350, doping regions are formed in an N-type

precursor. A set of patterned PV elements 2350 can be stacked and processed to form VMJ solar cells with improved performance.

[00139] **FIG. 24** presents a perspective illustration of an example embodiment of a textured vertical multi-junction (VMJ) photovoltaic cell 2405 with textured surface and that is formed by stacking unit cells 2410_1-2410_{10} along a direction normal to the plane of the unit cell(s); each unit cell(s) 2410_κ, with κ=1, 2,...10, consists of a PV element with a patterned dielectric coating and metal contact, as described herein. While in example textured PV cell 2405 a set of 10 unit cell(s) are illustrated, it is noted that textured VMJ photovoltaic cells can comprise M unit cell(s), with M a positive integer. Unit cell(s) in a texture VMJ photovoltaic cell, e.g., 2410_κ, can be embodied in unit cell(s) 2070_λ, 2180_λ, or 2350, or any other unit cell(s) produced as described herein. In photovoltaic cell 2405, textured surface 2412 is a V-grooved surface; however, other grooves or cavities of various shapes can be formed, e.g., U groove. The textured surface is formed onto a plane (*qrs*) that is exposed or substantially exposed to electromagnetic radiation as a result of processing the monolithic stack of unit cell(s), or PV elements with patterned metal contacts described herein; see, e.g., FIG. 20D. Incident light can be refracted in the plane 2430 having a normal vector *n* 2432. Such plane 2430 is parallel to the surface(s) of unit cell(s) 2410_κ onto which the patterned dielectric material is coated, and can include the cross section configuration of the grooves 2415—plane 2430 is substantially perpendicular to the direction of stacking unit cells 2410_κ. Texturing of surface of the monolithic stack of unit cell(s) 2410_κ, which leads to textured surface 2412, enables the refracted light to be directed away from the P+ and N+ diffuse doping regions without hindering photogeneration of carriers, thus effectively making the unit cells that compose the textured photovoltaic cell 2405 thinner, and reducing recombination losses as indicated supra. Moreover, an anti-reflection coating can be applied to the textured surface 2410 to increase incident light absorption in the cell.

[00140] In view of the example systems and elements described above, example methods that can be implemented in accordance with the disclosed subject matter can be better appreciated with reference to flowcharts in **FIGs. 25-8**. For purposes of simplicity of explanation, the methods described set forth herein are presented and described as a series of acts; however, it is to be understood and appreciated that the described and claimed subject matter is not limited by the order of

acts, as some acts may occur in different orders and/or concurrently with other acts from that shown and described herein. For example, it is to be understood and appreciated that a method described herein can alternatively be represented as a series of interrelated states or events, such as in a state diagram, or interaction diagram. Moreover, not all illustrated acts may be required to implement example method in accordance with the subject specification. Additionally, the example methods described herein can be implemented conjunctly to realize one or more features or advantages.

[00141] **FIG. 25** is a flowchart of an example method 2500 for producing VMJ solar cells with reduced carrier recombination losses according to aspects disclosed herein. The subject example method is not limited to solar cells and it also can be effected to produce any or substantially any photovoltaic cell. One or more component(s) or module(s) described herein can effect the subject example method 2500. At act 2510, a set of surfaces of a photovoltaic element (e.g., PV element 1910) are patterned with a dielectric coating. Patterning the PV element with the dielectric coating includes utilizing any suitable technique for produce one or more of the dielectric coatings discussed supra. As an example, patterning can proceed through deposition and photolithography techniques. As another example, etching techniques can also be employed to complement or supplement employed patterning protocols. Substantially any or any dielectric material can be employed to coat the set of surfaces. At act 2520, a metal contact is deposited onto one or more of the patterned surfaces of the PV element. Alternative or additional realization of act 2530 can include deposition of an ohmic contact or conductive contact onto the one or more of the patterned surfaces of the PV element. The material for the metal contact, or ohmic contact, can be embodied in substantially any or any conductive material, e.g., a low-resistivity doped semiconductor or a metal. In an aspect, the conductive material preferably has thermal coefficient(s) that nearly matches thermal coefficient(s) of semiconductor material of the PV element. In another aspect, the conductive material has bonding characteristics that facilitate stacking of patterned and metalized PV elements. In yet another aspect, pattern(s) of dielectric material coating(s) ensures that metallization of opposing surfaces results in regions of low resistance by aligning metal regions on disparate surfaces (e.g., 90 degree-misoriented striped openings in patterns 2330 and 2340 result in metal contact regions aligned along a stacking direction (e.g., z direction 2080). At act 2530, a set of patterned,

metalized photovoltaic elements is stacked to form a VMJ solar cell. It should be appreciated that such PV elements can include confined regions of diffuse doping as discussed above. At act 2540, the formed VMJ solar cell is processed to facilitate deployment in a PV device, optimize photovoltaic performance, or a combination thereof. Such processing can include various manufacturing steps or procedures such as cutting procedures, polishing procedures, cleaning procedures, integrating procedures, and the like. Such procedures can be directed, at least in part, to expose a specific crystalline plane to sunlight when the formed VMJ solar cell is deployed in a PV device. In one example, processing comprises cutting formed VMJ cell(s) so as to expose or substantially expose ⟨100⟩ crystal planes to sunlight in order to establish the lowest surface states for passivation.

[00142] **FIG. 26** is a flowchart of an example method 2600 for producing solar cells with reduced carrier recombination losses according to aspects described herein. The subject example method 2600 is not limited to manufacturing solar cells; example method 2600 also can be effected to produce any or substantially any photovoltaic cell. One or more component(s) or module(s) described herein can effect the subject example method 2600. At act 2610, a set of surfaces of a photovoltaic element (e.g., PV element 1910) are patterned with a dielectric coating. Patterning the PV element with the dielectric coating includes utilizing any suitable technique for produce one or more of the dielectric coatings discussed supra. As an example, patterning can proceed through deposition and photolithography techniques. As another example, etching techniques can also be employed to complement or supplement employed patterning protocols. Substantially any or any dielectric material can be employed to coat the set of surfaces. At act 2620, a patterned dielectric coating can be utilized to generate confined regions of diffuse doping in the PV element. The patterned dielectric coating can be employed as a mask that dictates the degree of confinement of doping regions. In an aspect, confinement of the doping regions can be nearly two-dimensional, with the doping substantively extending along one dimension and confined along two disparate directions. Confinement of doping regions also can be nearly three-dimensional, wherein doping in the PV element is limited to a set of one or more localized areas substantially smaller than the size of the PV element (see, e.g., FIG. 22). As an example, a striped pattern of dielectric material (e.g., pattern 2330), when utilized as a mask for doping, can lead to diffuse doping layers that are

substantially confined in two directions, e.g., the diffusion direction towards a center of a slab of nominally non-doped semiconductor material and the direction normal to the pitch or stripe in the patterned coating. Confined regions of diffused doping region(s) reduce volume thereof and mitigate photogenerated carrier recombination losses.

[00143] At act 2630, an ohmic contact is deposited onto one or more of the patterned surfaces of the PV element. The material for the ohmic contact, can be embodied in substantially any or any conductive material, e.g., a low-resistivity doped semiconductor or a metal. In an aspect, the conductive material nearly matches the thermal coefficient(s) of the semiconductor material e.g., Si; Ge; GaAs, InAs, or other III-V semiconducting compounds; II-VI semiconducting compounds; CuGaSe; CuInSe; CuInGaSe …, of the PV element and is suitable for alloying. As indicated supra, pattern(s) of dielectric material coating(s) ensures that deposition of an ohmic contact onto opposing patterned surfaces results in regions of low electrical resistance by aligning metalized regions on disparate surfaces (e.g., 90 degree-misoriented striped openings in patterns 2330 and 2340 result in metal contact regions aligned along a stacking direction (e.g., z direction 2080).

[00144] At act 2640, a set of patterned, metalized photovoltaic elements is stacked to form a solar cell. The set of photovoltaic elements that form the solar cell spans M elements, with M a natural number determined at least in part by a target operation voltage of the solar cell. In an aspect, the set of PV elements can be homogeneous or heterogeneous. In a homogeneous set each element, or unit cell, in the set is based on the same or substantially the same precursor, whereas in a heterogeneous set each element is based on disparate precursors. Disparate precursors can be based on the same semiconducting compounds, e.g., Si; Ge; GaAs, InAs, or other III-V semiconducting compounds; II-VI semiconducting compounds; CuGaSe; CuInSe; CuInGaSe, but differ in doping type or, for alloyed compounds, in alloying concentrations. In addition, such patterned, metalized PV elements include confined regions of diffuse doping as discussed above. At 2650, the solar cell is processed to facilitate deployment in a PV device, optimize photovoltaic performance, or a combination thereof. Processing can include various manufacturing steps or procedures such as cutting procedures, polishing procedures, cleaning procedures, integrating procedures, or the like. Such steps can be intended, at least in part, to expose a specific crystalline plane to sunlight when the formed solar cell is deployed

in a PV device. In one example, processing comprises cutting the formed solar cell(s) so as to expose or substantially expose (100) crystal planes to sunlight in order to establish the lowest surface states for passivation. It should be appreciated that the solar cell can be processed to expose or substantially expose other crystal planes, e.g., (*qrs*) planes such as (311)..

[00145] **FIG. 27** is a block diagram of an example system 2700 that enables fabrication of solar cells in accordance with aspects described herein. Deposition reactor(s) 2710 enable processing of semiconductor-base wafers to produce PV elements or unit cells that compose solar cells, e.g., VMJ solar cells, as described herein. Deposition reactor(s) 2710 and module(s) therein include various hardware components, software components, or combination(s) thereof, and related electric or electronic circuitry to accomplish the processing. In aspect, coater module(s) 2712 allows patterning a surface of a semiconductor wafer or substrate with a dielectric coating. The wafer or substrate can be nominally-undoped or doped, and is the precursor of PV elements utilized for production of the solar cells. As indicating above, patterning can be based upon deposition of the dielectric material via a suitable mask, photolithography, or etching. Deposition reactor(s) 2710 also include doping module(s) 2714 that allows inclusion of dopants within the semiconductor precursor of the PV elements. Dopants can form diffuse doping layers as described above (see, e.g., FIG. 19 or FIG. 23); however, doping module(s) 2714 also afford substantially any type of doping such as epitaxy-based doping, e.g., delta doping. In addition, doping module(s) 2714 allow formation of diffusion barriers that can prevent autodoping.

[00146] As described above, coating a PV element with a dielectric material can occur prior or subsequent to doping. Doping subsequent to patterned dielectric coating exploits such coating as a mask for generation of confined or nearly-confined doping regions (see, e.g., FIG. 22).

[00147] Metallization module(s) 2716 enables deposition of metallic layer(s) to a PV element that includes doping regions, extended or confined, and patterned dielectric coating(s). Metallization can be accomplished through deposition of semiconductor material with subsequent doping, or a metal material. In an aspect, such materials have thermal coefficient(s) that matches or nearly matches thermal coefficient(s) of PV element with doping regions.

[00148] Deposition reactor(s) 2710 can include sputtering chamber(s), epitaxy chamber(s), vapor deposition chamber(s); electron beam gun(s); source material holder(s); wafer storage; sample substrate; oven(s), vacuum pump(s); e.g., turbomolecular pump, diffusion pump; or the like. In addition, deposition reactor(s) 2710 can include computer(s), including processor(s) and memories therein, with memories being volatile or non-volatile; programmable logic controller(s); dedicated processor(s) such as purpose-specific chipset(s); or the like. Deposition reactor(s) 2710 also can include software application(s) such as operating system(s), or code instructions to effect one or more processing acts, including at least those described supra. Described hardware, software, or combination thereof, facilitate or enable at least a portion of the functionality of deposition reactor(s) 2710 and module(s) therein. A bus 2718 allows communication of information, e.g., data or code instructions; transfer of materials; exchange of processed elements; and so forth, amongst the various hardware, software, or combination(s) thereof, in deposition reactor(s) 2710.

[00149] Photovoltaic element(s) can be supplied to a package platform 2730 for further processing. An exchange link, e.g., a conveyer link, or an exchange chamber and electromechanical components therein, can supply the PV element(s); at least one of the exchange link or exchange chamber illustrated with arrow 2720. Assembly module(s) 2732 can collect a set of PV element(s) and allow stacking of each of the PV elements through a high-temperature process or step in order to produce a solar cell, e.g., a VMJ solar cell. The stack is transferred to a specification module(s) 2734 that completes the solar cell to a determined specification, e.g., the stack is sawed to allow exposure of a particular crystalline plane of the PV elements in the stack that form the solar cell. Such processing can be facilitated or allowed, at least in part, by test module(s) 2760, which can determine crystallographic orientation of the PV elements, or unit cells, in the solar cell; such determination can be established via X-ray spectroscopy, e.g., diffraction spectrum and rocking curve spectra.

[00150] For quality assurance or to meet specifications, test module(s) 2760 can probe precursor materials or processed materials various stages of solar cell manufacturing. As an example, test module(s) 2760 can probe density of openings in a patterned dielectric coating of PV element(s) to determine whether such density is adequate for an expected sunlight intensity, or photon flux, in a solar concentrator. As another example, test module(s) can determine defect density that can arise from

thermal cycling in a PV element with metallic layers, to establish if the material or process utilized for metallization is adequate. To at least such ends, test module(s) 2760 can implement or enable minority-carrier lifetime measurements, X-ray spectroscopy, scanning electron microscopy, tunneling electron microscopy, scanning tunneling microscopy, electron energy loss spectroscopy, or the like. Probe(s) implemented by test module(s) 2760 can be in situ or ex situ. Samples of precursor of processed materials or devices, e.g., solar cells, can be supplied to test module(s) via exchange links 2740 and 2750.

[00151] Processing unit(s) (not shown) can effect logic to control at least part of the various processes described herein in connection with operation of system 2700. Such processing unit(s) (not shown) can include processor(s) that execute code instructions that effect the control logic; the code instructions, e.g., program module(s) or software applications, can be retained in memory(ies) (not shown) functionally coupled to the processor(s).

[00152] What has been described above includes examples of systems and methods that provide advantages of the subject innovation. It is, of course, not possible to describe every conceivable combination of components or methodologies for purposes of describing the subject innovation, but one of ordinary skill in the art may recognize that many further combinations and permutations of the claimed subject matter are possible. Furthermore, to the extent that the terms "includes," "has," "possesses," and the like are used in the detailed description, claims, appendices and drawings such terms are intended to be inclusive in a manner similar to the term "comprising" as "comprising" is interpreted when employed as a transitional word in a claim.

50669-106D1

CLAIMS:

1. An electrolysis system comprising:

a vertical multi junction (VMJ) photovoltaic cell that includes a plurality of integrally bonded cell units, each cell unit with a plurality of layers that form a PN junction(s);

a textured surface of the VMJ photovoltaic cell for receipt of incident light, the textured surface for mitigation of bulk recombination losses for the VMJ photovoltaic cell, the textured surface facilitates confining light refraction of an incident light in a plane that cross sections the textured surface, the plane includes substantially repetitive cross sectional patterns, wherein light absorption is mitigated in p+ and n+ diffused doped regions of the VMJ:

an electrolyte that receives a current generated by the VMJ photovoltaic cell, a plurality of anodes and a plurality of cathodes formable by the integrally bonded cell units on a surface of the VMJ, to create the current that decomposes the electrolyte, and a plurality of metal layer protrusions, each protrusion bonded to one of the plurality of anodes and to one of the plurality of cathodes.

2. The electrolysis system of claim 1, the electrolyte is salt water.

3. The electrolysis system of claim 1, each cell units generates at least 0.6 volt.

4. The electrolysis system of claim 1, the VMJ photovoltaic cell has a grooved surface.

5. The electrolysis system of claim 4, the grooved surface is at least one of a V section, or U section, or combination thereof.

6. The electrolysis system of claim 1, each cell of the cell units includes a plurality of parallel semiconductor substrates that are stacked together, wherein a direction of stacking is substantially non-perpendicular to incident light that creates the current.

7. The electrolysis system of claim 6, a substrate includes impurity doped semiconductor material that form a PN junction.

8. The electrolysis system of claim 7 the substrate further includes a "built-in" electrostatic drift field that facilitates minority carrier movement towards the PN junction.

9. The electrolysis system of claim 7 the substrate having a back surface with reflection coatings.

10. The electrolysis system of claim 7 further comprising a buffer zone that safeguards the plurality of layers from at least one of a stress and strain induced on the VMJ photovoltaic cell.

11. The electrolysis system of claim 7, the buffer zone including substantially low resistivity material.

12. A method of electrolyzing an electrolyte comprising:

integrally bonding a plurality of active layers to form a VMJ photovoltaic cell;

generating a current from the VMJ cell for electrolysis of an electrolyte;

forming a plurality of anodes and cathodes that protrude from a surface of the VMJ cell, and

forming a plurality of metal layer protrusions, each protrusion bonded to one of the plurality of anodes and to one of the plurality of cathodes.

13. The method of claim 12 further comprising cooling the VMJ cell by a heat regulating assembly.

14. The method of claim 12 further comprising partially submerging the VMJ cell in the electrolyte.

15. The method of claim 12 further comprising

mitigating bulk losses in the VMJ cell via a textured surface of the VMJ cell that receives an incident light; and

confining refracted incident light in a plane that cross sections the textured surface, the plane includes substantially repetitive cross sectional patterns.

16. The method of claim 12 further comprising increasing mechanical stability of the VMJ cell *via* buffer zones.

17. The method of claim 12, the integrally bonding act further comprising stacking cell units.

18. The method of claim 15 further comprising alloying silicon wafers and aluminum interfaces to form the VMJ cell.

19. The method of claim 15 further comprising employing impurity doped semiconductor material to form PN junctions in the VMJ cell

20. An electrolysis system comprising:

decomposing means for decomposing an electrolyte *via* incident light comprising a plurality of anodes and cathodes on a surface of the decomposing means and comprising a plurality of metal layer protrusions, each protrusion bonded to one of the plurality of anodes and to one of the plurality of cathodes; and

means for mitigating bulk combination losses for the decomposing means, wherein refracted light is substantially confined in a plane that cross sections the means for mitigating bulk combination losses, the plane includes substantially repetitive cross sectional patterns; wherein light absorption is mitigated in p+ and n+ diffused doped regions of the decomposing means.

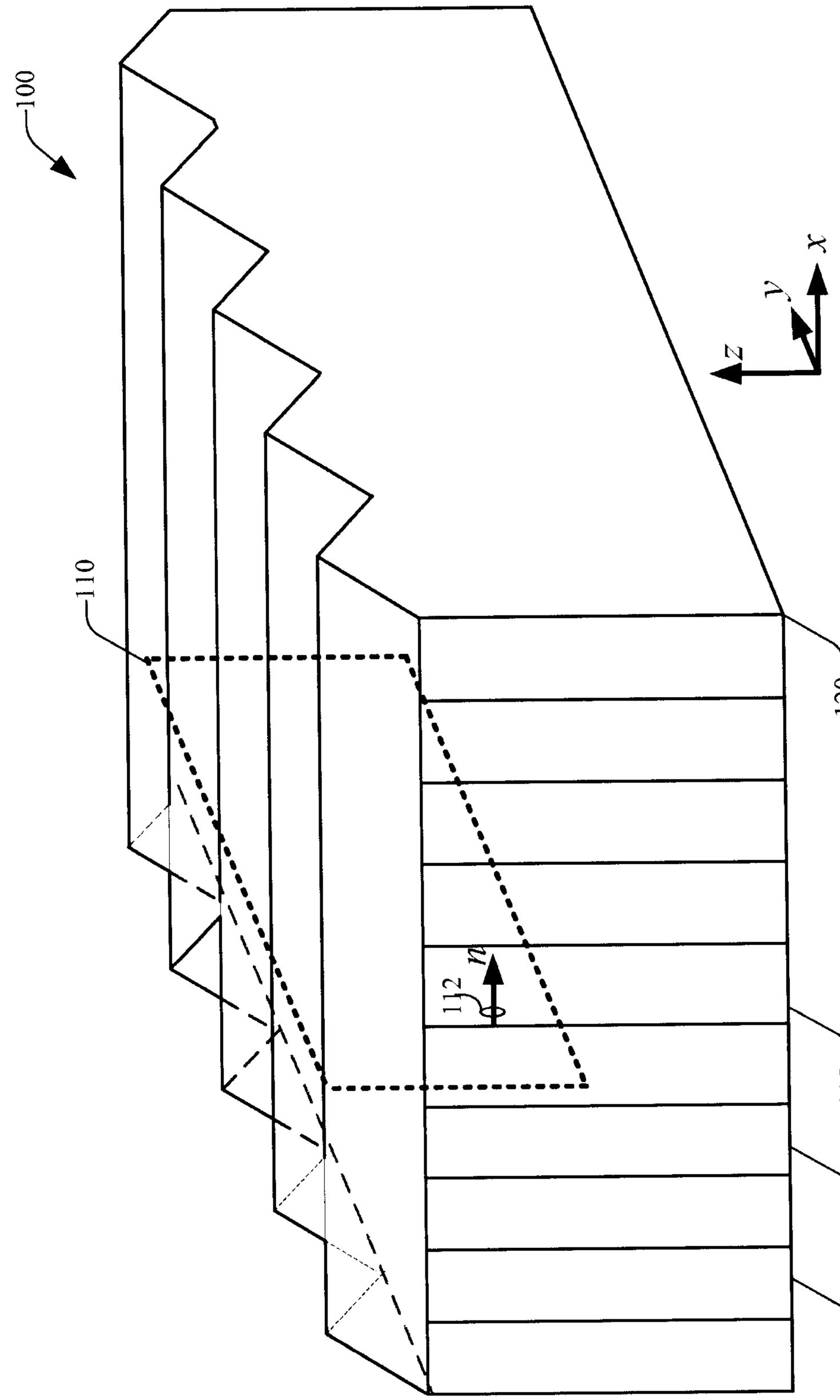

Fig. 1

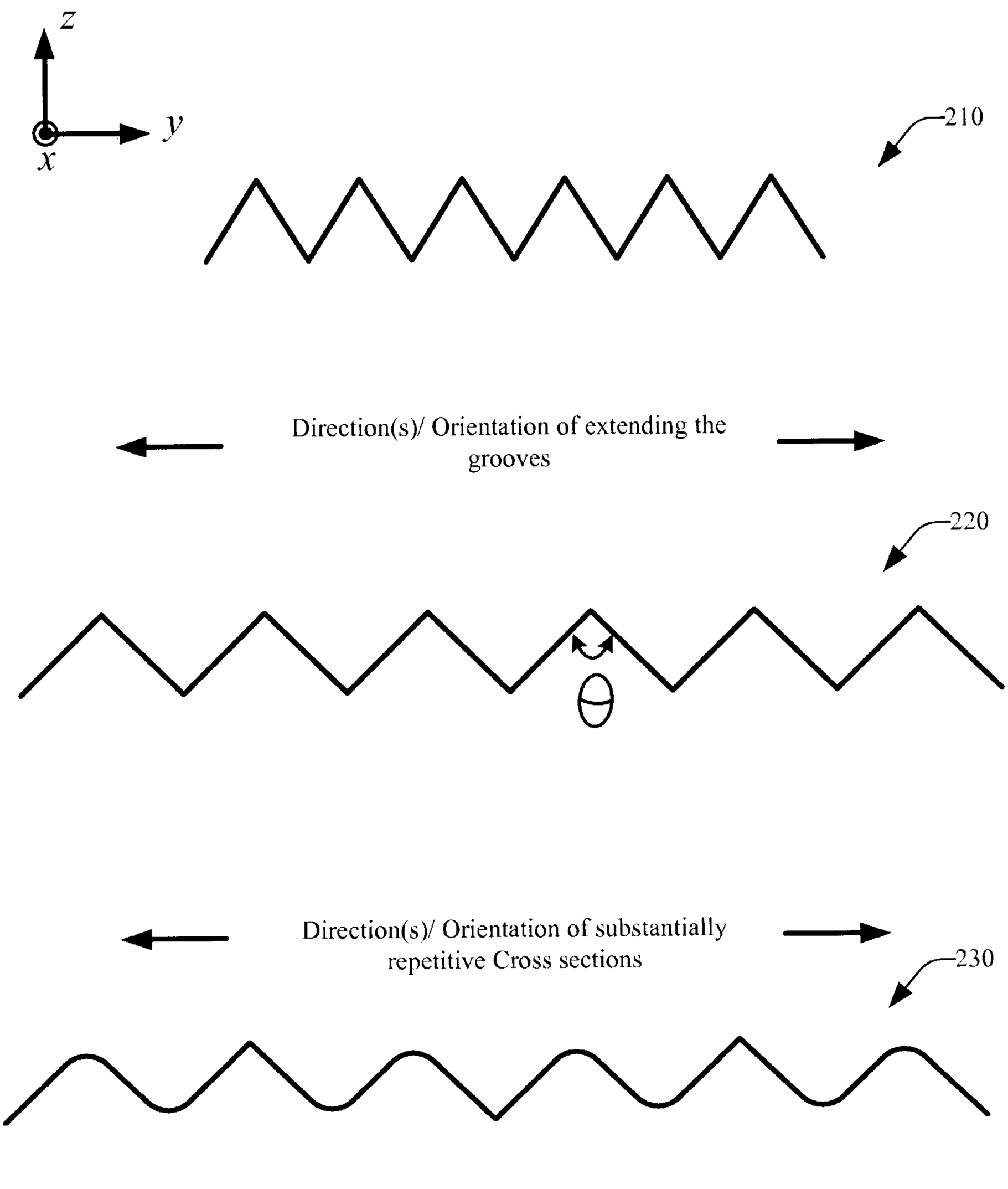
z
y
x
210
Direction(s)/ Orientation of extending the grooves
220
θ
Direction(s)/ Orientation of substantially repetitive Cross sections
230

Fig. 2

Stacking Direction(s)

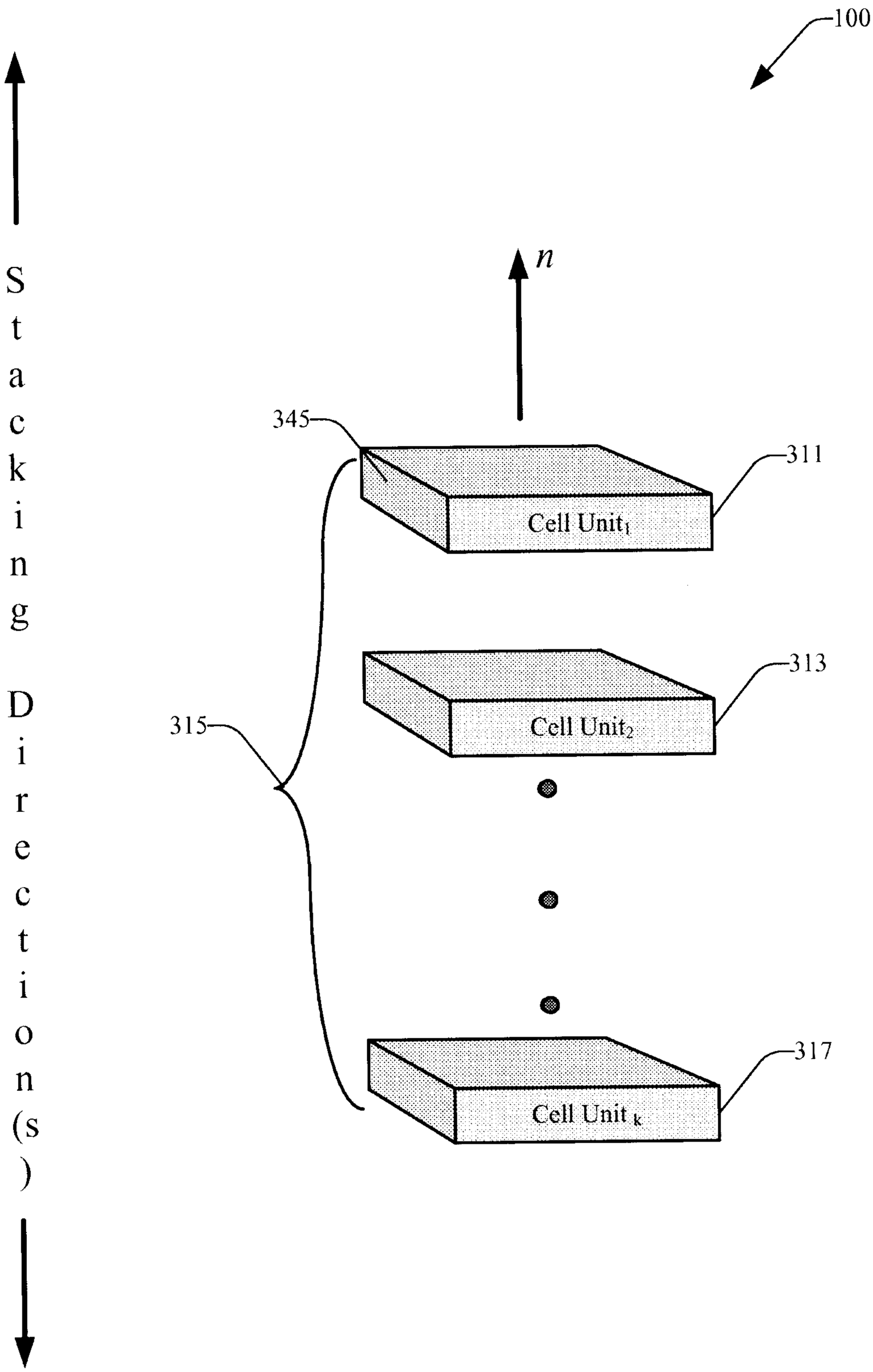

Fig. 3

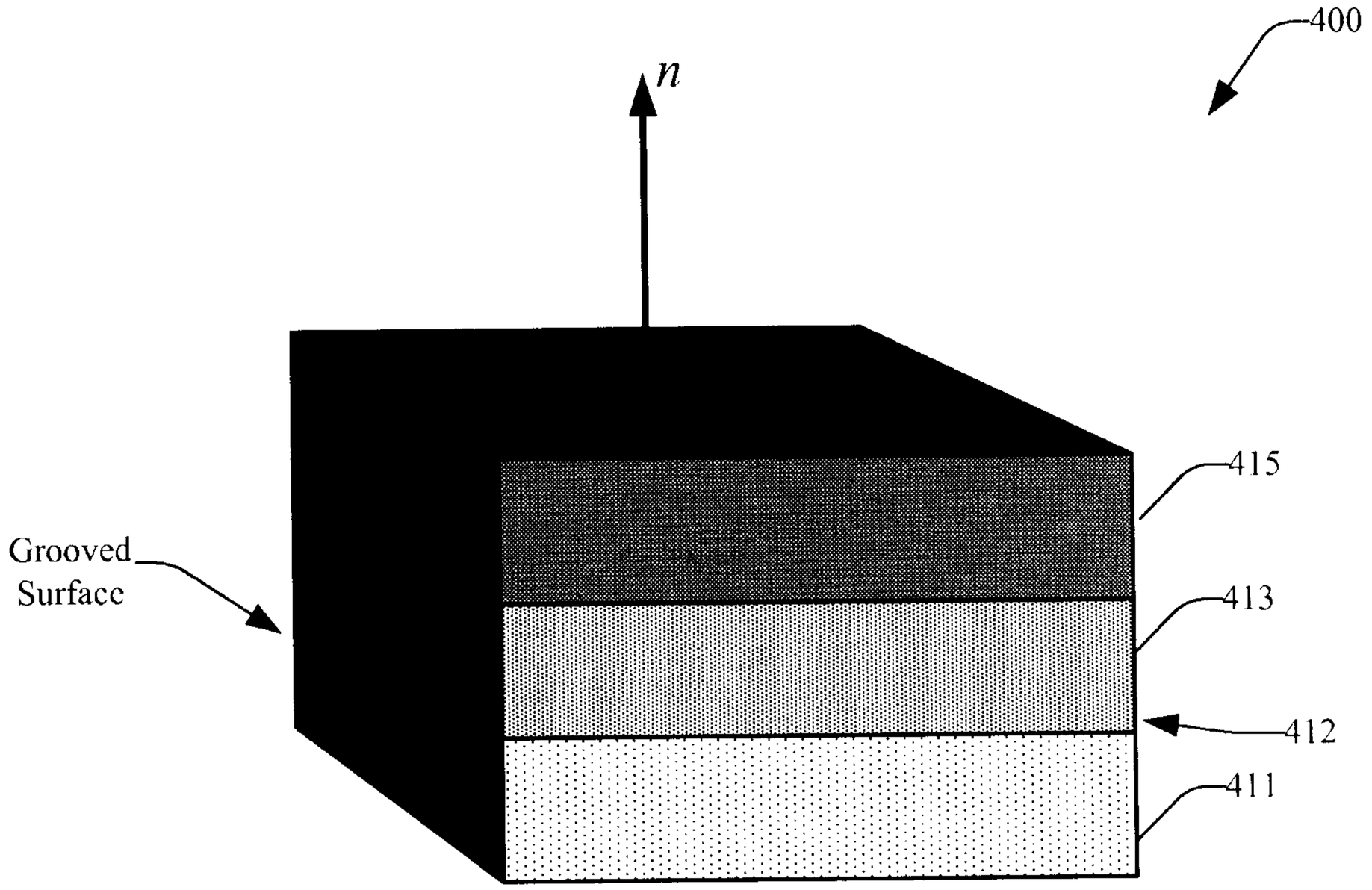

Fig. 4

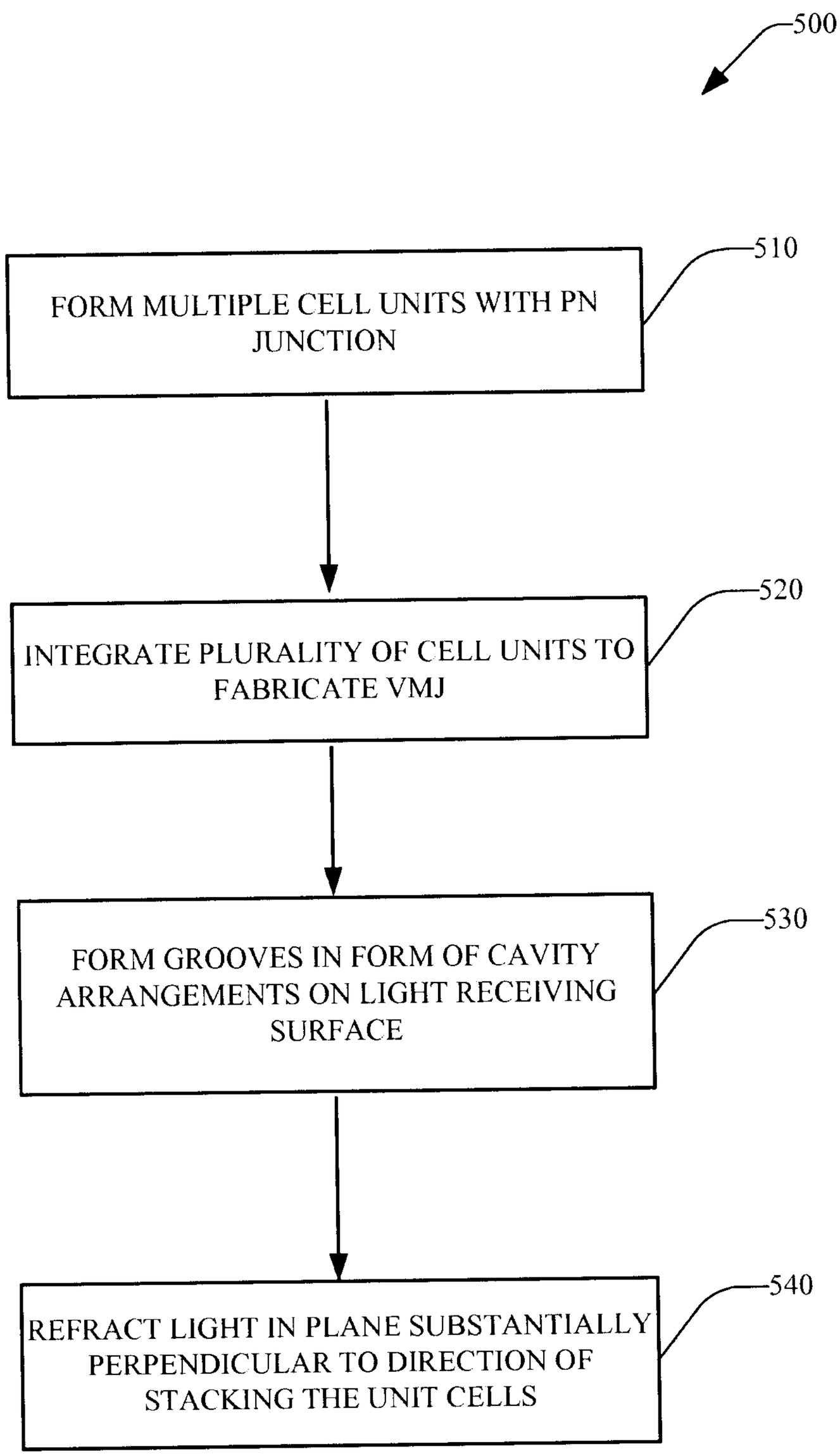
500
FORM MULTIPLE CELL UNITS WITH PN JUNCTION
510
INTEGRATE PLURALITY OF CELL UNITS TO FABRICATE VMJ
520
FORM GROOVES IN FORM OF CAVITY ARRANGEMENTS ON LIGHT RECEIVING SURFACE
530
REFRACT LIGHT IN PLANE SUBSTANTIALLY PERPENDICULAR TO DIRECTION OF STACKING THE UNIT CELLS
540

Fig. 5

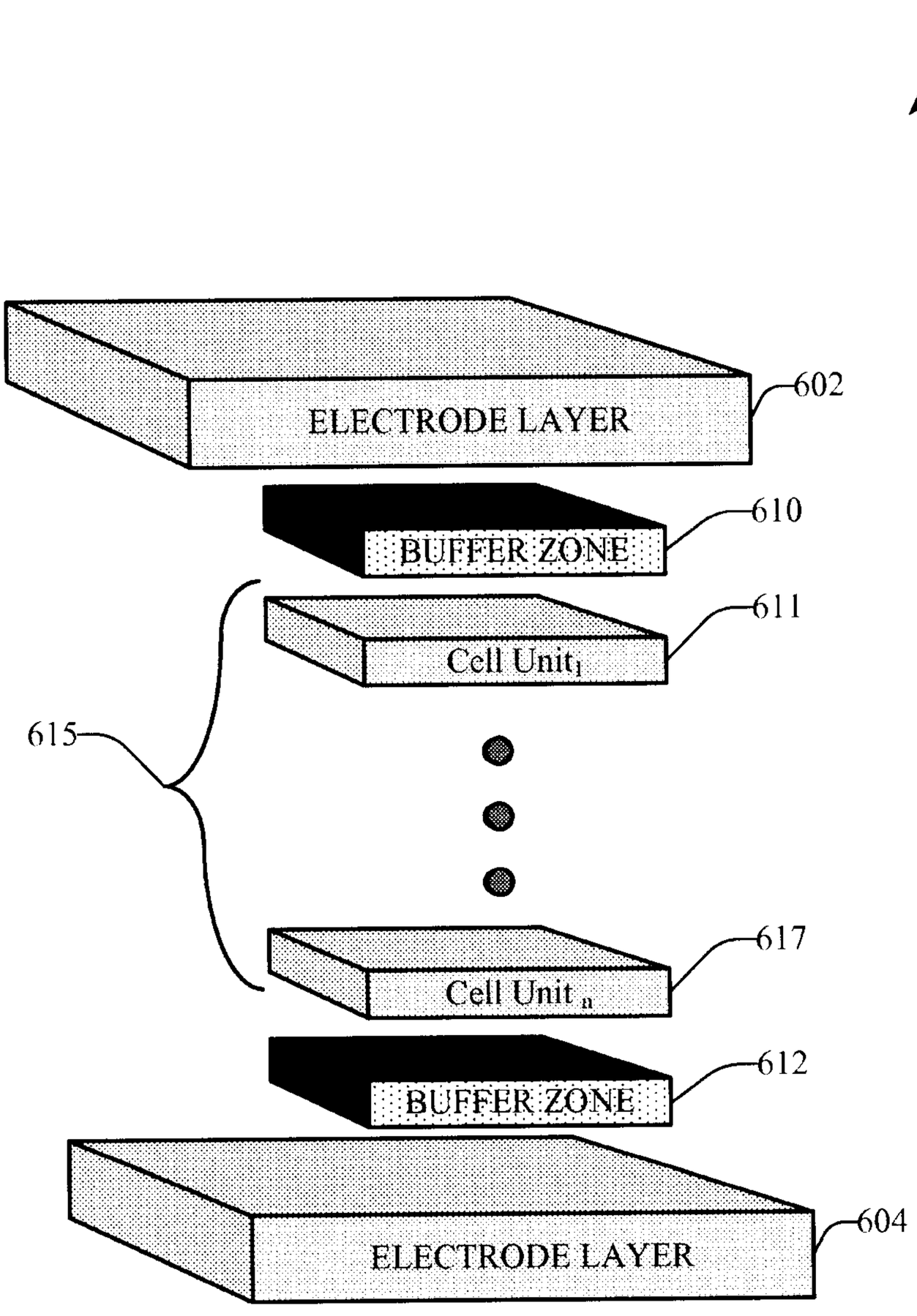
600
ELECTRODE LAYER
602
BUFFER ZONE
610
Cell Unit$_1$
611
615
Cell Unit $_n$
617
BUFFER ZONE
612
ELECTRODE LAYER
604

FIG. 6

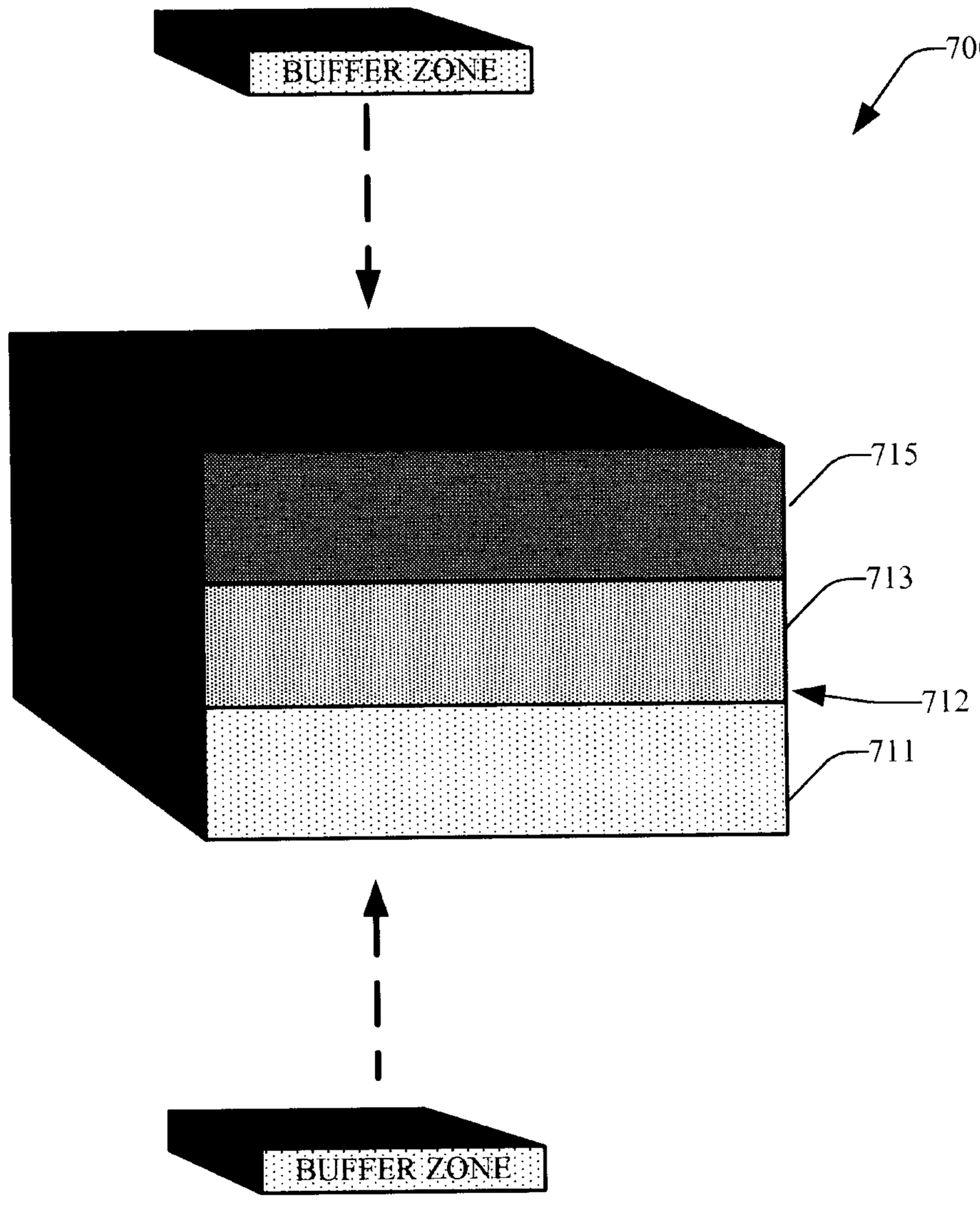

FIG. 7

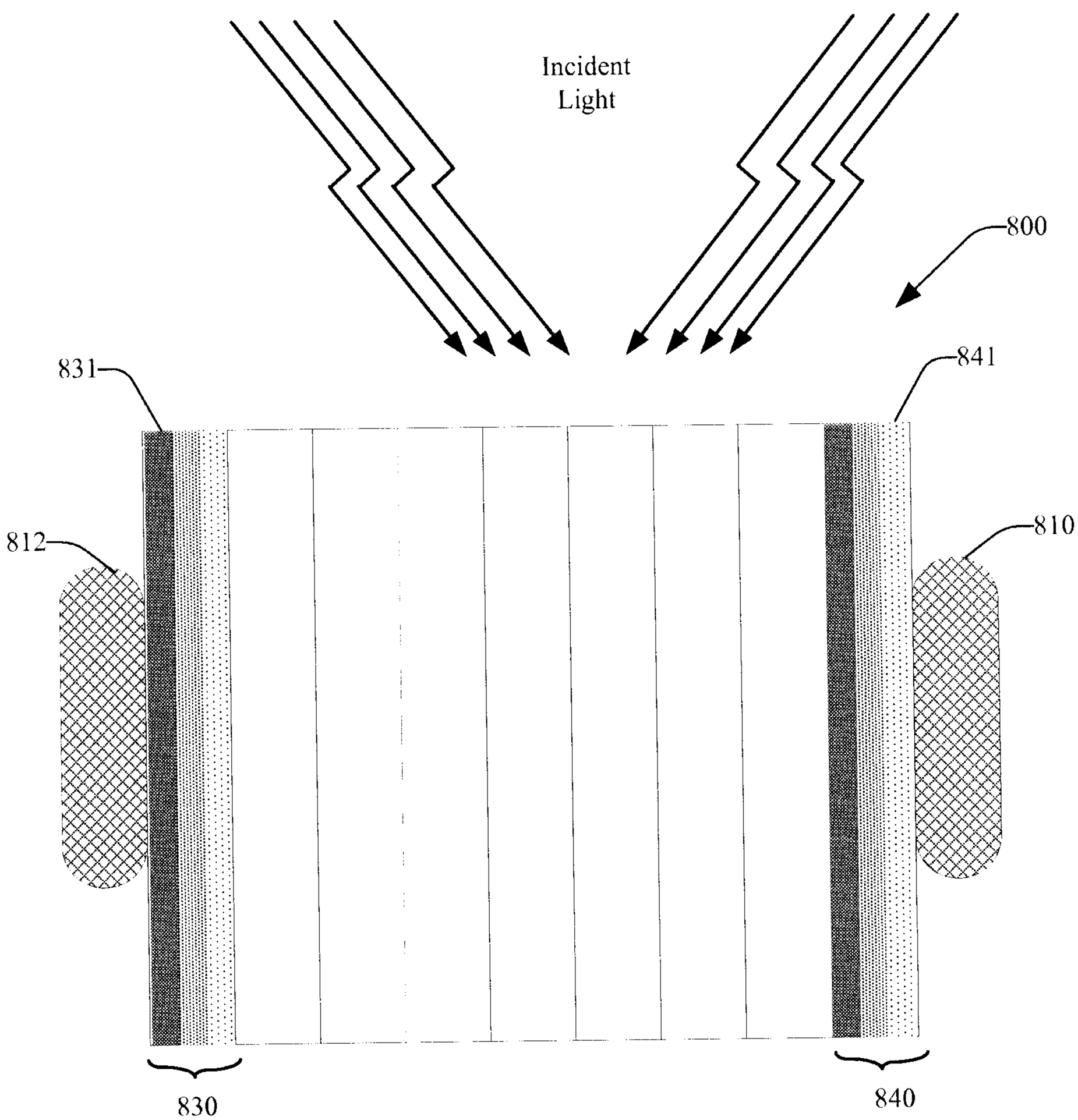

FIG. 8

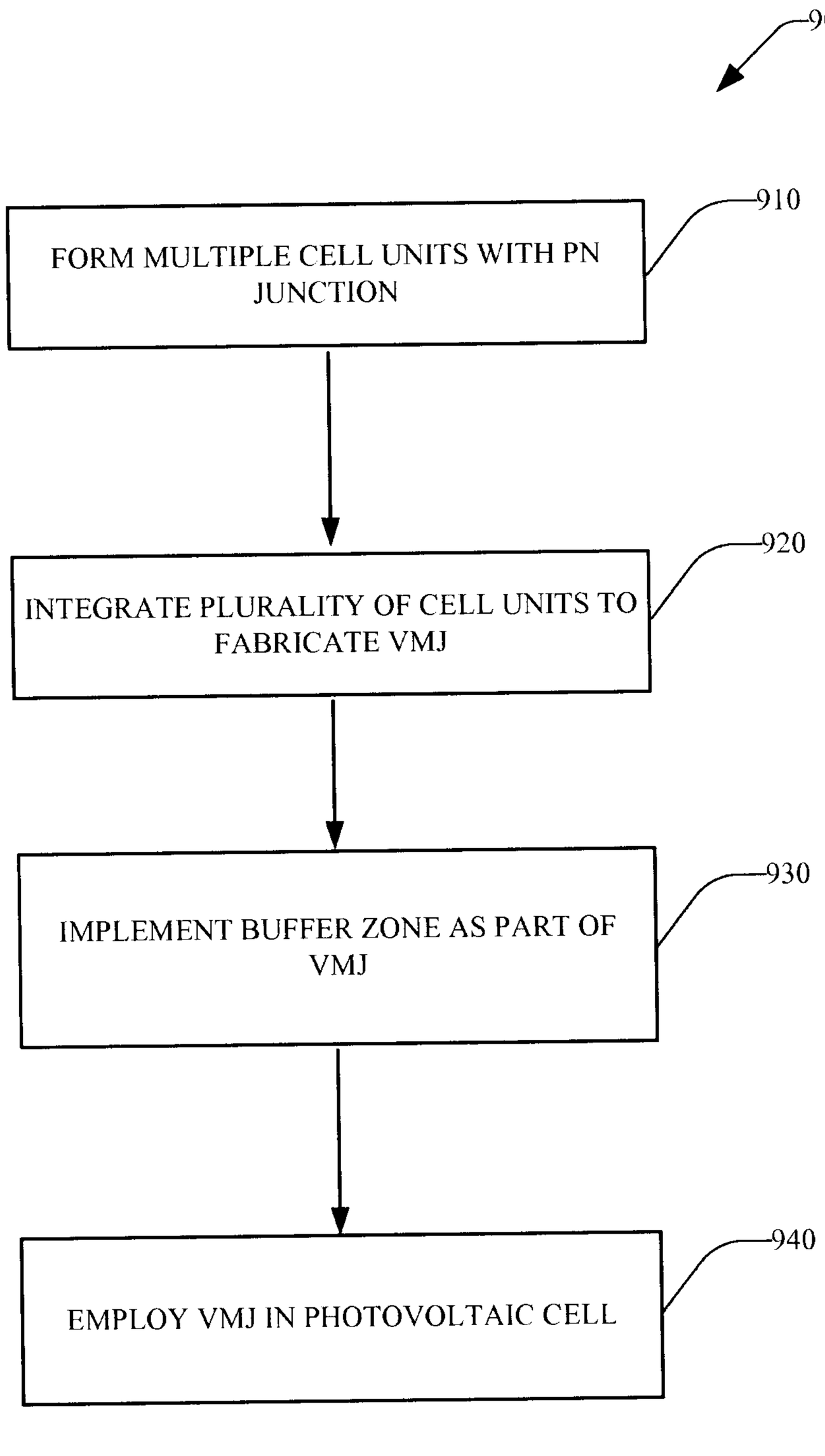
900
FORM MULTIPLE CELL UNITS WITH PN JUNCTION
910
INTEGRATE PLURALITY OF CELL UNITS TO FABRICATE VMJ
920
IMPLEMENT BUFFER ZONE AS PART OF VMJ
930
EMPLOY VMJ IN PHOTOVOLTAIC CELL
940

FIG. 9

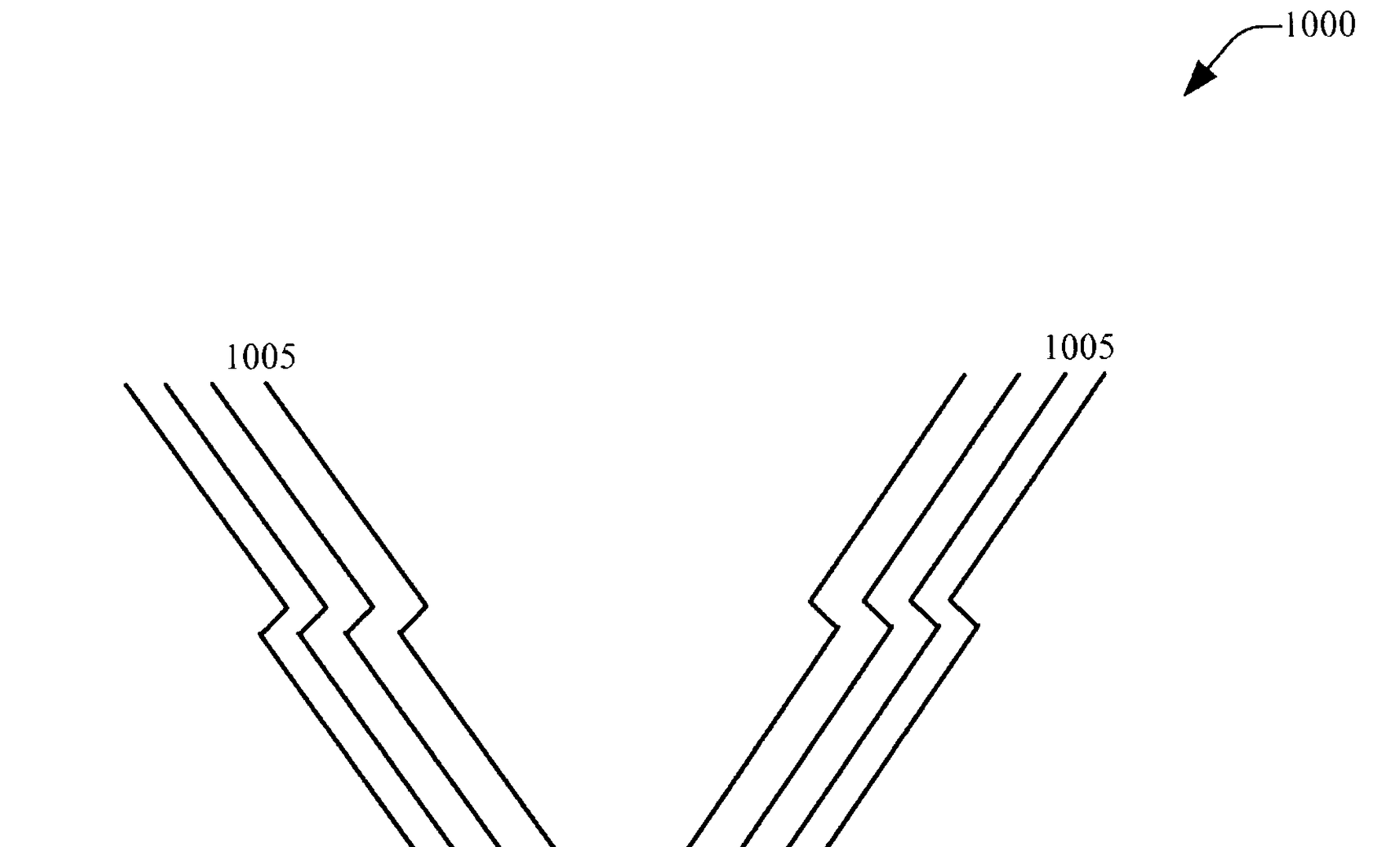
1000
1005
1005
1025
1023
PV_1
PV_2
PV_k
1027
1020
MODULAR ARRANGEMENT OF PHOTOVOLTAIC CELLS
ELECTRIC CURRENT

Fig. 10

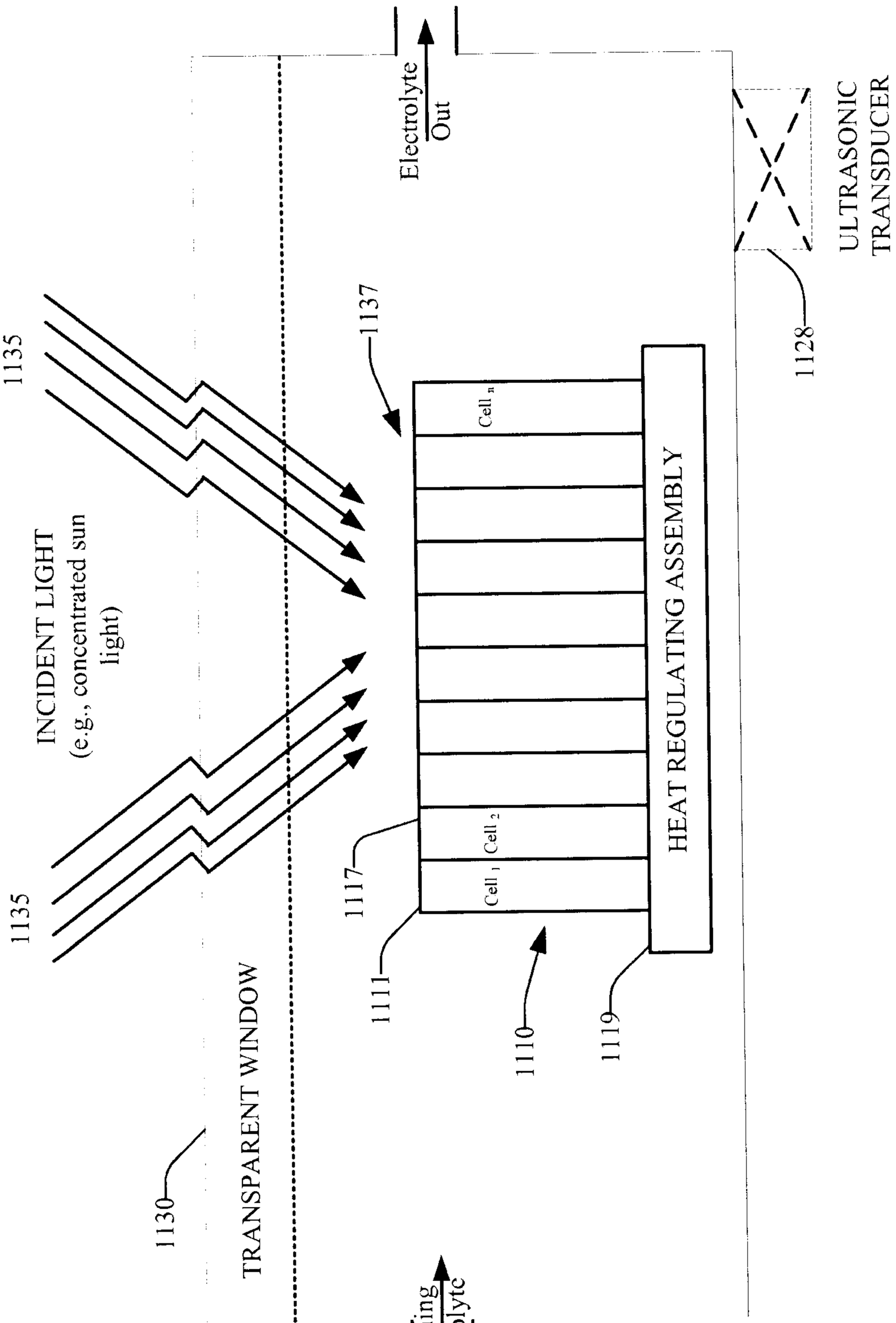
Electrolyte Out
1135
INCIDENT LIGHT
(e.g., concentrated sun light)
1135
1137
Cell n
HEAT REGULATING ASSEMBLY
ULTRASONIC TRANSDUCER
1128
1117
Cell 2
Cell 1
1111
1110
1119
TRANSPARENT WINDOW
1130
Incoming Electrolyte

FIG. 11

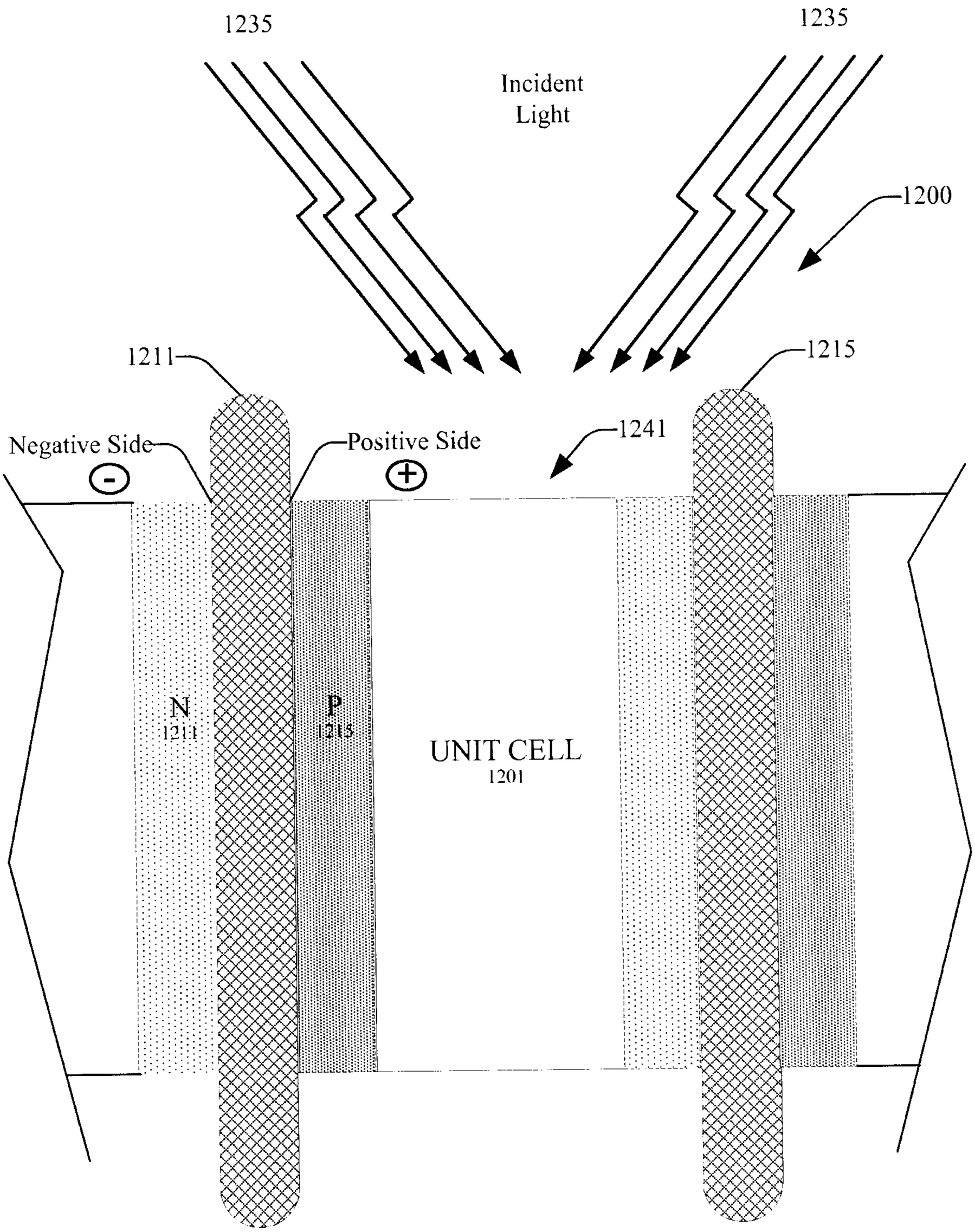
1235
Incident Light
1235
1200
1211
1215
1241
Negative Side
Positive Side
N
1211
P
1215
UNIT CELL
1201

FIG. 12

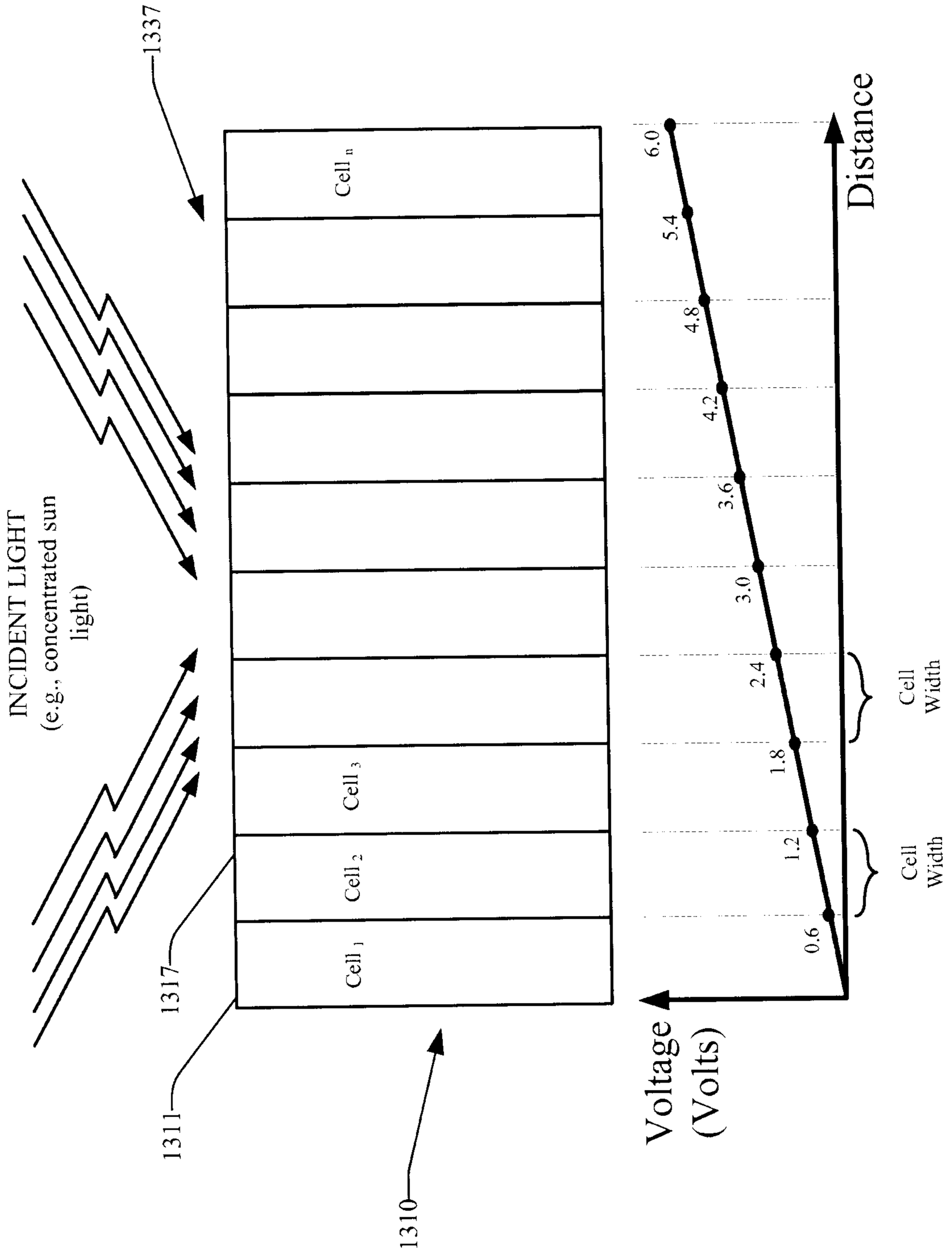
1337
INCIDENT LIGHT
(e.g., concentrated sun light)
Cell n
Cell 3
Cell 2
Cell 1
1317
1311
1310
6.0
5.4
4.8
4.2
3.6
3.0
2.4
1.8
1.2
0.6
Distance
Cell Width
Cell Width
Voltage (Volts)

FIG. 13

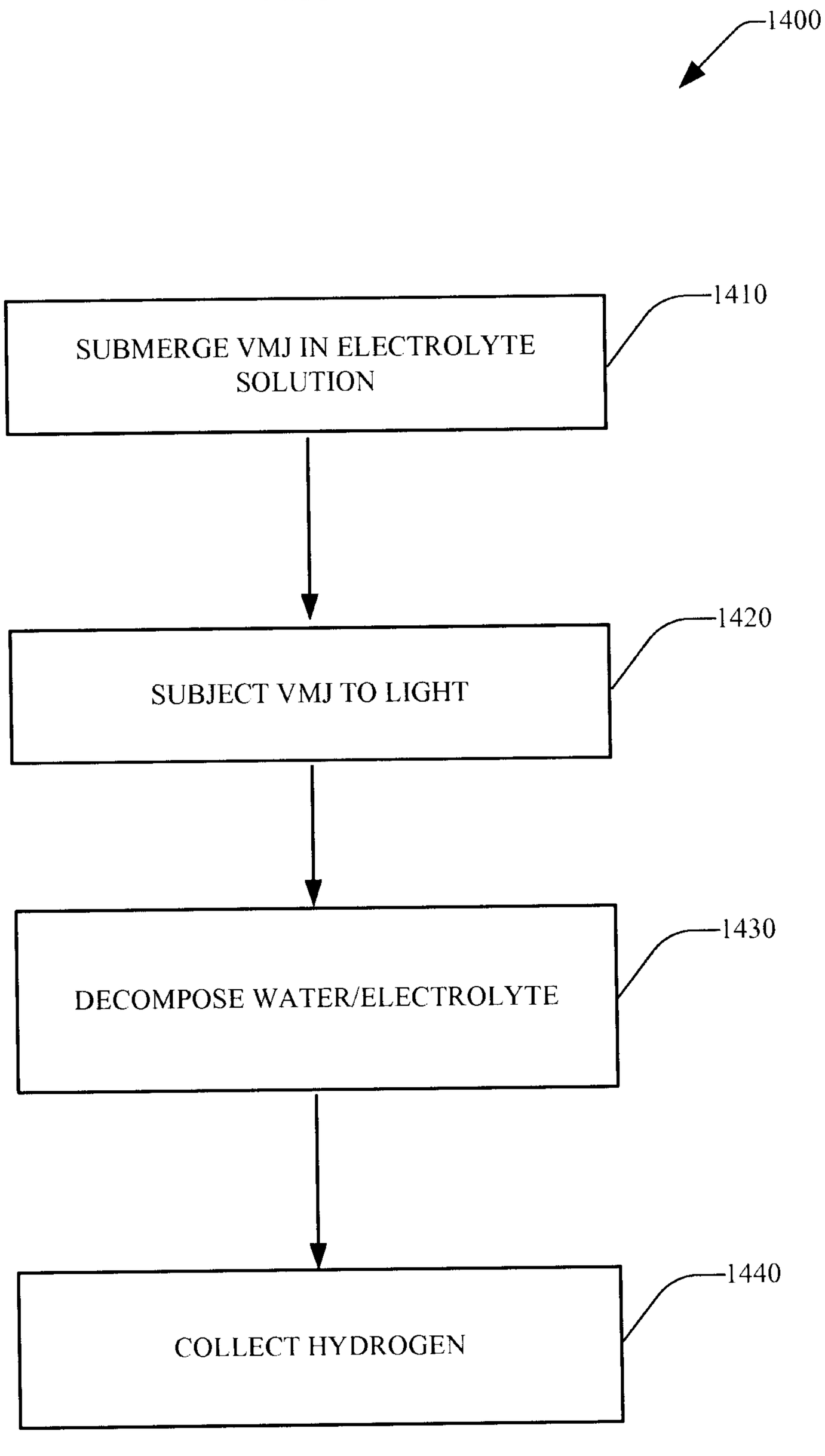
1400
SUBMERGE VMJ IN ELECTROLYTE SOLUTION
1410
SUBJECT VMJ TO LIGHT
1420
DECOMPOSE WATER/ELECTROLYTE
1430
COLLECT HYDROGEN
1440

FIG. 14

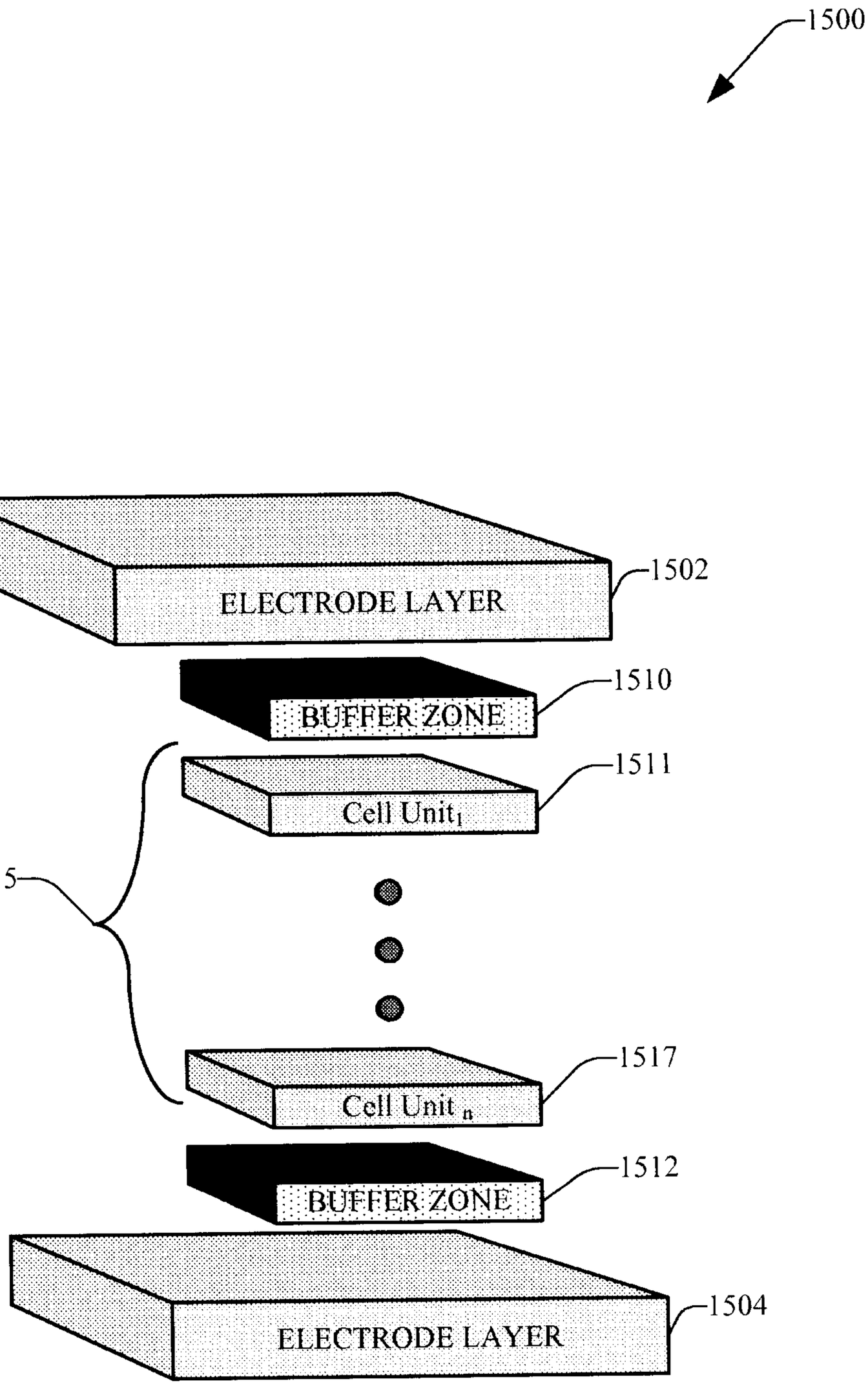
1500
ELECTRODE LAYER
1502
BUFFER ZONE
1510
Cell Unit$_1$
1511
1515
Cell Unit $_n$
1517
BUFFER ZONE
1512
ELECTRODE LAYER
1504

FIG. 15

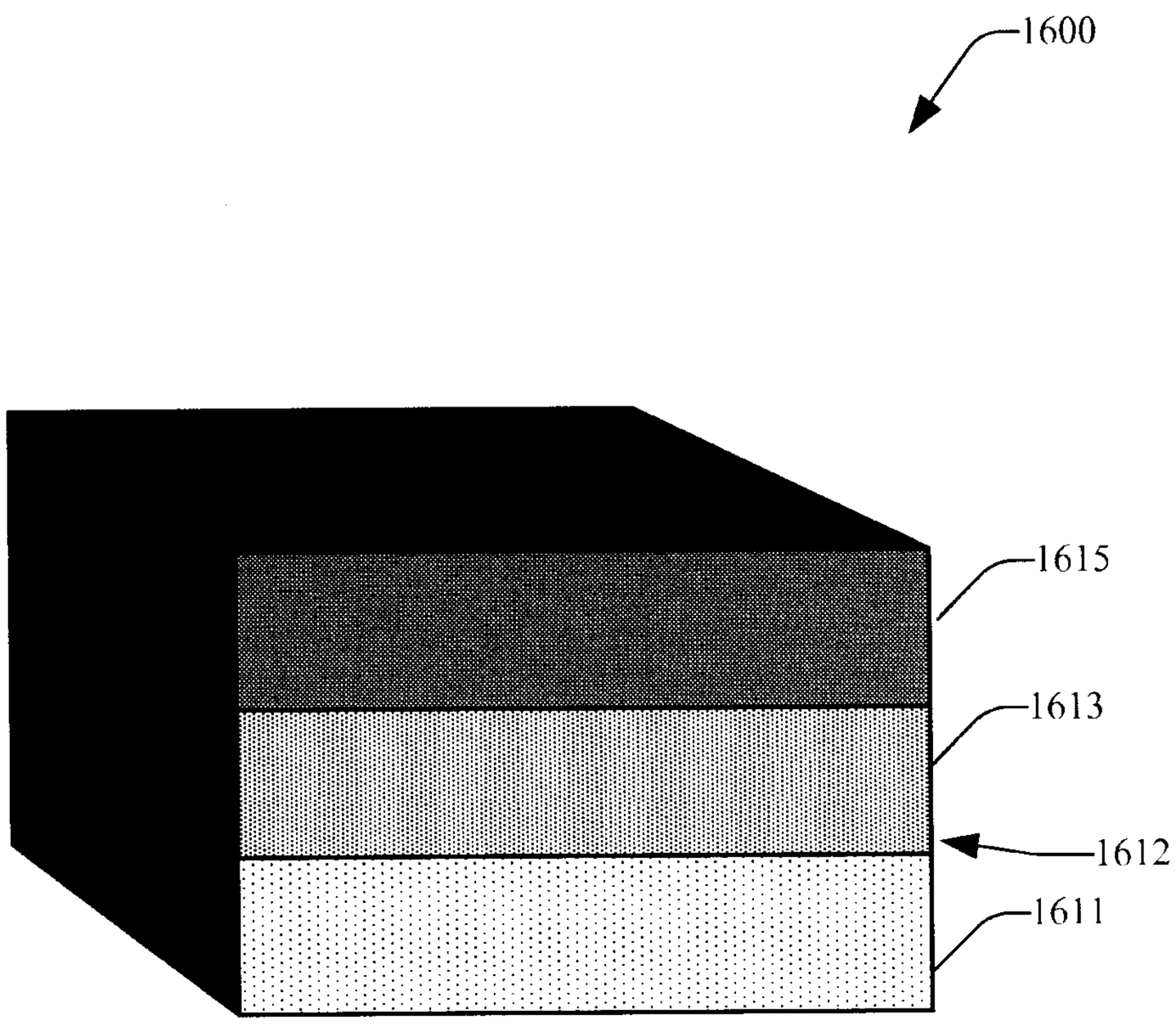

FIG. 16

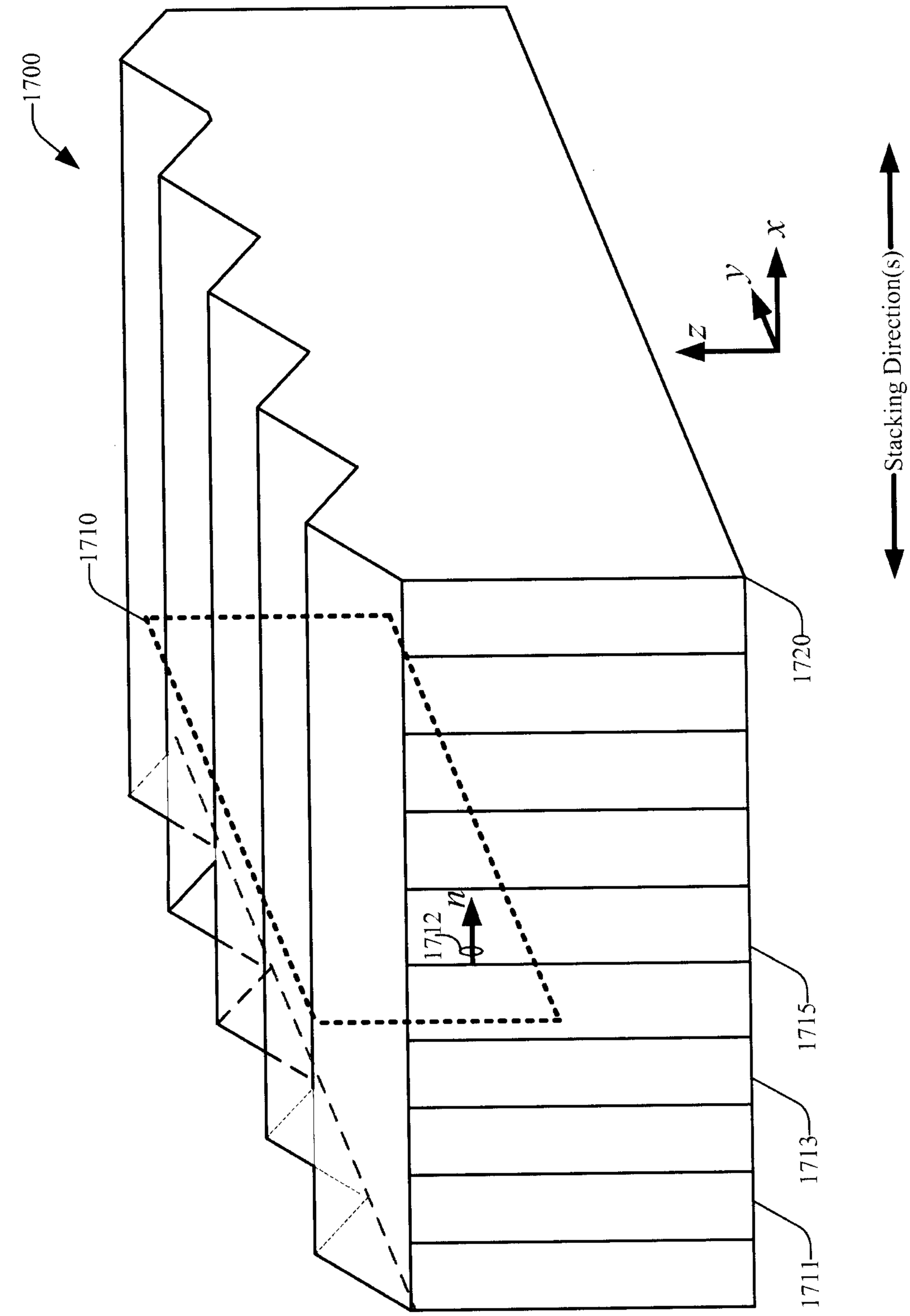
1700
1710
1720
1712
1715
1713
1711
x
y
z
n
Stacking Direction(s)

FIG. 17

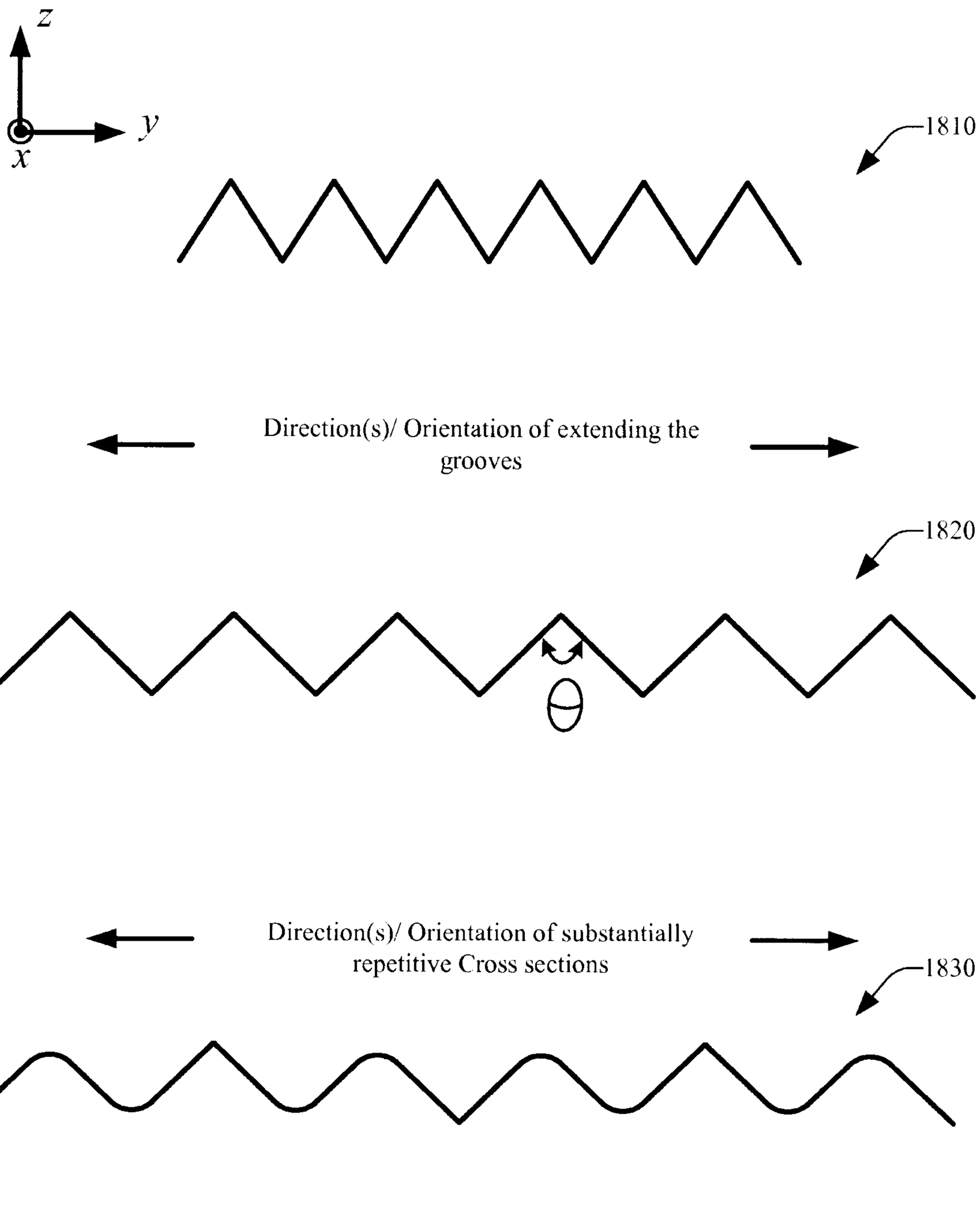
z
y
x
1810
Direction(s)/ Orientation of extending the grooves
1820
θ
Direction(s)/ Orientation of substantially repetitive Cross sections
1830

FIG. 18

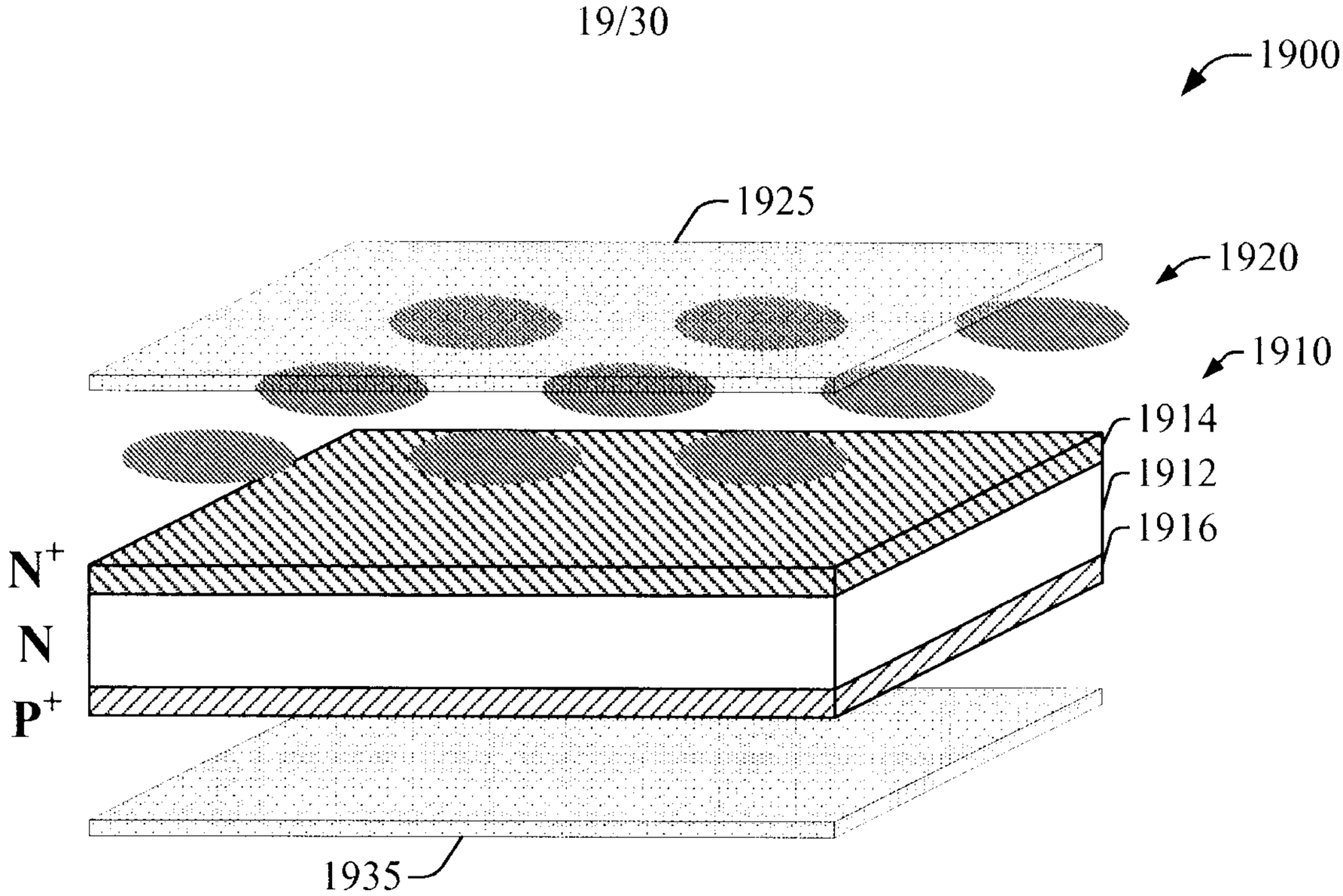

FIG. 19A

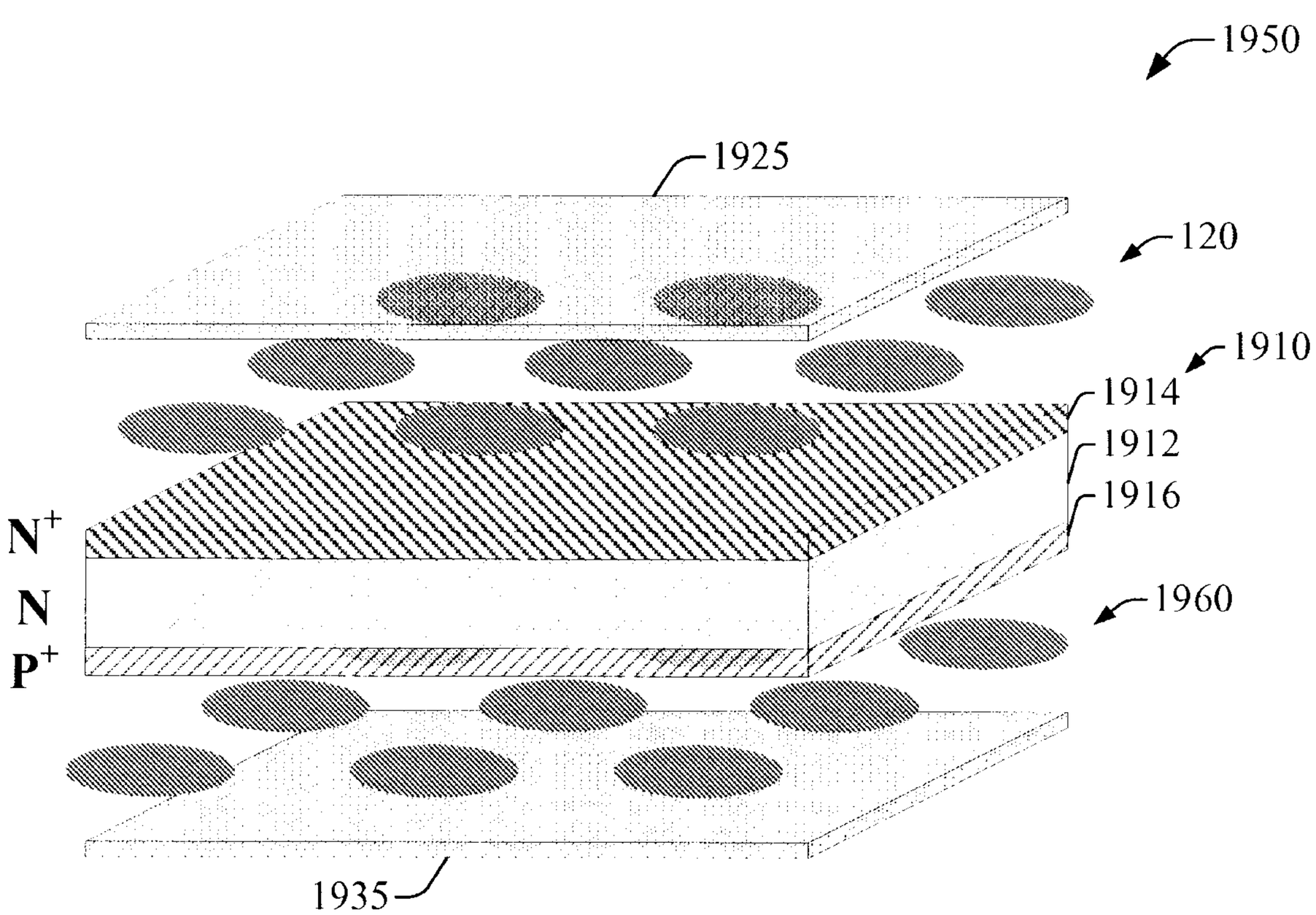

FIG. 19B

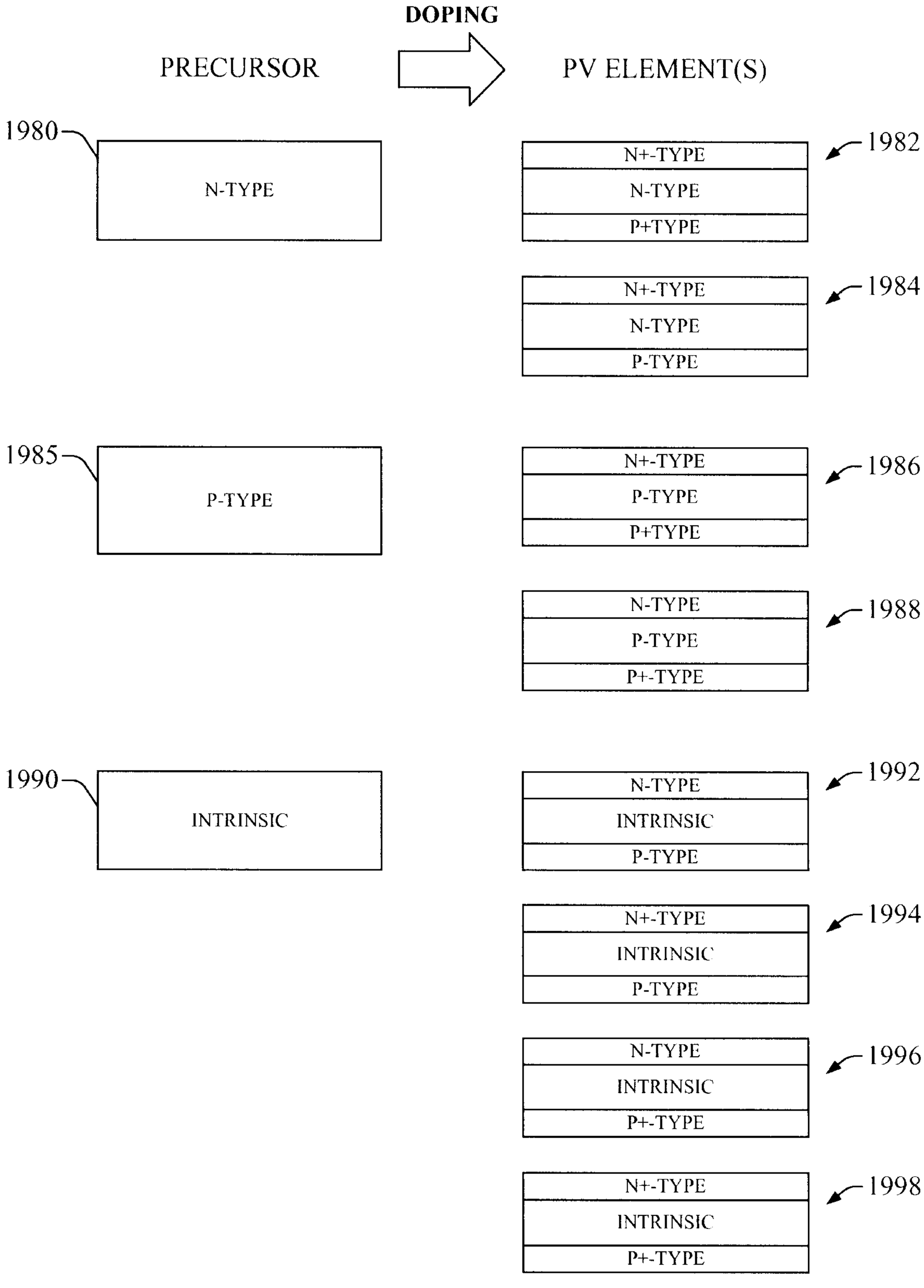
DOPING
PRECURSOR
PV ELEMENT(S)
1980
N-TYPE
N+-TYPE
N-TYPE
P+TYPE
1982
N+-TYPE
N-TYPE
P-TYPE
1984
1985
P-TYPE
N+-TYPE
P-TYPE
P+TYPE
1986
N-TYPE
P-TYPE
P+-TYPE
1988
1990
INTRINSIC
N-TYPE
INTRINSIC
P-TYPE
1992
N+-TYPE
INTRINSIC
P-TYPE
1994
N-TYPE
INTRINSIC
P+-TYPE
1996
N+-TYPE
INTRINSIC
P+-TYPE
1998

FIG. 19C

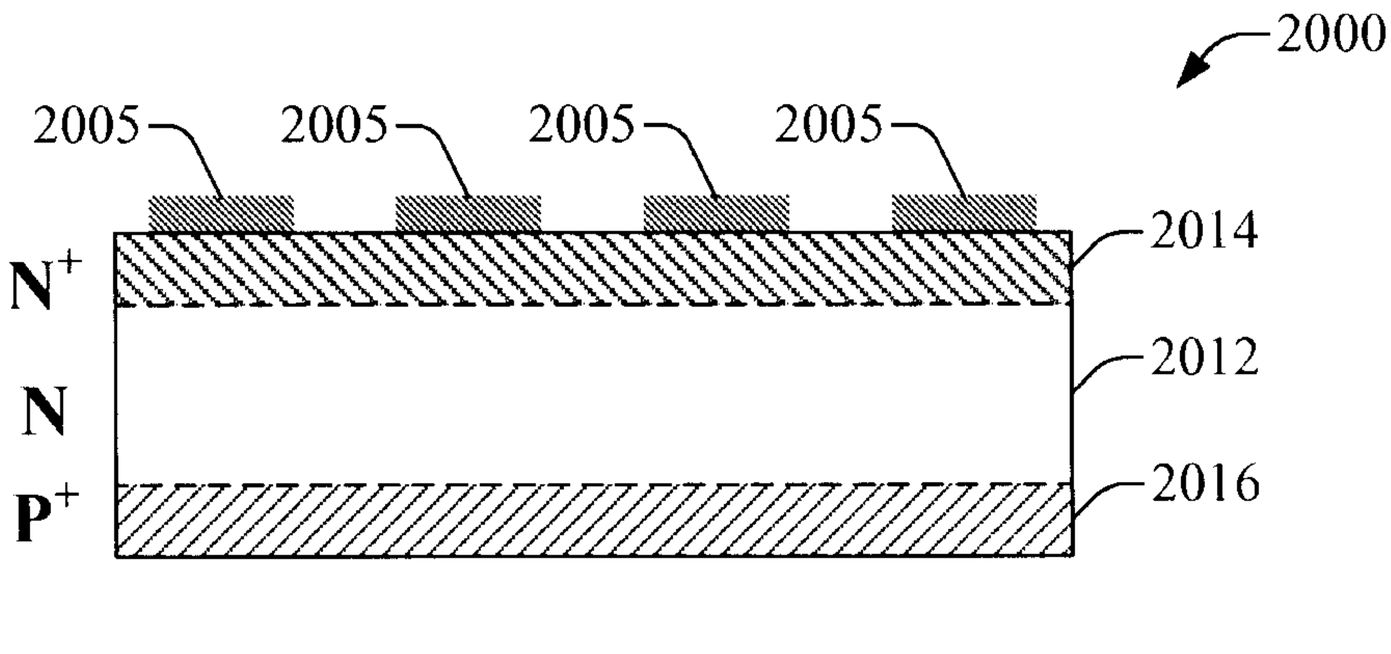

FIG. 20A

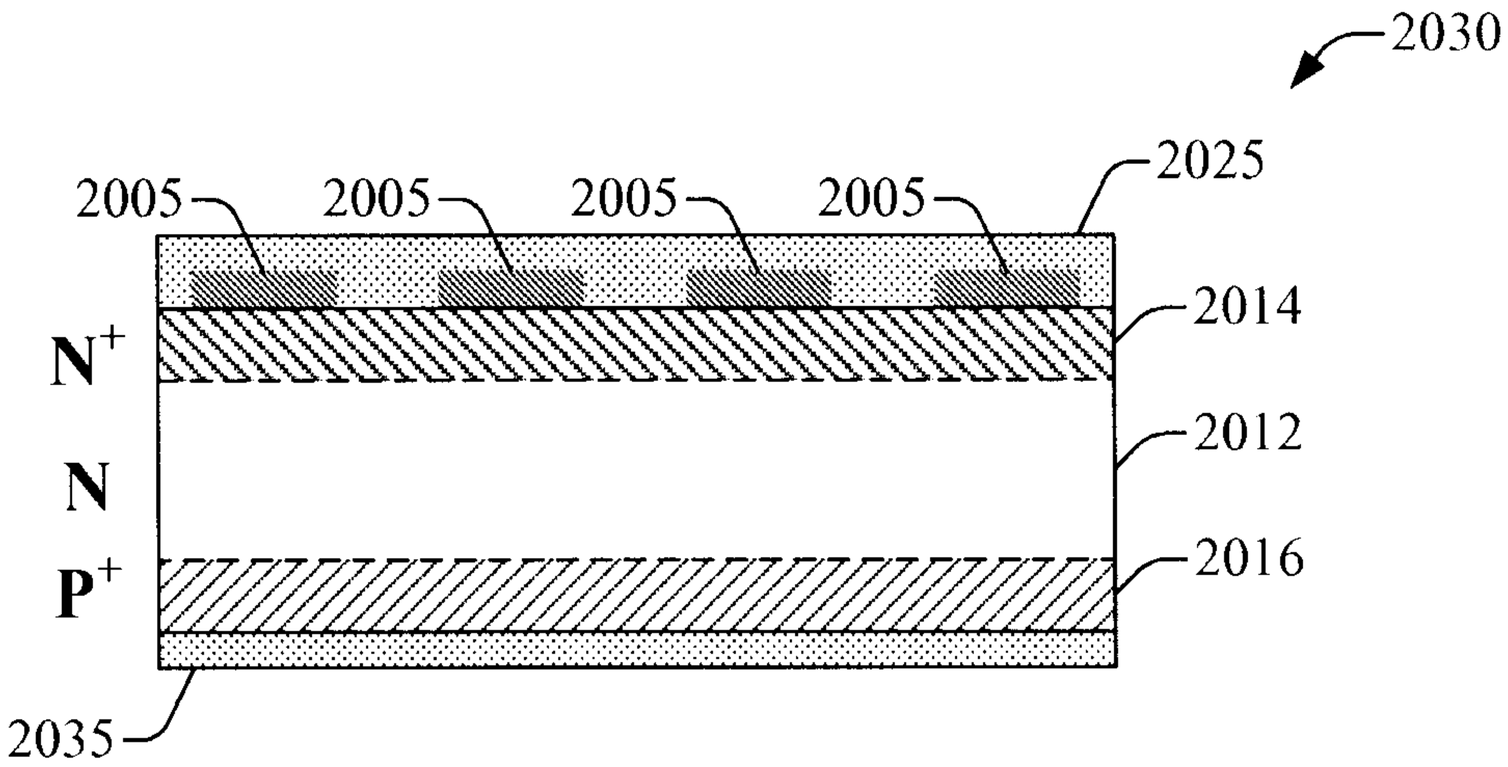

FIG. 20B

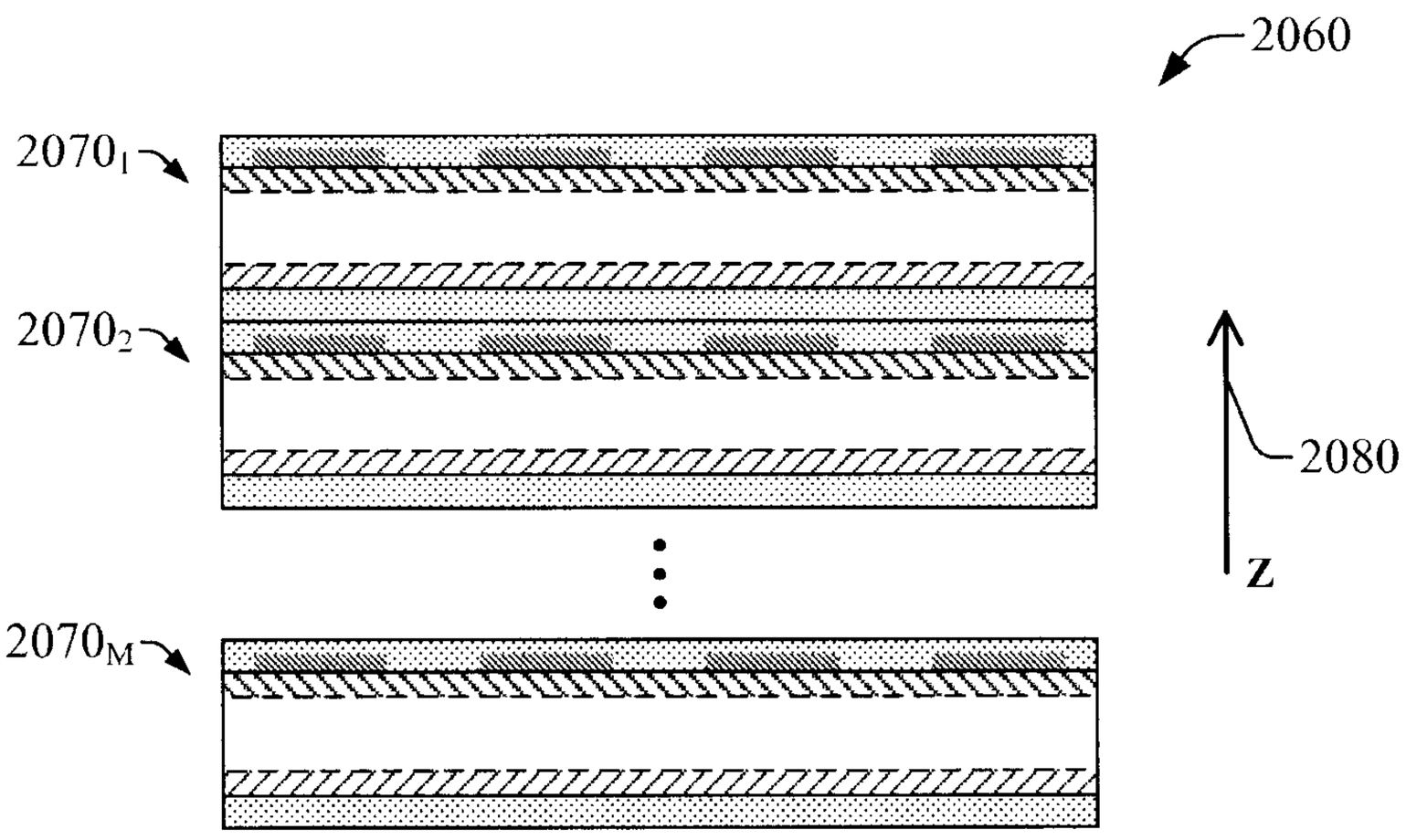

FIG. 20C

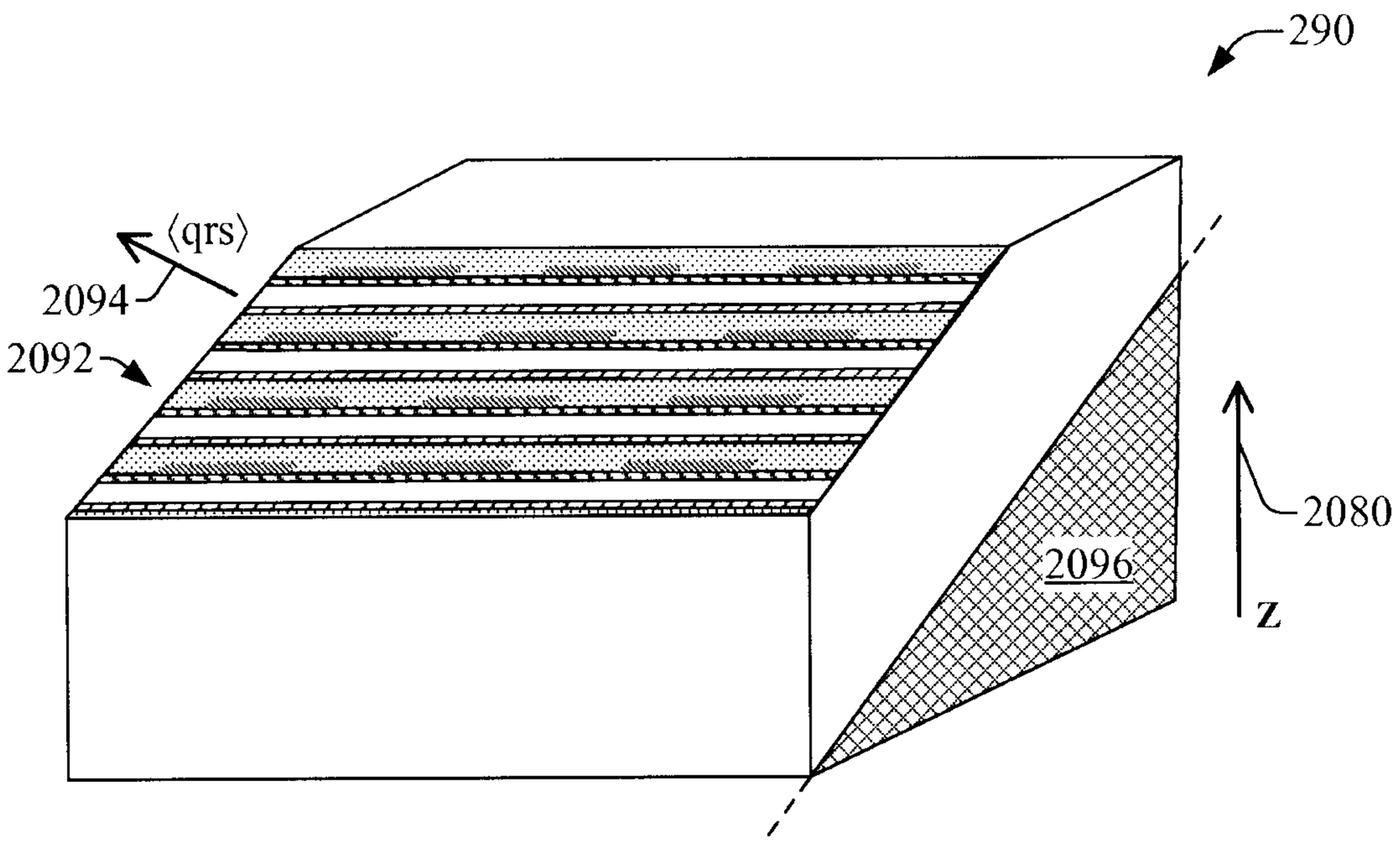

FIG. 20D

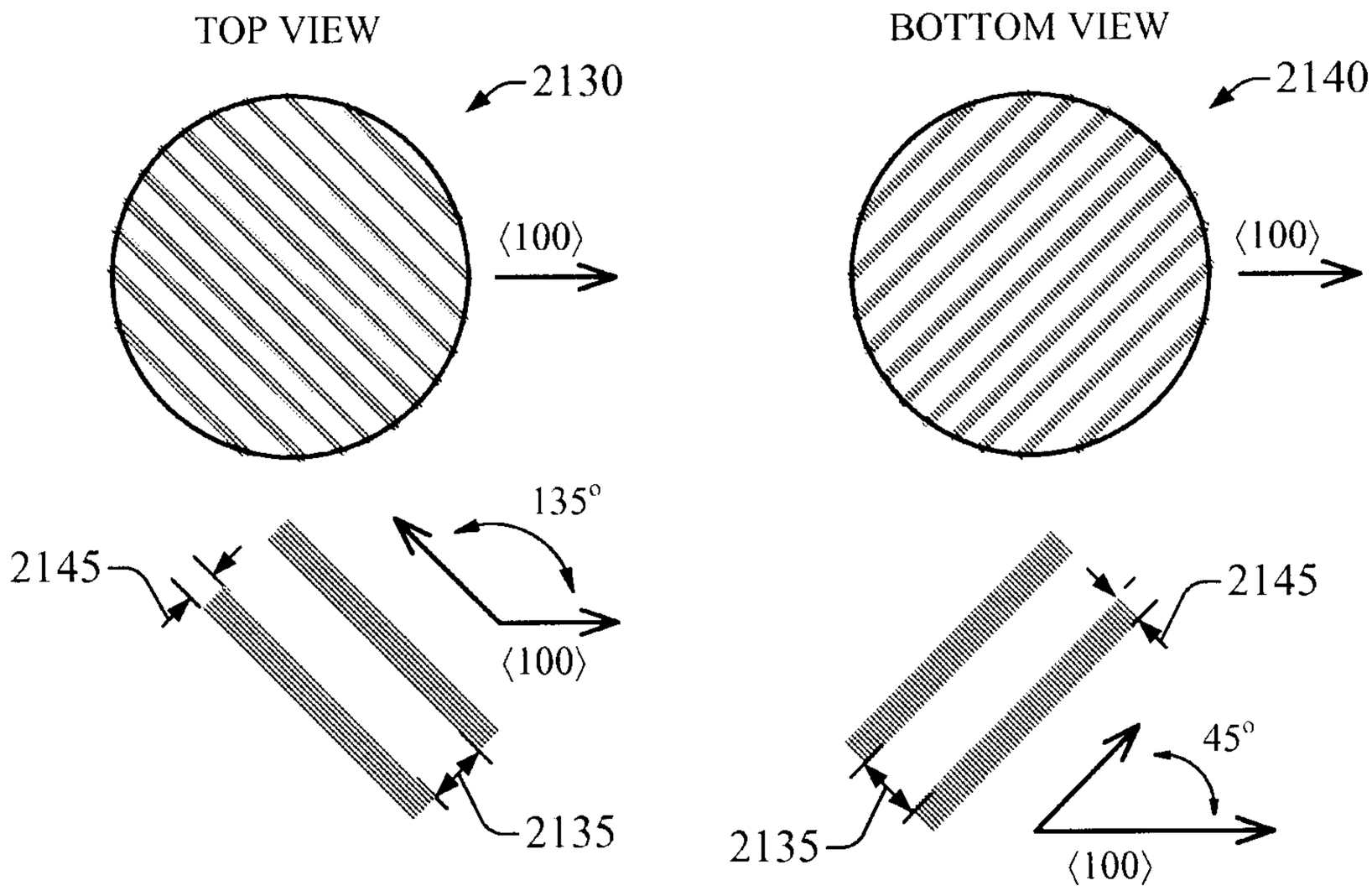

FIG. 21A

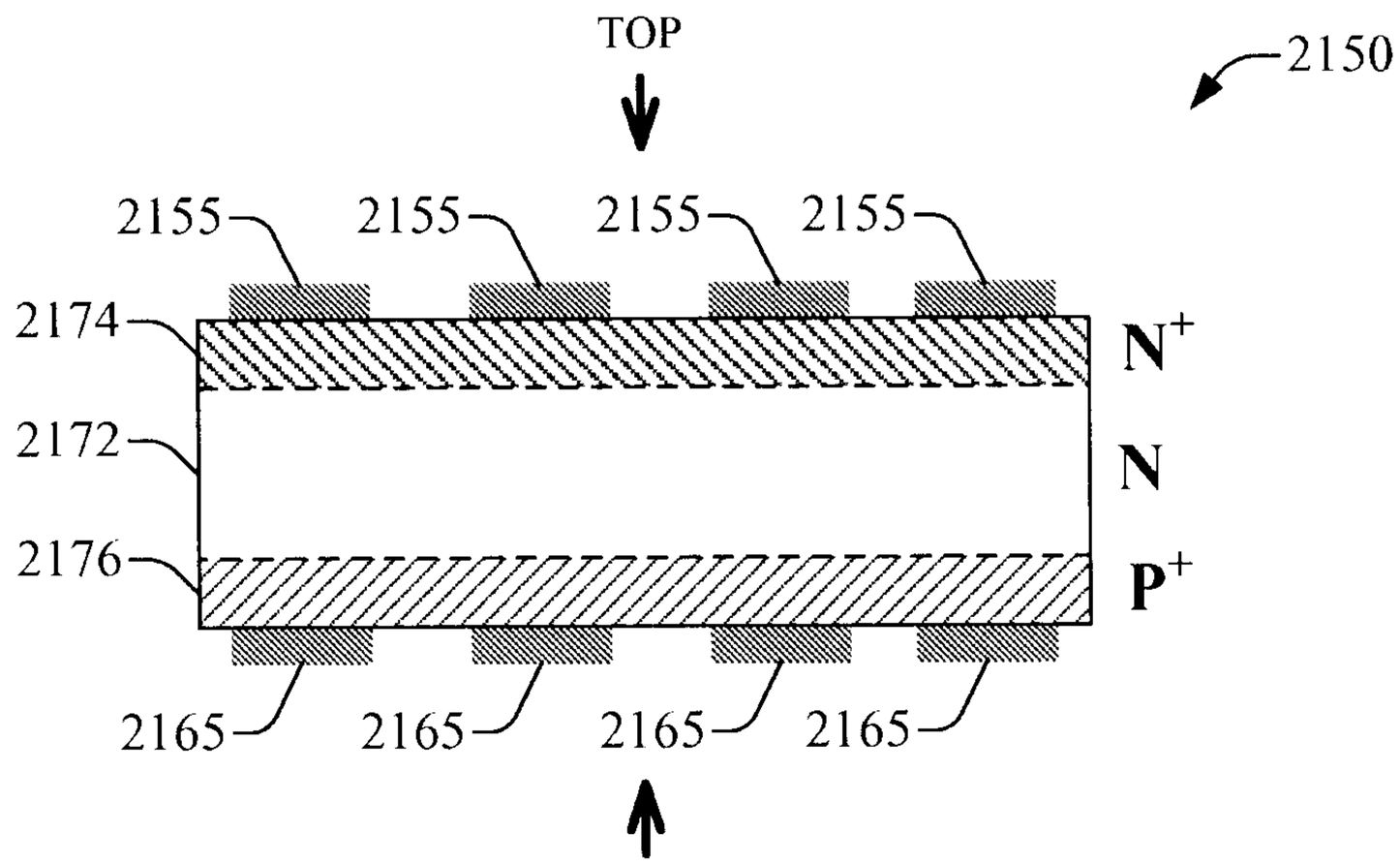

FIG. 21B

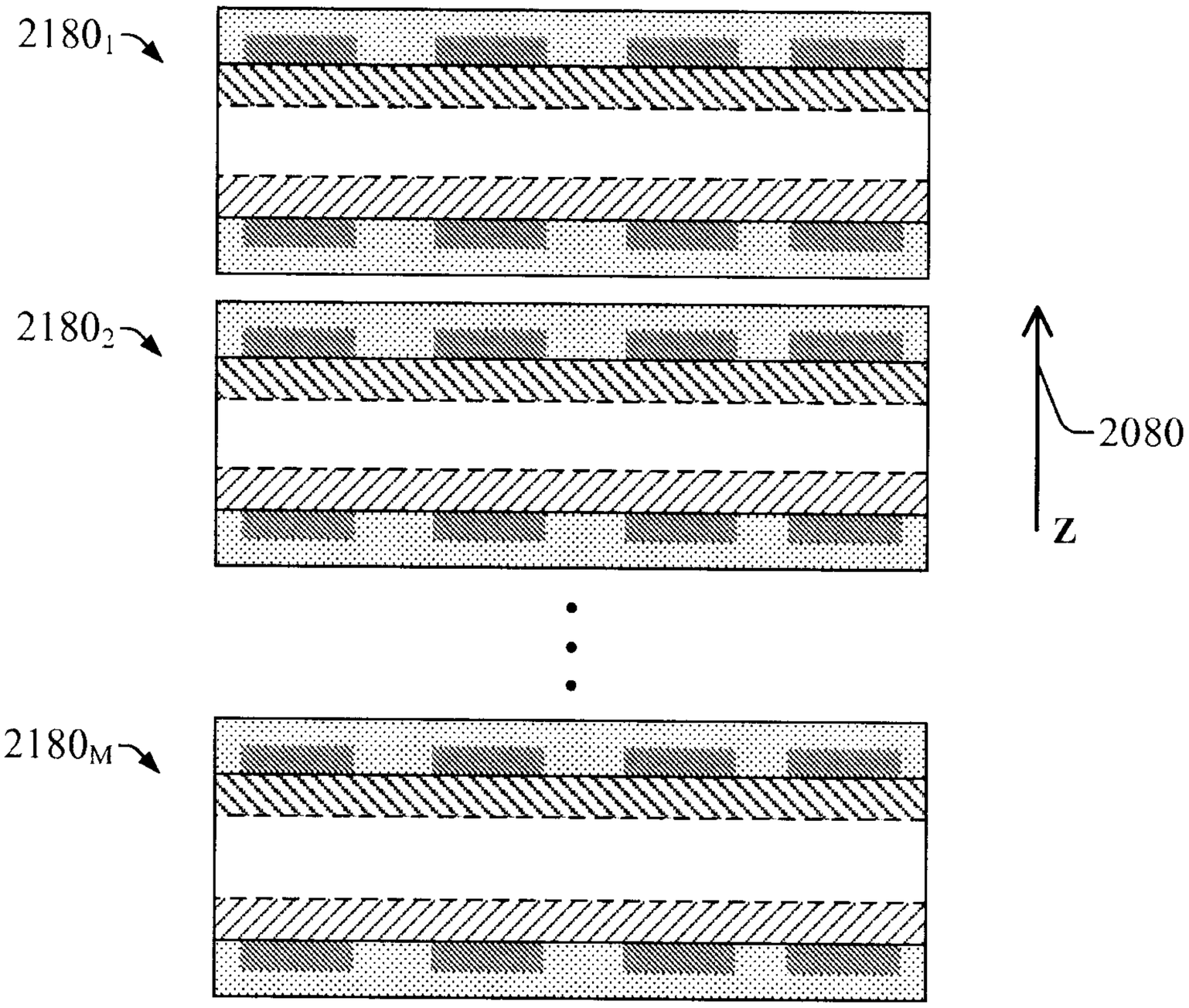

FIG. 21C

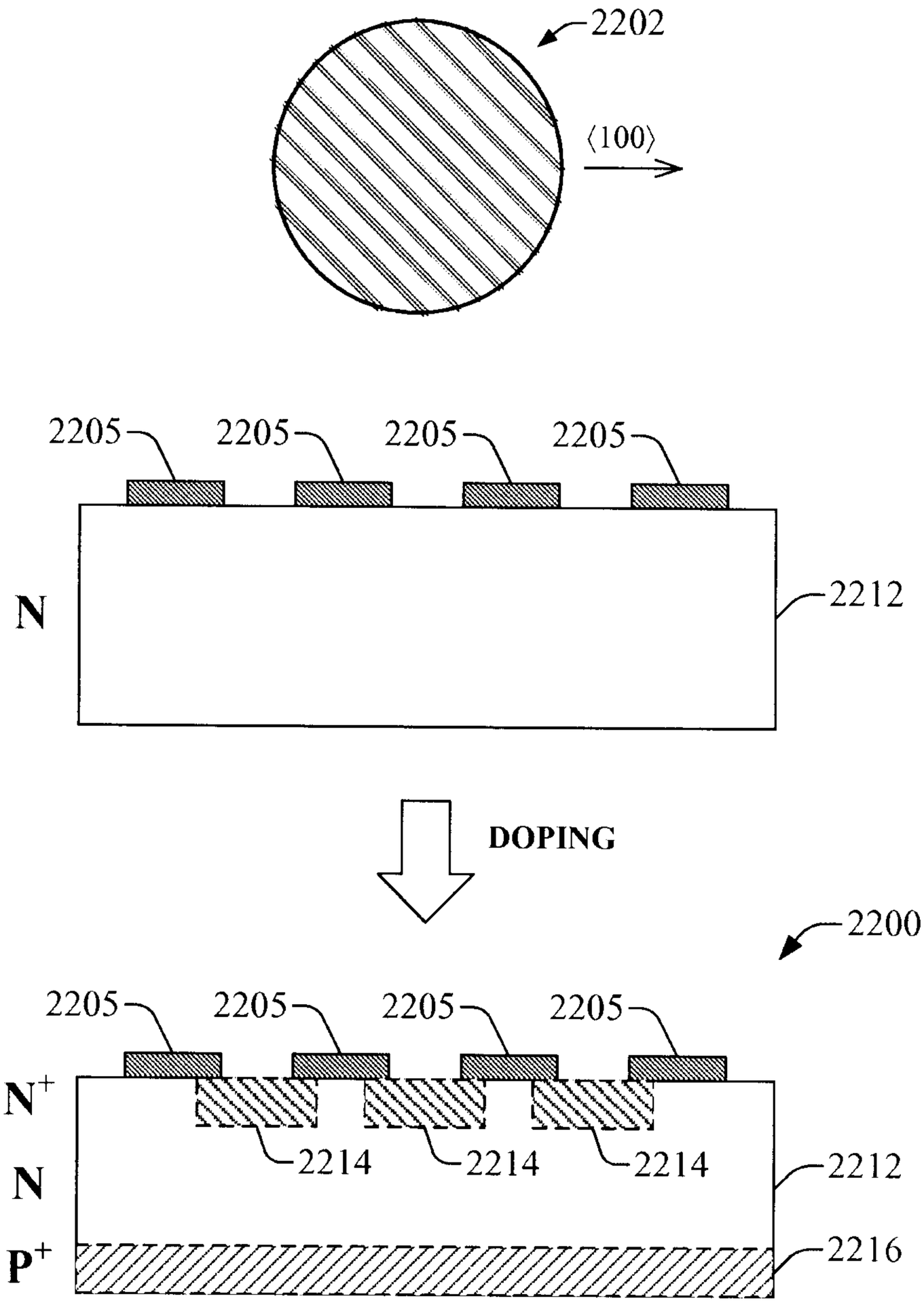
2202
⟨100⟩
2205
2205
2205
2205
N
2212
DOPING
2200
2205
2205
2205
2205
N+
N
P+
2214
2214
2214
2212
2216

FIG. 22

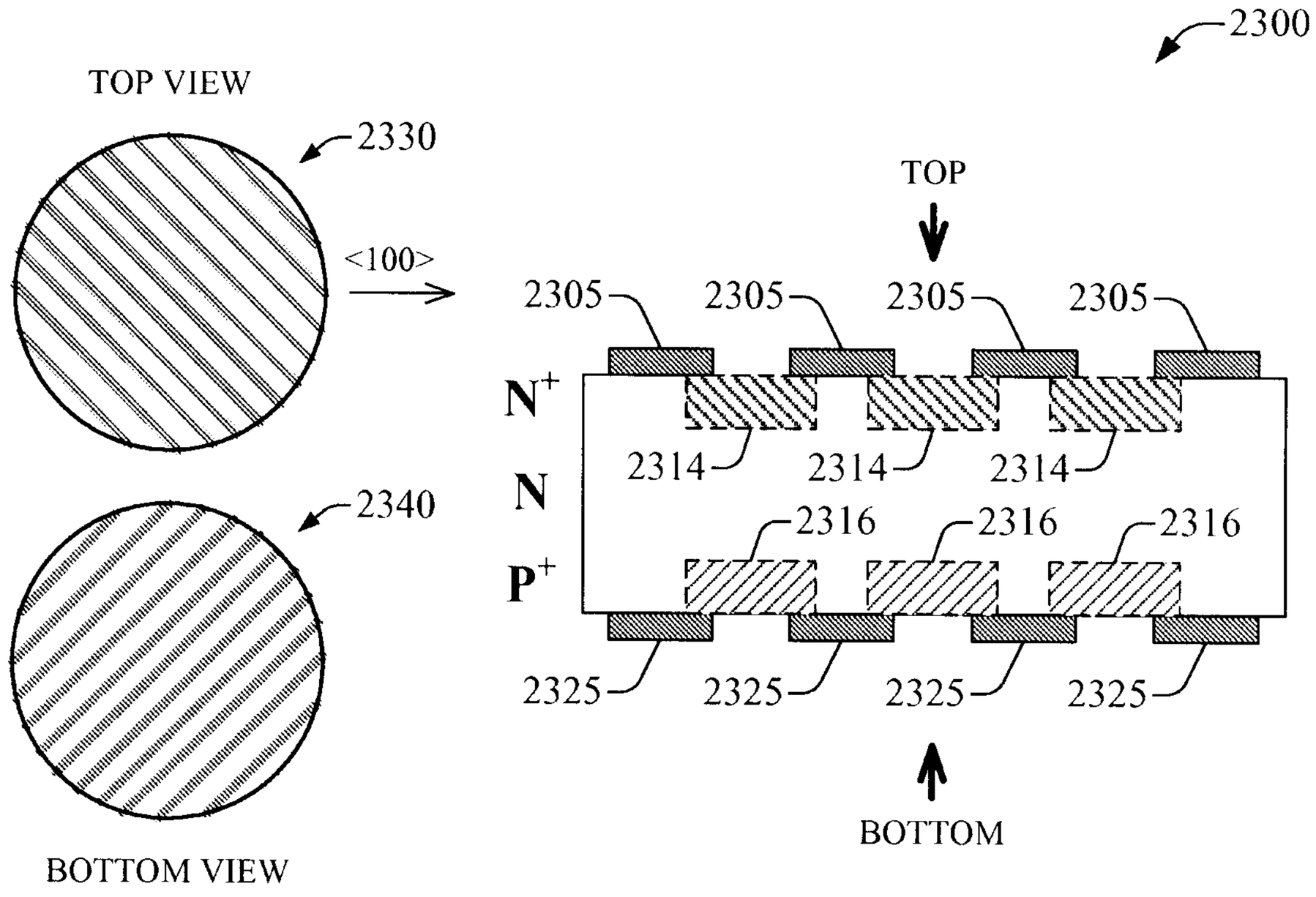

FIG. 23A

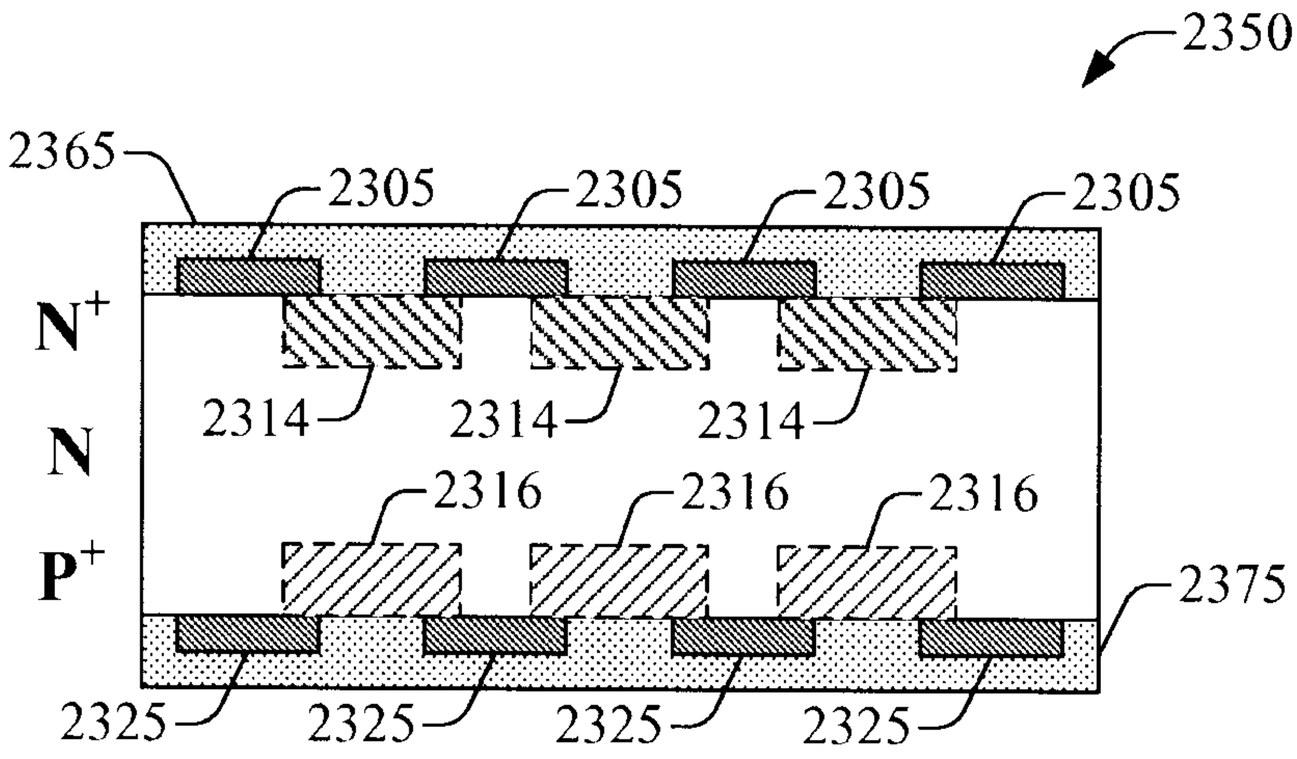

FIG. 23B

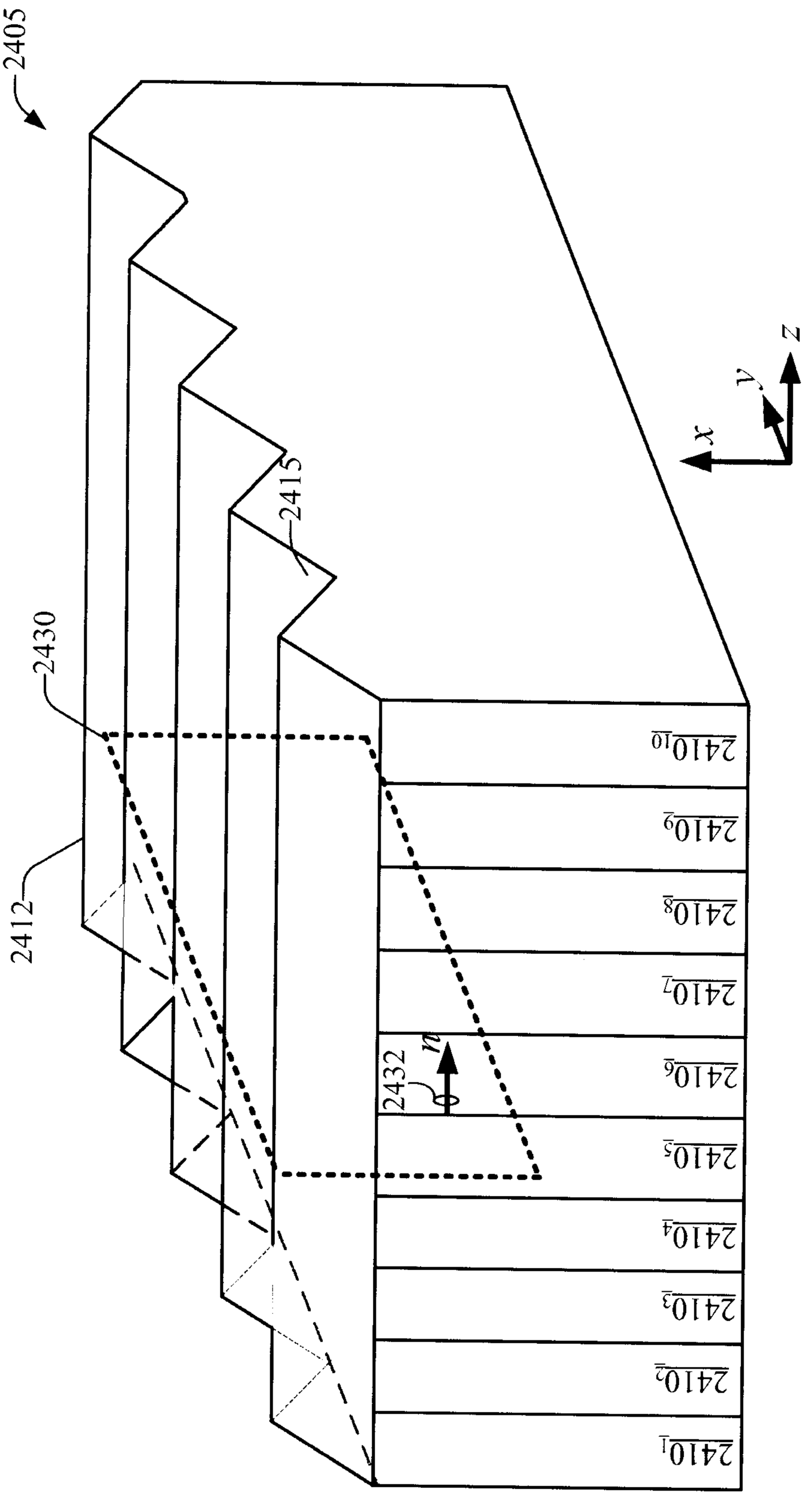
2405
2430
2415
2412
2432
2410_{10}
2410_9
2410_8
2410_7
2410_6
2410_5
2410_4
2410_3
2410_2
2410_1
x
y
z
h
STACKING DIRECTION

FIG. 24

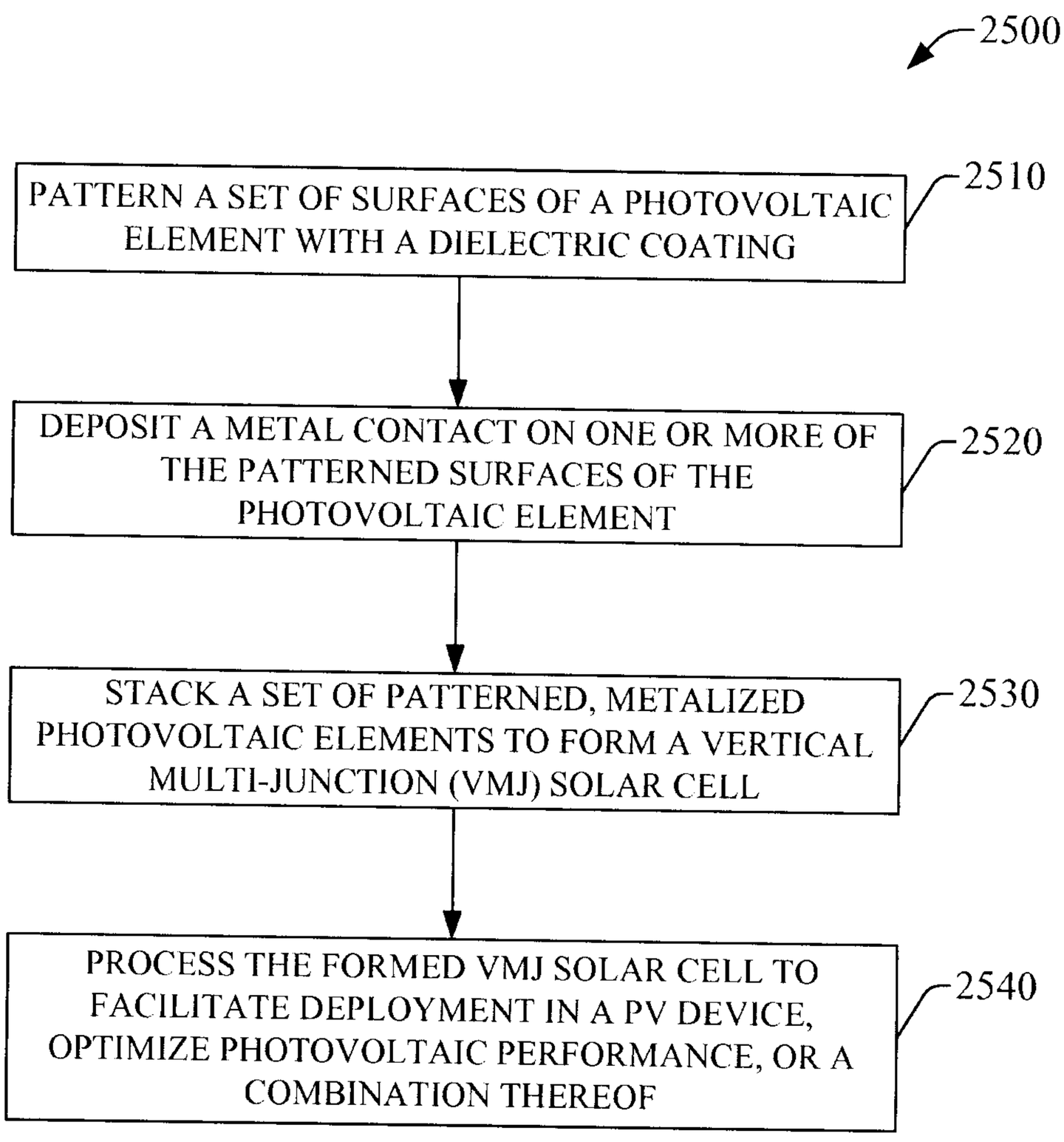
2500
PATTERN A SET OF SURFACES OF A PHOTOVOLTAIC ELEMENT WITH A DIELECTRIC COATING
2510
DEPOSIT A METAL CONTACT ON ONE OR MORE OF THE PATTERNED SURFACES OF THE PHOTOVOLTAIC ELEMENT
2520
STACK A SET OF PATTERNED, METALIZED PHOTOVOLTAIC ELEMENTS TO FORM A VERTICAL MULTI-JUNCTION (VMJ) SOLAR CELL
2530
PROCESS THE FORMED VMJ SOLAR CELL TO FACILITATE DEPLOYMENT IN A PV DEVICE, OPTIMIZE PHOTOVOLTAIC PERFORMANCE, OR A COMBINATION THEREOF
2540

FIG. 25

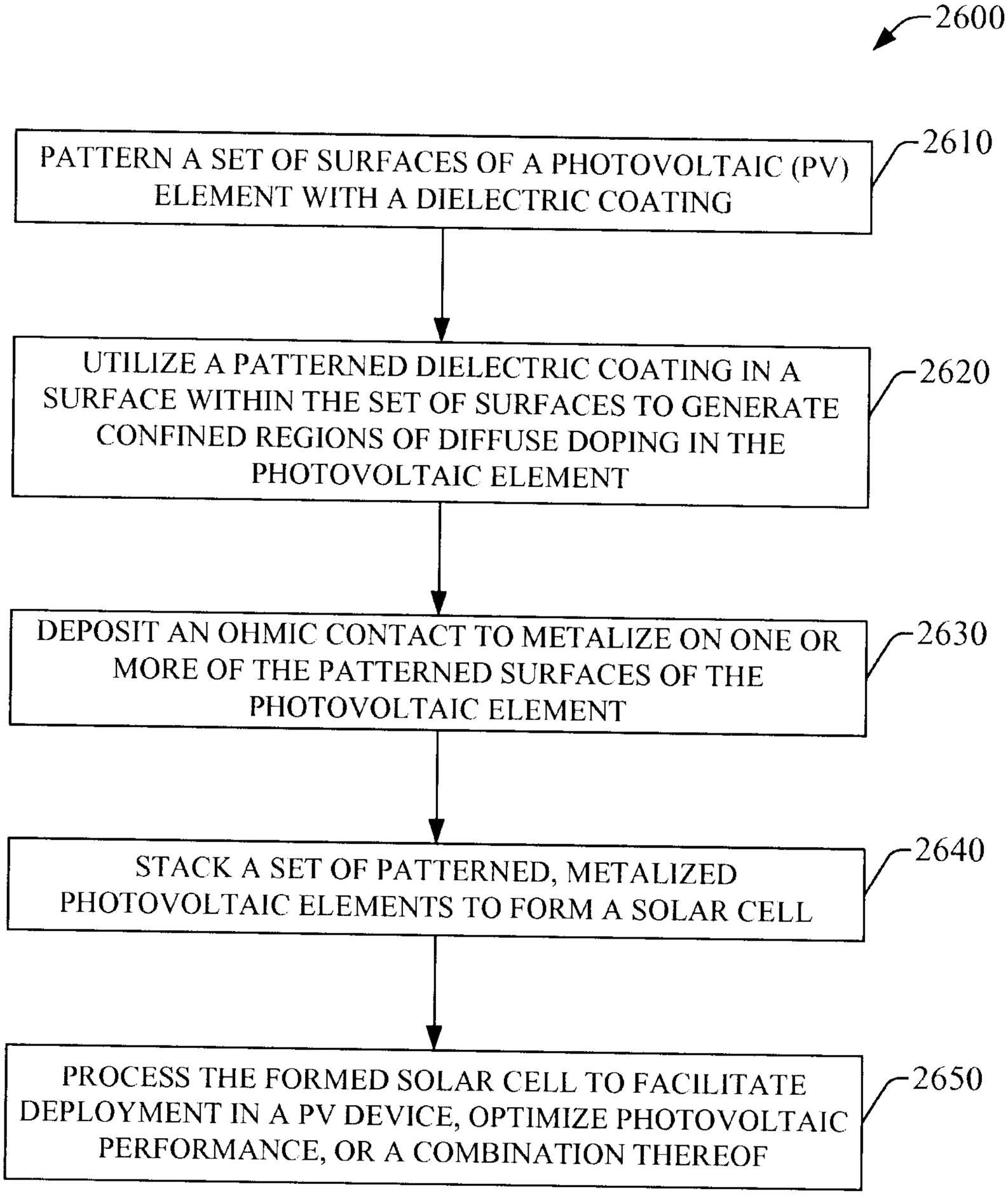
2600
PATTERN A SET OF SURFACES OF A PHOTOVOLTAIC (PV) ELEMENT WITH A DIELECTRIC COATING
2610
UTILIZE A PATTERNED DIELECTRIC COATING IN A SURFACE WITHIN THE SET OF SURFACES TO GENERATE CONFINED REGIONS OF DIFFUSE DOPING IN THE PHOTOVOLTAIC ELEMENT
2620
DEPOSIT AN OHMIC CONTACT TO METALIZE ON ONE OR MORE OF THE PATTERNED SURFACES OF THE PHOTOVOLTAIC ELEMENT
2630
STACK A SET OF PATTERNED, METALIZED PHOTOVOLTAIC ELEMENTS TO FORM A SOLAR CELL
2640
PROCESS THE FORMED SOLAR CELL TO FACILITATE DEPLOYMENT IN A PV DEVICE, OPTIMIZE PHOTOVOLTAIC PERFORMANCE, OR A COMBINATION THEREOF
2650

FIG. 26

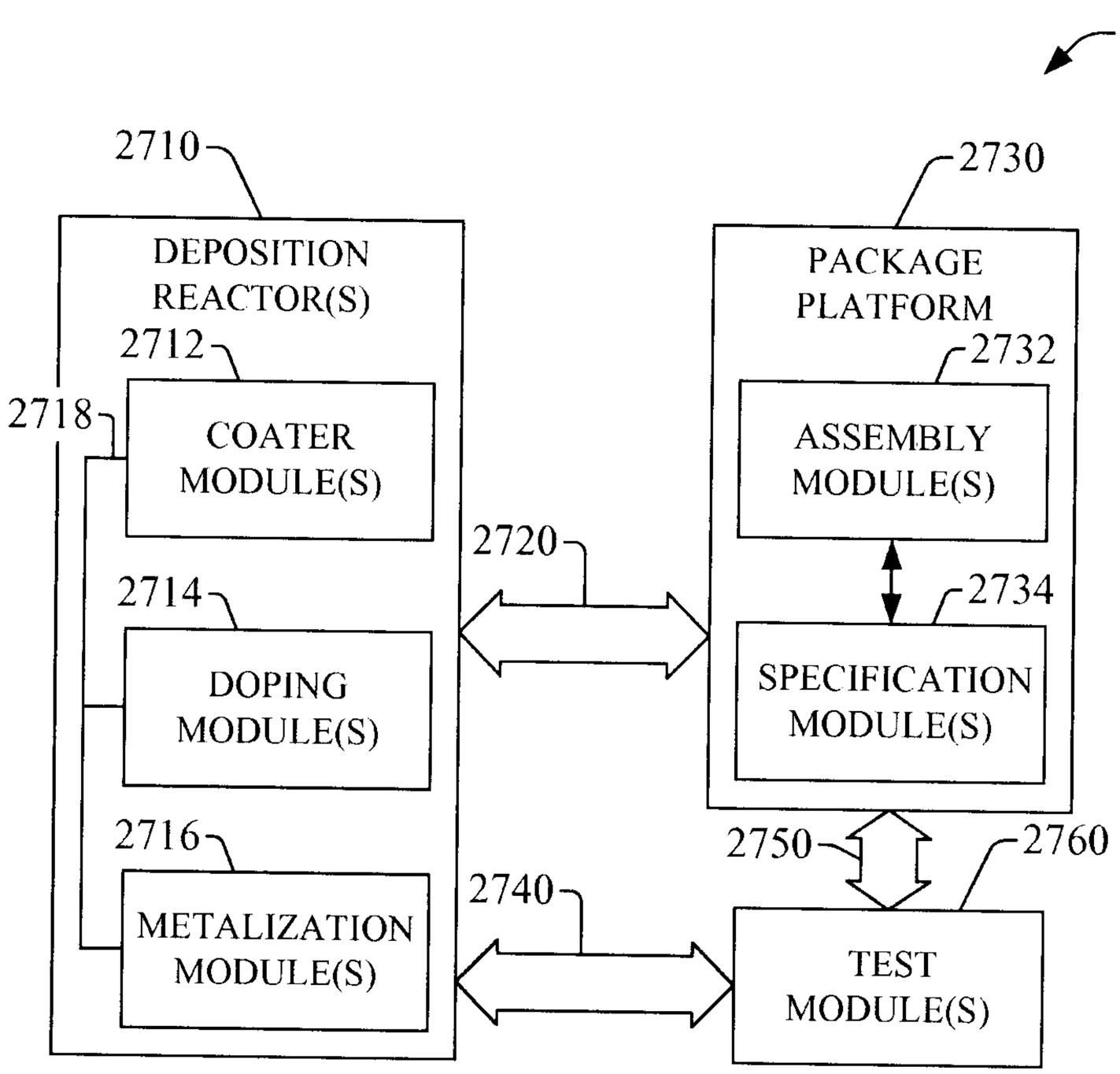
2700
2710
DEPOSITION REACTOR(S)
2712
2718
COATER MODULE(S)
2714
DOPING MODULE(S)
2716
METALIZATION MODULE(S)
2720
2730
PACKAGE PLATFORM
2732
ASSEMBLY MODULE(S)
2734
SPECIFICATION MODULE(S)
2750
2760
2740
TEST MODULE(S)

FIG. 27

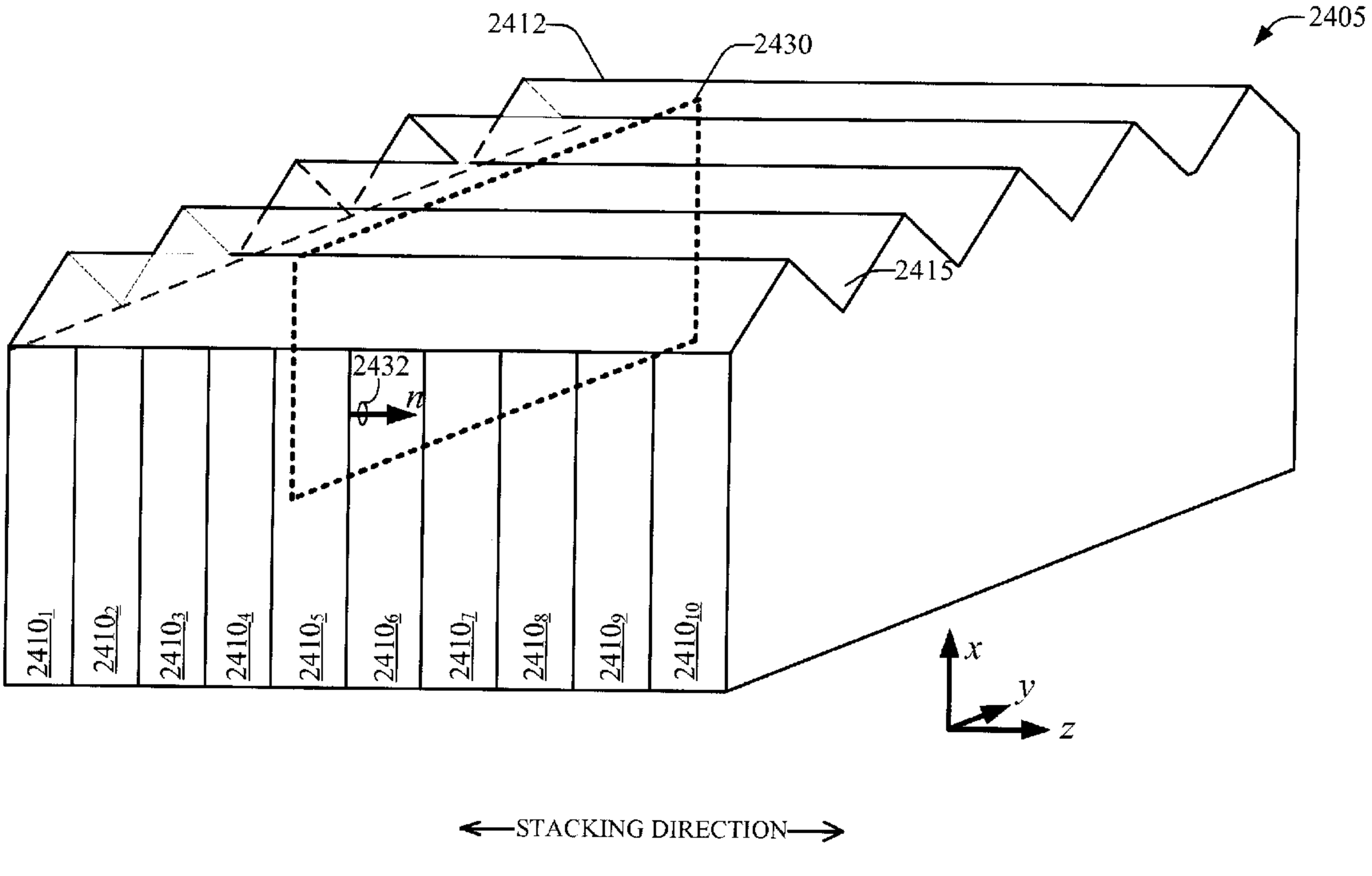
2412
2430
2405
2415
2432
n
2410₁
2410₂
2410₃
2410₄
2410₅
2410₆
2410₇
2410₈
2410₉
2410₁₀
x
y
z
STACKING DIRECTION